Dear Editor and Reviewers,

We highly appreciate your interest in our work and the long list of detailed and very constructive comments that were provided. We think that these comments were very helpful to improve the manuscript and, in particular, to sharpen its objectives.

In the revised version of the manuscript we made the following main changes: (1) a more detailed and more explicit explanation of the objectives and novelty of the manuscript, (2) clarifications on the local character of this study, (3) a more detailed discussion on the assumptions in and limitations of the analysis and (4) a revision of several figures so as to best provide the necessary information for the reader.

Please find below our replies to all Editor and reviewer comments as well as a track changed version of the revised manuscript.

Thank you very much for your consideration, and best regards,

Markus Hrachowitz (on behalf of all co-authors)

Replies to comments of the Editor

Comment:

The paper was reviewed by 4 reviewers and the response already highlights the potential relevance of the paper.

Reply:

We highly appreciate this positive assessment.

Comment:

However, the reviewer - and in particular #2-4, highlighted many points that need to be considered in a major revision before the paper can be reconsidered. Please put special attention to the following points: The research objectives and in particular the novel aspects of your analysis needs to be strengthen. Its is not clear what is really new in this study except a new catchment and dataset. A clear assessment of the models potential and limitations. And also clearly show the generality of the results versus the special aspects of the catchment studied.

Reply:

We completely agree that in the objectives and novelty of our analysis have not been clearly communicated in the original manuscript. We have now provided more detailed explanations and sharpened the focus of the manuscript. The novel aspects in our work are that we have set out (1) to describe __why__ deforestation in the Wüstebach caused the previously observed

changes in the hydrological partitioning, (2) to quantify changes in system properties and the associated model parameters as a consequence of deforestation and (3) to quantify the resulting effects on travel times.

We have also made it clearer now that the analysis and the associated interpretation are location specific.

Comment:

Finally, knowing the catchment quite well myself, I was wondering why only streamflow and isotope data has been used to constrain the model? I think the observations of soil moisture, groundwater wells and throughfall in this catchment would help to further constrain the model and hence reduces the uncertainty of the TTD considerably.

Reply:

It is true that in the Wüstebach a wealth of alternative data is available. Yet, to meaningfully use these data in catchment-scale models is not trivial. Many of these data remain point/plot-scale observations, which may or may not be representative for the catchment-scale (we simply do not know). To limit both, false negatives and false positives, we therefore deliberately decided not to use these data in our study. We believe that the underlying issue, i.e. the upscaling of hydrological variables, which is at the core of many problems in hydrology, is a formidable task that can fill several PhD projects but which is in the end outside the scope of this paper. Another problem, specifically related to soil moisture data is that there are no reliable and detailed catchment-scale estimates of root depth available in the Wüstebach. As the soil moisture store in the root-zone is the primary research target of this study (and as it can be estimated with the approach outlined in the manuscript), imposing assumptions on the depth of root-accessible soil moisture would be rather unhelpful for our analysis.

Replies to comments of Reviewer #1

Comment:

This paper analyses the results of a deforestation experiment on the Wüstebach experimental catchment using conceptual flow and transport models. Overall the paper uses interesting approaches, but needs better structuring, and a more appropriate title.

Reply:

We thank the reviewer for the overall positive assessment of our study as well as for her/his thoughtful and detailed comments.

Comment:

This paper essentially focuses on the Wüstebach catchment, a 0.39 km2 catchment in Germany. Clearly this catchment is a small and specific area. Whatever is found on this catchment cannot have general relevance, considering the place and scale dependence of hydrological processes. The title, however, is very trenchant and general, which contrasts with the specificity of the case study. I suggest a more specific title, more reflective of the individual headwater catchment that has been used in the analyses.

Reply:

On re-reading the title we agree with the reviewer and realize that the title is more general than intended. To better reflect the location specificity but also to place more emphasis on the actual objective and innovative aspect of this study we will reformulate the title into: "Reduction of vegetation-accessible water storage capacity after deforestation affects travel time distributions and increases young water fractions in a headwater catchment."

Comment:

The introduction is very general, and projects a status quo that is much broader of what is needed to introduce this specific study. The readers unavoidably end up asking themselves: what is already known about this specific catchment? The Wüstebach catchment has been the object of a countless number of studies, which analysed the results of the deforestation experiment, and modelled its behaviour using many modelling approaches (https://experimental-hydrology.net/wiki/index.php?title=W%C3%BCstebach_long-term_experimental_catchment). In particular, Wiekenkamp et al. (2016) already analysed issues related to water balance, potential evaporation, and water storage associated to deforestation. I can see that the authors here use different methods. However, that in this catchment "Deforestation reduces the vegetation-accessible water storage in the unsaturated soil" (part of the paper title) is already clear from Wiekenkamp et al. (2016), and other studies (e.g. works by Stockinger) have analysed the isotope data and evaluated MRT. These references are cited in the current manuscript. But they are not discussed to provide a clear motivation for the current paper, and to justify the novelty of the results.

Reply:

The reviewer is completely correct in saying that the Wüstebach study catchment has over the past years been subject to numerous studies. We highly appreciate the notion of the reviewer that for the reader the added value and innovative aspects of this study may not be completely clear yet. We agree that it will therefore be helpful for the reader to more explicitly describe how this study fits into the context of previous work in the Wüstebach and which knowledge it specifically adds.

Briefly, the Wiekenkamp et al. (2016) paper quantified in an elegant study the effects of deforestation on the partitioning of water fluxes, based on discharge and eddy covariance observations. Overall, they found that deforestation decreased actual evaporation/transpiration, which led to higher levels of soil moisture and eventually to increases in discharge. In contrast, the aim of our study was to establish a quantitative mechanistic link between these observed decreases in transpiration and changes to sub-surfaces properties of the system (and thus model parameters) to provide an explanation of __why__ deforestation reduces evaporative fluxes and increased soil moisture and discharge – after all the atmospheric water demand (here approximated by potential evaporation) remained stable pre- and post-deforestation.

Similarly, detailed previous work of some of our co-authors (Stockinger at al., 2019) quantified travel times and changes therein over time while Wiekenkamp et al. (2020) found evidence for increased post-deforestation occurrence of preferential flows. As an extension of that work, we here quantify the effect of deforestation on subsurface system properties and found that changes in these subsurface properties can to some extent explain __why__ deforestation affects travel times and in particular young water ages in the Wüstebach.

Overall our results provide evidence that post-deforestation changes in the water balance and the hydrological response dynamics can, to a large part, be traced back to changes in the soil pore space that can be *__accessed__* by evaporative fluxes (i.e. evaporation and/or transpiration) to satisfy atmospheric water demand. Vegetation, through its root system, can access pores and efficiently extract water from them for transpiration in, relatively spoken, deep parts of the soil. Soil evaporation, in contrast, can only extract water from comparably much shallower parts of the soil, due to increasingly limited turbulent exchange with depth. In other words, after the top soil is dry, soil evaporation is largely "blocked" while root-water uptake from deeper soil layers for transpiration can continue. In case of deforestation, plants are removed and the associated transpiration stops. The pore space that was accessed by transpiration before, can after deforestation then not be accessed by evaporative fluxes (i.e. soil evaporation) anymore and soil moisture levels in these pores remains longer close to field capacity. Informally spoken, this pore volume is thus lost as "reservoir" for evaporative fluxes.

In contrast to previous studies, where this pore volume is either estimated as model calibration parameter or based on very scarce data of root depths and soil porosities, our results here suggest (1) that this root-accessible pore volume ($S_{U,max}$) and its change due to deforestation can be meaningfully estimated from water balance data at the catchment-scale, (2) that it is therefore also a meaningful and directly observable catchment-scale effective parameter for use in process-based models and, most importantly (3) that changes in that hydrologically relevant subsurface property/model parameter can explain much of __why__ the hydrological response as well as travel times and young water fractions changed after deforestation.

We will provide a more detailed context of previous studies together with a more explicit definition of the objectives of this study and how they fit into the context and actually <u>link</u> the results of previous studies.

Comment:

The motivation for the choice of methods is unclear. E.g. why conceptual models, and SAS are chosen for the problem at hand? Wouldn't the result be obtainable with much simpler methods? It seems to me that if I look at the abstract or conclusions, a simple water balance calculation, and simple hydrograph separation techniques could have been sufficient to end up with the same outcomes. I understand that the authors are proposing a more elaborate approach. But why is that necessary?

Reply:

The motivation for the choice of the modelling strategy, i.e. a process-based hydrological model with an integrated SAS-function based tracer module, is closely linked to our overall objective of this study, i.e. to develop a better understanding of <u>why</u> the water balance, the hydrological response dynamics as well as the travel times in the Wüstebach catchment were subject to change after deforestation even though climatic conditions did largely not change. We wanted to understand (1) which (subsurface) system property was most affected by deforestation, (2) if this real-world property (or when used in models: parameter) and its change after deforestation can be meaningfully quantified at the catchment-scale and (3) if changes in this property can explain the observed post-deforestation changes in the water balance, response dynamics and travel times.

The simpler methods referred to by the reviewer are powerful tools to quantify overall hydrological system characteristics. However, due to their simplicity they mostly need to remain process-agnostic and can therefore provide us only with limited information on the underlying processes and mechanistic reasons. We will clarify this in the revised manuscript.

Comment:

The authors mention that they use an extensive multi-objective strategy, but in the end they use a single objective function. True that the objective function aggregates multiple objectives, but this cannot be defined multi-objective optimization, which would require determining the Pareto-front between the various objectives.

Reply:

We respectfully but strongly disagree with this comment. Only because multiple performance metrics f (i.e. objectives and criteria) were compressed into one summary statistic does not mean that the parameter selection strategy was not based on multiple objectives.

It is true that the solution space of a multi-objective optimization problem typically spans a front of pareto-optimal solutions. However, this pareto front only quantifies uncertainties arising from the choice and weight of and the trade-offs between the individual objectives. It does not account for data uncertainty and the idea of behavioural models, like in the GLUE framework (Beven and Binley, 1992). To embrace that we here did not treat *<u>only</u>* the actual pareto optimal solutions as feasible but also potential solutions behind the pareto front, i.e. we applied the GLUE method in a multi-dimensional case. This is schematically illustrated in Figure R1 below for a theoretical multi-objective evaluation based on two performance metrics f_1

and f_2 (note that the analysis of this manuscript was based on n=12 performance metrics instead, but based on the same reasoning).

We first defined a performance threshold for each individual performance metric f. Only solutions that fell within that threshold for each performance metric were kept as behavioural. The resulting solution space then implicitly contains the pareto front. Based on that we then further evaluated each solution that was kept as behavioural based on its multi-dimensional distance D_E from the "perfect model". The "best" solution is the one with the shortest distance D_E, thus inherently also being a point on the pareto-front. All other solutions accepted as feasible are further away from the "perfect model" and can be located on the pareto front or behind it.

If less (or in the extreme case only one) performance metrics than used in our analysis (n=12) had been used, the subset of retained behavioural solutions would be larger and their associated performances in terms of D_E different, which clearly demonstrates the effect of multiple performance metrics even when compressed into one summary statistic D_E. The above outlined strategy not only includes all pareto optimal solutions but also allows for additional uncertainty, thereby not only being defined as but actually extending and going beyond classic multi-objective parameter selection strategies as also similarly described and formalized by various recent papers (e.g. Efstradiadis and Koutsoyiannis, 2010; Gharari et al., 2013).
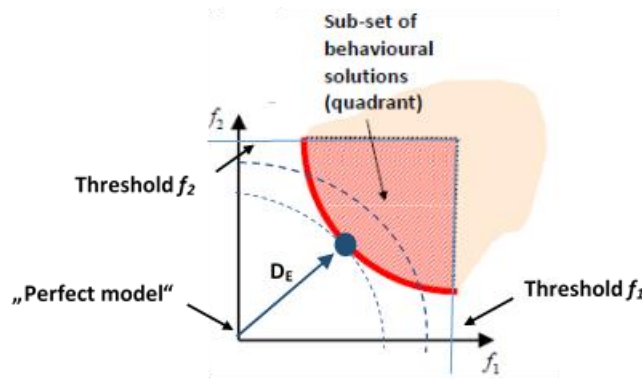
Figure R1: Schematic sketch of two-dimensional model performance space as defined by two performance metrics f_1 and f_2 (i.e. multi-objective). The theoretical "perfect model" would plot in the origin. The yellow shade indicates all model solutions. The light blue lines indicate the respective behavioural thresholds for f_1 and f_2 below which solutions are kept as behavioural and thus feasible. The red shaded area indicates the two-dimensional space of solutions accepted as behavioural. The bold red line indicates the set of pareto optimal solutions and the blue circle the single "best" solution with the lowest distance D_E to the "perfect model". The dashed blue circles-arcs indicate iso-performance levels in terms of D_E, i.e. solutions that have equal distances from the "perfect model" (after Gharari et al., 2013)

Comment:

I would have preferred to see separate results and discussion sections, to see separate the outcome of this work from the outcomes of other works. Currently the blend adds to the confusion of not being able to appreciate the value of the current work compared to earlier work on the specific catchment.

Reply:

We acknowledge and appreciate this comment. However, given the stepwise nature of the analysis we would strongly prefer to have the results of the individual steps closely associated to the interpretation thereof. However, we will strengthen and clarify the link to previous studies in the revised manuscript.

Comment:

Not clear to me why the Su,max of the model would be reflective of available water storage. For example, the model could have an Su,max of 200, but the variable storage between the reservoir can vary between e.g. 30 and 40 over one year, or between 10 and 150. So, Su,max sets an upper bound, but the real variability of the storage can be much smaller. The observation that 10.000 mm of water is necessary to attenuate the isotope signal suggests that indeed Su,max can be much larger than the dynamic range experienced by the catchment.

Reply:

*The reviewer is absolute right in stating that $S_{U,max}$ is an upper bound. To further reply to this interesting comment it will be helpful to upfront remind us again of how $S_{U,max}$ is actually defined. In the original manuscript, $S_{U,max}$ is described as the "pore volume between field capacity and permanent wilting point that is within the reach of active roots" and in the text referred to as "vegetation-accessible water storage **capacity**" and thus the **maximum** vegetation-accessible water storage volume in the unsaturated soil.*

As such, the upper limits of $S_{U,max}$ are by definition physically bound by

(1) Depth of groundwater table. Although fluctuating, the groundwater table in the study catchment remains at depths below 1 m for much of the year even in the riparian zone (Bogena et al., 2015) and can be expected to be considerably deeper on the hillslopes. Thus assuming a conservative upper bound of catchment-average depth of the groundwater table at ~ 5 m (assuming that the lowest groundwater table at each point in the catchment is at the elevation of the nearest stream), porosity of the silty clay loam (Bogena et al., 2018) soil of 0.4 and field capacity at a relative pore water content of 0.5 suggests an upper limit of $S_{U,max}$ at ~ 1000 mm.

(2) Root-depths. However, actual roots are often shallower than these 5m of the groundwater table. Although sufficient detailed data on root depths are not available in the study catchment, there is no evidence for systematic and wide-spread roots extending to below 0.5 m. This is broadly consistent with direct experimental evidence that roots of temperate forests in general (Schenk and Jackson, 2002) and Picea species in particular mostly remain rather shallow (< 1 m; e.g. Schmid and Kazda, 2001) and with indirect evidence that Picea species rarely tap groundwater and are thus comparatively shallow (e.g. Evaristo and McDonnell, 2017). As a conservative back-of-the-envelope calculation, assuming a maximum plausible

catchment-average root depth of 2 m (which comes close to the average observed soil depth reported in Graf et al., 2014), porosity of the silty clay loam (Bogena et al., 2018) soil of 0.4 and field capacity at a relative pore water content of 0.5 suggests an upper limit of $S_{U,max}$ at ~ 400 mm.

Thus given these estimates, we think it is very unlikely that $S_{U,max}$ is much larger than that. In addition, there is increasing and robust evidence that the magnitude of $S_{U,max}$ is actually based on optimality principles (e.g. Kleidon, 2004; Schymanski et al., 2008; Guswa et al., 2008; Yang et al., 2016; Speich et al., 2018 and many more): individual plants which have survived and are thus present in an ecosystem were well adapted to past conditions. This entails that they have root systems __large enough__ to provide them with access to enough water, __but not more than that__. Unnecessary allocation of resources to subsurface growth (and maintenance) would have led to a lack of resources for above-surface growth. These plants would have eventually lost out in competition for light. By extension, the question of how much water was necessary to be stored (i.e. held below field capacity and thus against gravity) and accessible for vegetation (i.e. $S_{U,max}$) can then be inferred from what vegetation *actually* transpired under extreme conditions (here: dry spells with 20 year return periods), as done in this manuscript.

However, please also note that as mentioned above, here and in many other landscapes world-wide (e.g. Fan et al., 2017) most roots do not extend to the depth of the groundwater table. This leads to the presence of an unsaturated zone __below__ the root zone. This zone is hydrologically largely "passive" as it is outside the influence of roots and given its relatively deep position essentially also outside the influence of soil evaporation: evaporative fluxes can therefore not extract water from pores in this part of the subsurface and water entering this zone only undergoes some delay before it is released from that zone again as groundwater recharge or direct drainage to a stream (e.g. through preferential flow paths). As no significant volumes of water can be drained below field capacity the unsaturated soil below the root zone remains close to field capacity for much of the year (except for the moments when a wetting front passes through). This is illustrated by the much lower variability in soil moisture content in these deeper soil layers (see e.g. Graf et al., 2014). Albeit being hydrologically largely passive (at least at time-scales of more than a few days dS/dt~0), this transitional zone between the root zone and the groundwater provides a mixing volume for tracers. This was implemented in one of our recent studies (Hrachowitz et al., 2015). However, here we finally decided not to explicitly account for this effect as it requires 2 additional model calibration parameters, i.e. the size of the mixing volume and the time lag for releasing water. After intensive model testing it was found that these two parameters cannot be well constrained at all. In particular the size of the mixing volume showed considerable trade-offs with the parameter of the passive mixing volume $S_{S,p}$ here. Instead of explicitly representing this volume as individual model component, we therefore implicitly accounted for this additional mixing volume in $S_{S,p}$. It can thus be assumed that, in reality, part of the 10.000 mm of $S_{S,p}$ is actually a mixing volume in the transitional zone. It plausible to assume that here the magnitude of this volume does realistically not exceed ~500-600mm (i.e. the difference between the storage capacity above the groundwater and the root zone – see (1) and (2) above).
We will clarify this in the revised manuscript.

Comment:

In terms of isotopes, it seems from the figure that there is an increase in the variability of the inputs. This leads to the question of how different are the inputs in the two periods, and whether the increase in young water fraction can be partly attributed to non-stationary inputs.

Reply:

*The variability in the observed precipitation isotope inputs indeed slightly increased after deforestation (mostly due to higher sampling frequency) from a standard deviation of ~3.2 ‰ to ~3.8 ‰, while the stream water isotope variability remained stable at a standard deviation of ~0.2 ‰. This entails that the damping ratio between precipitation slightly increased and the input signal was thus proportionally more strongly damped. Following our current understanding of tracer dynamics, a higher damping ratio is associated with older water (e.g. McGuire and McDonnell, 2006). We therefore believe that, if this slight change in variability had an effect, it would rather **decrease** than increase young water fractions.*

Comment:

From the uncertainty analysis, it appears that some parameters, e.g. Rs,max, are poorly constrained. But I am guessing that this parameter can strongly affect the behaviour of the Su reservoir, which is the key storage analysed in this paper. Any comment on this?

Reply:

As correctly observed by the reviewer, some model parameters are less well constrained than others, which remains a problem in essentially all inverse model implementations in environmental sciences. It is also true that the specifically mentioned parameter $R_{S,max}$ has some influence on $S_{U,max}$. However, the results suggest that the absolute magnitudes of the associated flux $R_{S,H}$ are too low (i.e. < 10% of the water balance) to significantly influence $S_{U,max}$. This is further supported by the fact that $S_{U,max}$ is, for conceptual model standards, very well constrained: no matter the value of $R_{S,max}$, $S_{U,max}$ remains within the same narrow range. We will add this to the discussion in the revised manuscript.

References:

Beven, K., & Binley, A. (1992). The future of distributed models: model calibration and uncertainty prediction. Hydrological processes, 6(3), 279-298.

Bogena, H. R., Bol, R., Borchard, N., Brüggemann, N., Diekkrüger, B., Drüe, C., ... & Missong, A. (2015). A terrestrial observatory approach to the integrated investigation of the effects of deforestation on water, energy, and matter fluxes. Science China Earth Sciences, 58(1), 61-75.

Bogena, H.R., Montzka, C., Huisman, J.A., Graf, A., Schmidt, M., Stockinger, M., ... & Lücke, A. (2018). The TERENO-Rur Hydrological Observatory: A multiscale multi-compartment research platform for the advancement of hydrological science. Vadose Zone Journal, 17(1).

Efstratiadis, A., & Koutsoyiannis, D. (2010). One decade of multi-objective calibration approaches in hydrological modelling: a review. Hydrological Sciences Journal–Journal Des Sciences Hydrologiques, 55(1), 58-78.

Evaristo, J., & McDonnell, J. J. (2017). Prevalence and magnitude of groundwater use by vegetation: a global stable isotope meta-analysis. Scientific reports, 7(1), 1-12.

Fan, Y., Miguez-Macho, G., Jobbágy, E.G., Jackson, R.B., & Otero-Casal, C. (2017). Hydrologic regulation of plant rooting depth. Proceedings of the National Academy of Sciences, 114(40), 10572-10577.

Gharari, S., Hrachowitz, M., Fenicia, F., & Savenije, H. H. G. (2013). An approach to identify time consistent model parameters: sub-period calibration. Hydrology and Earth System Sciences, 17(1), 149.

Graf, A., Bogena, H.R., Drüe, C., Hardelauf, H., Pütz, T., Heinemann, G., & Vereecken, H. (2014). Spatiotemporal relations between water budget components and soil water content in a forested tributary catchment. Water resources research, 50(6), 4837-4857.

Guswa, A.J. (2008). The influence of climate on root depth: A carbon cost- benefit analysis. Water Resources Research, 44(2).

Hrachowitz, M., Fovet, O., Ruiz, L., & Savenije, H.H.G. (2015). Transit time distributions, legacy contamination and variability in biogeochemical 1/fα scaling: how are hydrological response dynamics linked to water quality at the catchment scale?. Hydrological Processes, 29(25), 5241-5256.

Kleidon, A. (2004). Global datasets of rooting zone depth inferred from inverse methods. Journal of Climate, 17(13), 2714-2722.

McGuire, K. J., & McDonnell, J. J. (2006). A review and evaluation of catchment transit time modeling. Journal of Hydrology, 330(3-4), 543-563.

Schenk, H.J., & Jackson, R.B. (2002). Rooting depths, lateral root spreads and below- ground/above- ground allometries of plants in water- limited ecosystems. Journal of Ecology, 90(3), 480-494.

Schmid, I., & Kazda, M. (2001). Vertical distribution and radial growth of coarse roots in pure and mixed stands of Fagus sylvatica and Picea abies. Canadian Journal of Forest Research, 31(3), 539-548.

Schymanski, S.J., Sivapalan, M., Roderick, M.L., Beringer, J., & Hutley, L B. (2008). An optimality-based model of the coupled soil moisture and root dynamics. Hydrology and earth system sciences, 12(3), 913-932.

Speich, M.J., Lischke, H., & Zappa, M. (2018). Testing an optimality-based model of rooting zone water storage capacity in temperate forests. Hydrology and Earth System Sciences, 22(7), 4097-4124.

Stockinger, M. P., Bogena, H. R., Lücke, A., Stumpp, C., & Vereecken, H. (2019). Time variability and uncertainty in the fraction of young water in a small headwater catchment. Hydrology & Earth System Sciences, 23(10).

Wiekenkamp, I., Huisman, J. A., Bogena, H. R., Lin, H. S., & Vereecken, H. (2016). Spatial and temporal occurrence of preferential flow in a forested headwater catchment. Journal of hydrology, 534, 139-149.

Wiekenkamp, I., J.A. Huisman, H.R. Bogena, and H. Vereecken (2020): Spatiotemporal Changes in Sequential and Preferential Flow Occurrence after Partial Deforestation. Water 12(1), 35.

Yang, Y., Donohue, R.J., & McVicar, T.R. (2016). Global estimation of effective plant rooting depth: Implications for hydrological modeling. Water Resources Research, 52(10), 8260-8276.

Replies to comments of Reviewer #2

Comment:

The specific goals of the work, as stated in the introduction, are to analyse the observed post-deforestation changes through the lenses of change in the plant-available storage. The latter is a topic where the leading author has developed extensive research in the last years. Based on this main goal, the authors formulate three hypotheses that form the basis for the results and discussion. The goals of the manuscript fully fit the scope of the journal, the data is of high quality and the methodology appears elaborate and generally appropriate. The authors produce a very large number of results, which may even be enough material for two papers, and I think this is where the manuscript becomes difficult to navigate. Although the overarching questions are clearly outlined in the introduction, the focus of the paper gets somewhat lost across the numerous results and analyses. For example, I find the water age analysis too detailed and beyond the main point of the article. I believe the focus of the manuscript should be narrowed and the material more selected to provide a cleaner storyline. Overall, while I believe these results deserve publication, I think major improvements on the manuscript structure and focus are required.

Reply:

We thank the reviewer for her/his interest in our work. We highly appreciate the thought- and insightful comments and the overall positive assessment of our manuscript. We will address all comments in detail below.

Comment:

Novelty and relevance: I think the paper introduction is well developed but I somewhat miss the novelty and relevance of the results. E.g. what did we not know before? Does novelty lie specifically in the quantitative (rather than qualitative) evaluation of change?

Reply:

We agree, as also pointed out to Reviewer #1, that the research objectives and in particular the novel aspects of our analysis were not defined clearly enough in the original manuscript.

Briefly, previous analyses in the study catchment documented changes in the individual water balance components (i.e. evaporation and discharge, Wiekenkamp et al., 2016, 2020) and also fluctuations in young water fractions (Stockinger et al., 2019) in the years after deforestation. In contrast, the aim and novelty of our study here was to establish a link between these observed changes in the water balance components and deforestation-induced changes in (sub-)surface system properties (and thus model parameters) and to explore and quantify possible mechanistic processes that cause these changes, eventually providing a possible explanation of __why__ these changes occurred.

Our results provide evidence that changes in $S_{U,max}$ (and to a minor degree, in I_{max}), a hydrologically relevant and directly quantifiable subsurface property/model parameter, can explain much of __why__ the hydrological response as well as travel times and young water fractions changed after deforestation.

We will clarify this in the revised manuscript.

Comment:

Visual assessment of model results: Figures are all high-quality but they are not always informative. Figure 2 is particularly important because it shows time series of modelled and observed variables, but it is rather ineffective and it should be redesigned.

Reply:

We agree that Figure 2 can be improved. We will adapt as described in detail below.

Comment:

Model purpose: the model produces a large number of outputs and I appreciate that the authors clearly discuss the limitation of the modelling framework. I think it would be good to declare upfront the capabilities of such a model. For example, given its design and the data used to assess its performance, what can the model be reasonably used for in this context?

Reply:

We agree. We will provide some more information on that in the model description section. Briefly, the model used is a current-generation catchment scale, process-based, semi-distributed model based on conceptual parametrizations and which is coupled with a tracer tracking module formulated based on the SAS-function concept. As such it is valuable to quantify catchment-scale water balance and tracer dynamics. In particular and most importantly, instead of merely aggregating largely unknown surface and subsurface heterogeneities, it allows to account for their integrated effects on the hydrological response. The main limitation of such a model approach is missing spatial detail and the use of catchment-scale effective parameter that sometimes cannot be well constrained by the model calibration process.

Comment:

Also it seems that the model would in principle be able to estimate the age of evaporative fluxes, but the authors do not show such results. Why? And why is the model not used to estimate the (change in) partitioning between Q and ET?

Reply:

The reviewer is right in assuming that the model also provides age estimates of evaporative fluxes (and any other system internal flux). In a deliberate decision we chose not to use these model outputs in the analysis as these outputs do not have any direct data support and are thus subject to considerable uncertainty. While stream water age estimates are of course also subject to uncertainties, they are more reliably and directly constrained by stream water tracer samples. We will clarify this in the revised manuscript.

The model is in fact already used to estimate the partitioning, although not directly between Q and ET, but instead (in fact containing the equivalent information to Q/E_A) expressed as the runoff ratio C_R (i.e. Q/P or $(1-E_A)/P$). The runoff ratio is also one of the calibration objectives in our model implementation (i.e. $E_{R,CR}$) as shown in Table 3 and Figure 5 and discussed at several points in the original manuscript (e.g. l.454-456 or l.488-490).

In addition, we believe that the analysis is already quite comprehensive and the manuscript rather long, as also remarked on above by the reviewer. Additional information will make it difficult to keep the manuscript focussed.

Comment:

Estimates of SU,max: the reduction in SU,max after deforestation is very pronounced. I'd appreciate some discussion of how a 21% reduction of forest cover may lead to a 50% reduction in SU,max. Does the location (riparian area VS hillslope) play a role? Would you expect important differences if the deforestation had occurred away from the river network? Could this model be used to make such a prediction?

Reply:

This is a very interesting observation. We are similarly surprised by the strong effect and also remarked on that in the original manuscript (l.421). One statement we can make here, and which is supported by data, is that the model results suggest that the reduction of $S_{U,max}$ in the completely clear-cut riparian zone was considerably higher than on the only partially deforested hillslopes (see Table 2, Figure 6 and l.509-511). While this indicative ranking and also the strong reduction of $S_{U,max}$ in the clear-cut riparian zone are plausible (~ 130 mm; l.511), the ~ 75 mm reduction in the only partially deforested hillslope zone (l.510) indeed generates questions. Of course, it cannot be excluded that deforestation affects other properties in the subsurface and that these changes may feed back onto $S_{U,max}$ (as discussed in l.503-505 in the original manuscript). An alternative explanation could be that after deforestation in 2013, the remaining forest on the hillslopes, that was homogeneously planted in 1946 (Graf et al., 2014) was thinned in 2015, thereby likely reducing catchment-scale vegetation water demand and thus also $S_{U,max}$, as compared to the pre-deforestation period. We, however and unfortunately, do at this point not have the necessary data to further test and substantiate this hypothesis.

We will extend the discussion on this in the revised version of the manuscript.

Comment:

Age analysis: as mentioned before, I think this is a very complete analysis but it seems to go too deep compared to the scope of the paper. There are several concepts and results that appear complex (e.g. not just the TTD/RTD ratio or the young water fraction, but also their sensitivities to wetness, before and after deforestation) and would fit a paper that specifically focuses on the effects of deforestation on catchment residence times. But given the broader objectives, a selection of the results might help clarify the message.

Reply:

We agree, that a comprehensive selection of results is presented and that the manuscript may benefit from a bit less detail. We will therefore remove the results/discussion on the differences between TTD and RTD and try to shorten some of the other aspects.

Comment:

Title: isn't it obvious that deforestation "affects" travel times? Can suggest how it affects them

Reply:

Probably it is indeed intuitively obvious. However, to our knowledge it has not yet been explicitly shown in a detailed analysis. To highlight the direction of the effect, we suggest to adapt the title to: "Reduction of vegetation-accessible water storage capacity after deforestation affects travel time distributions and __increases__ young water fractions in a headwater catchment."

Comment:

50-56: very long sentence. Consider breaking it

Reply:

Agreed. Sentence will be rephrased.

Comment:

70-71: unclear sentence

Reply:

Agreed. Sentence will be rephrased.

Comment:

93-96: this sentence includes some slang. Consider rephrasing. Also, it partly seems a repetition of lines 49-52

Reply:

We are not sure what the reviewer is exactly referring to as "slang" in this sentence: "Transpiration extracting soil water below that therefore effectively generates a root-zone water storage reservoir between field capacity and permanent wilting point that is characterized by a storage capacity $S_{U,max}$, i.e. a maximum vegetation-accessible storage volume, and that is at any given moment filled with a specific water volume $S_U(t)$, depending on the past sequence of water inflow and release."

It is true that the sentence is partly a repetition, but we believe it is necessary to explicitly clarify the difference between $S_{U,max}$ and $S_U(t)$. We will try to rephrase the sentence.

Comment:

98: "With increasing storage, the hydrological memory of a system increases" → can be easily misinterpreted because one may think that, for a system with a given water storage, streamflow age would increase when the storage increases, but it is usually found (e.g. Harman, 2015, Water Resources Research) that the opposite applies.

Reply:

This is indeed a delicate problem, mainly due to the unfortunate and confusing terminology available to us. In fact the term "storage" can be used in ways that have subtle differences. Consider the following simplified, illustrative thought experiment, distinguishing 4 situations:

(1) *a small storage reservoir that is half-filled with water and from which water can only slowly drain at the bottom. Water will stay and mix in this volume for some time (i.e. little storage leads to old ages that eventually leave the reservoir) before being drained.*

(2) *In a second step, this storage reservoir is filled and overtops. Much of the overtopping water has little opportunity to mix with older water in the reservoir and bypasses the storage volume (i.e. at such high storage states, much of the outflowing water will thus be very young)*

(3) *a second storage reservoir that is __larger__ than the one above is, just as above in (1), half-filled with water and from which water can only slowly drain at the bottom. Water will stay and mix in this volume for some time (i.e. little storage leads to old ages that eventually leave the reservoir). However, the difference to (1) is that although the degree of filling of the storage reservoir is the same, the actual storage volume is larger, which leads – under complete mixing to older ages than in (1), as reflected in basic equation for mean turnover times T=volume/flux.*

(4) *In a last step, this larger storage reservoir is filled and overtops. Much of the overtopping water has little opportunity to mix with older water in the reservoir and bypasses the storage volume (i.e. at such high storage states, much of the outflowing water will thus be very young). However, under most conditions there is still __some__ exchange with the old water in the large storage reservoir. Although younger than in a half-filled large storage volume (3), the outflowing water may still be older than the outflowing water from the full small storage volume (2).*

In summary, while the use of the term storage in the Harman (2015) paper refers to the degree-of-filling of a storage reservoir with given size, i.e. (1) and (2), we use the term storage here to refer to the absolute size of a storage reservoir, i.e. (3) and (4).

We will clarify this in the revised manuscript.

Comment:

Figure 2: this figure is very important for the manuscript but I find it rather inefficient. Subplot (a) does not seem to show anything that a reader could grasp. Subplot (c) is very compressed –it is never easy to compress 7 years of data into a single pane l– but then it is almost impossible to inspect the results. Subplot (d) is uninformative because tracer in stream water is not shown at an adequate scale. Is tracer precipitation data really useful here? If you really want to show it, maybe you could report some monthly means (so we get at least the seasonality of the input) and on a rescaled y-axis?

Reply:

We agree that efficiently showing the most relevant results over longer time periods for multiple variables in figures is challenging. We also agree that Figure 2 can benefit from some adaptions. We therefore propose the following changes.

Subplot (a): we will replace daily values by monthly values. This should make the plot easier to read.

Subplot (c): we think it is important to give the reader an overall impression of the hydrological response to be able to place it into sufficient context. We thus would like to keep subplot (c) as is, but to add either (1) an additional subplot, showing zoomed-in version of one individual year pre- and one year post-deforestation, or (2) detailed individual plots for each year in figures in the Supplementary Material. We will test and evaluate both alternatives.

Subplot (d): We had a long and intensive discussion on exactly this question and, in the end, made the deliberate decision in the original manuscript to show the tracer signals in the way we did. Of course the reviewer is right in saying that detailed, small scale fluctuations in stream water tracer cannot be seen in this figure. The underlying question for us was, which information is in fact the most relevant to convey here. We finally decided that it is more relevant to illustrate the degree of damping that precipitation tracer signals experience before they reach the stream. This is a direct indicator of the age of stream water and can only be seen when both variables are plotted at the same scale. In the case of this study catchment, when the tracer signal is attenuated to a degree that the stream water composition plots almost as a straight line, little fluctuations around this line are difficult to interpret: how much of it is due to real effects? How much is due to mere noise, resulting from observational uncertainties? This is also discussed in some detail in the original manuscript (l.474-479). However, we also acknowledge that the reader may want to see exactly this detail. Thus we propose the same as for subplot (c) and we will add an additional subplot with a zoomed-in version for one individual year pre- and one year post-deforestation. In addition, we will follow the reviewer's excellent suggestion to integrate the precipitation signals to monthly time-scales for better readability of the figure.

Comment:

162: "To quantify effects of deforestation on SU,max and, as a consequence of that, on the age structure of water" I find this slightly misleading as it seems that the age structure is only affected through SU,max (and not directly).

Reply:

Deforestation reduces the catchment-scale pore volume that can be accessed by roots, i.e. $S_{U,max}$. This also reduces $S_{U,max}$ as mixing volume. The size of a mixing volume directly affects water ages (see replies above). Changes in water age structure are thus a consequence of a reduction of this mixing volume. We will clarify this in the revised manuscript.

Comment:

166: similar to 162, I don't see why you estimate the effects of these changes only. Aren't the two problems partially separate? You can get to (2) even without (1) or am uncorrect?

Reply:

It is correct that quantifying changes in $S_{U,max}$ does not __require__ an a priori check if the general water balance partitioning pattern changed. However, under relatively stable climatic conditions (as in the study catchment during the study period), changes in the partitioning are a reliable indicator of changes in some (a priori unknown and unquantified) system properties (and thus model parameters), frequently related to changes in vegetation cover (e.g. van der Velde et al., 2014; Jaramillo et al., 2018). If, in contrast, no such changes in the partitioning are observed, changes to system properties are much less likely. We therefore wanted to first establish that there actually was a significant change between the pre- and post-deforestation partitioning pattern detectable with our method (and not only with the method used in Wiekenkamp et al., 2016) and to use this as basis for the subsequent hypothesis that deforestation affects $S_{U,max}$ and that this effect can be quantified.

Comment:

Eq 39 and 41: what is the horizontal bar above the lowercase omega?

Reply:

We agree, this looks confusing. This is not an overbar – the italic style of this MS Word font, when used in the equation editor only appears to have an overbar. It is in fact only a normal omega character.

Comment:

336: this explains how you translate a physical process into a model component. But I recommend explaining why a "passive" storage is needed. It is not a model artefact, but rather the real amount of water that is involved in the transport process. Other good classic references for this is "Birkel, C., C. Soulsby, and D. Tetzlaff (2011), Modelling catchment-scale water storage dynamics: Reconciling dynamic storage with tracer- inferred passive storage, Hydrol. Processes, 25(25), 3924–3936, doi:10.1002/hyp.8201"

Reply:

This is indeed an excellent suggestion. We will make this more explicit and add the above reference.

Comment:

353: Ok fine, but how do you initialize the model? Which d18O initial composition is assigned to the different compartments?

Reply:

We initialized the model using different initial isotope compositions for the individual storage components: assuming that only groundwater flows from S_S sustain low flows during the dry season, we used the mean isotope stream water composition of the time steps with the 5% lowest flows as initial composition in S_S and $S_{S,p}$. For S_U we used the long-term volume weighted mean precipitation value of the months April-September, preceding the start of the model in October. S_I and S_F were, due to their small sizes, assumed to be empty. The model was then primed with a 5-year warm-up period before 10/2009, which was a copy of the data from actually available observations.

We will add this information in the revised manuscript.

Comment:

385: I suggest replacing "the data" with "results"

Reply:

Agreed.

Comment:

408: start with "In our study, "

Reply:

Agreed.

Comment:

417: SU,max = 90+-149? If the standard deviation is much larger than the mean, wouldn't it be better to avoid completely this exercise? Or maybe mention it here but not stress it later as a real result, given it comes with considerable uncertainty?

Reply:

We agree that these uncertainties are quite high. We still believe it is worth to report it, to give the reader a sense of a, albeit uncertain, plausible range. Due to the uncertainties, we do, on purpose, not use these values for any quantitative analysis. We have explicitly stressed and acknowledged that in the original manuscript (l.418-420). We will further clarify this in the revised manuscript.

Comment:

428 and 435: as noted in comments on Figure 2, it is difficult to judge from this figure because too much data is compressed in it and the scaling does not look appropriate

Reply:

We will adapt Figure 2 as described in our reply to one of the comments further above.

Comment:

Figure 5: please add some legend to make the colouring more intuitive

Reply:

Agreed.

Comment:

Figure 6: why showing cumulative frequencies? I find it difficult to evaluate how much parameters are constrained from these curves.

Reply:

Ok. We will add histograms to also show the associated frequency distributions in these plots.

Comment:

440: "...show that most model parameters are reasonably well identified" but it is difficult to actually evaluate

Reply:

We will adapt Figure 6 as described above to make it easier to see.

Comment:

494: if I haven't stressed this enough, this is invisible in the figure

Reply:

Agreed. Figure 2 will be adapted as described above.

Comment:

513: I do not see how a value of 120 falls "reasonably well" into a "plausible" range [-59, 239]

Reply:

We are not sure what the reviewer exactly wants to express here. In our understanding, a value of 120 is very close to the central value (i.e. 149) of the interval spanned by [-59, 239] and thus also falls into this range.

Comment:

519: I get the point, but cannot really evaluate overlapping from figure 6. Rather from table 2. Then I see that Lp is the only other parameter with a significant change pre-post deforestation. Might this be worth of a comment?

Reply:

We will adapt Figure 6 as described above. It is true the parameter L_P does change, but, and this seems to be a misunderstanding, it is by far __not__ the only parameter with a significant change as shown in Table 2 in the original manuscript. The parameters that are directly related to vegetation ($S_{U,max}$, I_{max}) change the most and they do so in a more pronounced way in the fully deforested riparian zone, i.e. the range of $S_{Umax,R}$ is reduced from 194-287 mm to a range of 53-122 mm, while $I_{max,R}$ is reduced from 0.8-4.5 mm to 0.0-0.9 mm.

The reductions in the partially deforested hillslope parameters are less pronounced but still statistically significant (p<0.05) for $S_{U,max,H}$ from 233-309 mm to 118-249 mm and for $I_{maxh,H}$ from 0.8-4.5 to 0.1-1.7 mm.

Most other posterior parameter distributions (i.e. parameters not directly related to vegetation) do not experience a significant change (Table 2).

Comment:

534: [again on figures] "is evident", but nothing is evident from figure 2d

Reply:

Agreed. Figure 2 will be adapted as described above.

Comment:

541-566: this is a nice analysis but I wonder whether it is really necessary as it is more about general TTD and RTD dynamics rather than on effects of deforestation. In other words, this seems to go beyond the scope of the manuscript. A large simplification would make the manuscript easier to read.

Reply:

We will try to shorten this section. In particular, we will remove the analysis and interpretation of RTDs. However, we would really like to keep the mechanistic interpretation of the results, which is ultimately the part of the objectives of this paper.

Comment:

544: please specify how you computed Fyw because a reader will expect it is estimated using kirchner's 2016 method.

Reply:

The young water fraction was here defined as the fraction of water younger than three months. This value was here directly extracted from the associated travel time distributions (TTDs). We will clarify this in the revised manuscript.

Comment:

33: the change in Fyw from 0.11 to 0.13 does not seem significant considering the possible uncertainties in the estimate.

Reply:

This is correct. We will clarify this in the revised manuscript.

Comment:

Figure 2d: typo in the permil symbol in the y-axis label.

Reply:

Ok.

Comment:

70: the vegetation...presentS

Reply:

This is a misunderstanding. The sentence should read as: "The vegetation, i.e. a collective of individual different plants within an area of interest that is present at any given moment at any given location, has survived."

Comment:

264: it is reaches

Reply:

Will be corrected.

Comment:

548: "Stream water can contain Fyw" is not a correct formulation. Rather "stream water can contain up to 30% of young water" or similar

Reply:

Will be corrected.

Comment:

532-534: please reformulate this initial sentence, which is unclear The terminology"partly much lower" (452) and "partly considerable" (572) is a bit odd

Reply:

Will be corrected.

Comment:

425: title: Deforestation effects "on the catchment model" sounds a bit odd

Reply:

Will be rephrased.

References:

Graf, A., Bogena, H.R., Drüe, C., Hardelauf, H., Pütz, T., Heinemann, G., & Vereecken, H. (2014). Spatiotemporal relations between water budget components and soil water content in a forested tributary catchment. Water resources research, 50(6), 4837-4857.

Jaramillo, F., Cory, N., Arheimer, B., Laudon, H., Van Der Velde, Y., Hasper, T. B., ... & Uddling, J. (2018). Dominant effect of increasing forest biomass on evapotranspiration: interpretations of movement in Budyko space. Hydrology and Earth System Sciences, 22(1), 567-580.

Stockinger, M. P., Bogena, H. R., Lücke, A., Stumpp, C., & Vereecken, H. (2019). Time variability and uncertainty in the fraction of young water in a small headwater catchment. Hydrology & Earth System Sciences, 23(10).

Van der Velde, Y., Vercauteren, N., Jaramillo, F., Dekker, S. C., Destouni, G., & Lyon, S. W. (2014). Exploring hydroclimatic change disparity via the Budyko framework. Hydrological Processes, 28(13), 4110-4118.

Wiekenkamp, I., Huisman, J. A., Bogena, H. R., Lin, H. S., & Vereecken, H. (2016). Spatial and temporal occurrence of preferential flow in a forested headwater catchment. Journal of hydrology, 534.

Wiekenkamp, I., J.A. Huisman, H.R. Bogena, and H. Vereecken (2020): Spatiotemporal Changes in Sequential and Preferential Flow Occurrence after Partial Deforestation. Water 12(1), 35.

Replies to comments of Reviewer #3

Comment:

This manuscript presents a study on the effect of deforestation on catchment hydrology. In this manuscript mainly a modeling approach is used. Using this modeling approach, the authors find that runoff increases after deforestation and also catchment travel time distributions. While this is an interesting point, I have a number of concerns with the study as it is presented now.

Reply:

We appreciate the reviewer's interest in our work and her/his thoughtful comments. We provide detailed clarifications in the list below.

Comment:

While the study uses a valuable data set is not fully clear to me how exactly this paper goes beyond the studies that have already been published using this catchment and its data set. Conclusions 1 and 2 basically confirm earlier studies, and the other conclusions are based on modeling with a number of assumptions (as discussed be-low). In general, it would be important that the authors relate their findings more to the previous findings using the same catchment to show the added value of this study clearly.

Reply:

We agree with the reviewer that the objective and novelty of our study was not communicated in a clear enough way in the original manuscript.

Briefly, previous analyses in the study catchment documented changes in the individual water balance components (e.g. evaporation and discharge, Wiekenkamp et al., 2016) and also some minor fluctuations in young water fractions (e.g. Stockinger et al., 2019) in the years after deforestation. Yet, these contributions did not provide quantitative mechanistic explanations of __why__ these changes occurred.

The aim and novelty of our study is therefore to explore and quantify a possible mechanistic process that causes these changes. Our results provide some evidence that changes in $S_{U,max}$, a hydrologically relevant and directly quantifiable subsurface property/model parameter, can explain much of __why__ the hydrological response as well as travel times and young water fractions changed after deforestation.

We will make this clearer in the revised version and we will also more explicitly discuss our results with respect to the results of the above studies.

It is also true that Conclusion #1 in the original manuscript essentially only supports the results of a previous study (i.e. Wiekenkamp et al., 2016), albeit estimated with a different method and over a different time period. We will clarify this in the revised manuscript.

In contrast, we are not aware of any study in the Wüstebach that quantifies the effect of deforestation on $S_{U,max}$, i.e. Conclusion #2. Our results, however, provide a puzzle-piece of supporting evidence for the potential generality of $S_{U,max}$ reductions due to

24

deforestation as they are consistent with results from catchments in different climatic and geomorphic settings (Nijzink et al., 2016; cited in the original manuscript).

Comment:

An obvious limitation of this study is in the use of only one catchment. As valuable as the data set is results might not be generally valid unless they can be confirmed using a larger data set including several catchments.

Reply:

We completely agree. However and unfortunately, we are not aware of any other catchment world-wide, where the necessary data are available and the necessary conditions for such a study are met.

Briefly, which minimum information is required to do such an analysis?

*At least a few years, pre- and deforestation respectively, with (1) daily water balance observations (P, E_P, Q; which are without doubt available from a many catchments world-wide), (2) (bi-)weekly tracer composition in precipitation and stream water and (3) well **documented deforestation** of a **significant fraction** of a catchment and that occurred during a sharply defined, **short period**, which falls **within the time period of available water balance and tracer data**.*

For example, while for the Plynlimon experimental catchment, long time series of water balance and tracer observations are available, deforestation occurred only gradually over many years (or decades), each time only affecting a small fraction of the catchment, and was partly offset by regrowth. In addition, much of the deforestation did temporally not overlap with the availability of tracer data. In another example, for the HJ Andrews experimental watershed, where well documented, significant deforestation took place over short, well-defined time periods, no tracer data are available for that period. Similar limitations apply to other locations, making such an analysis highly problematic.

As much as we wanted to provide a more generally valid analysis, we remain limited by the available data. We nevertheless strongly believe that in such a case, detailed analyses and process understanding developed from anecdotal case studies, such as this one, can be valuable to shape our understanding of what could happen and which processes occur – without claiming generality of the phenomenon.

We also agree that the title and the framing of the original manuscript may have misled the reader into hoping for a more general analysis. We will therefore adapt the title to "Reduction of vegetation-accessible water storage capacity after deforestation affects travel time distributions and increases young water fractions in a headwater catchment." to emphasize the local character of this study. In addition, we will make this clearer in the introduction.

Comment:

The most obvious effect of deforestation on catchment hydrology obviously is the re-moved interception. Here the authors largely ignore interception by the use of so-called effective precipitation. It is important to note that effective precipitation was determined by modeling using a very simple approach with a constant interception storage. This means that the results might have been implicitly affected by the calculation of the effective precipitation.

Reply:

While we agree with the reviewer that interception plays a role in forest systems, we respectfully disagree with the statement that the "most obvious effects" of deforestation relate to interception. Leaving aside the fact that, of course, visually the effect is large, many studies world-wide demonstrate that transpiration not only exceeds interception evaporation (e.g. Jasechko et al., 2013; Coenders-Gerrits et al., 2014; Schlesinger et al., 2014; Wei et al., 2017; Mianabadi et al., 2019), but that transpiration is actually the largest water flux from many terrestrial systems (Jasechko, 2018).

The reviewer's notion that we "largely ignore interception" is probably a misunderstanding as we use a standard technique, successfully tested and used in current-generation catchment-scale model formulations to account for interception (e.g. Fenicia et al., 2008; Samaniego et al., 2010; Gao et al., 2014; Nijzink et al., 2016). It is true that we use an interception capacity I_{max} which defines the __maximum__ volume of water that can be stored in the interception storage reservoir $S_I(t)$ at each time step t before overflowing, as defined by equations 9, 17, 18 and 19 in the original manuscript. At each time step t, this reservoir fills (via precipitation $P(t)$), drains (via evaporation $E_I(t)$ and overflow $P_E(t)$) and stores water (whatever water volume does not overflow as P_E and cannot be evaporated as E_I within a time step is carried over as storage $S_I(t)$ to the next time step).

It is thus important to note that __not the interception storage $S_I(t)$__, i.e. the intercepted volume of water at each time step, is constant, __but the maximum volume of water I_{max}__ that can be stored in the reservoir at each time step is constant. In other words, the degree of filling of the interception reservoir varies each day up to a maximum volume of I_{max}.

The modelled fluxes related to interception evaporation are broadly consistent with plots-scale observations thereof: the model suggests a mean ratio $P/P_E \sim 1.35$ (5/95th interval: $1.19 - 1.51$) for the growing season, while Stockinger et al. (2015) reported an observed $P/P_E \sim 1.41$ (± 0.19).

The underlying problem that prevents a more detailed formulation of this process is that, on larger scales, such as catchments, we have by far insufficient data (even in experimental catchment such as the Wüstebach) to warrant a meaningful, more detailed formulation of the interception process (and many other processes), as also described with an illustrative example in Hrachowitz and Clark (2017; see section S2 of the Supplementary Material therein).

The limited influence of interception evaporation on $S_{U,max}$ and the associated interpretations are explicitly described in lines 411-415 and shown in Figures 4b and 4c in the original manuscript.

Comment:

The isotope data is used to parameterize the passive storage volume. As I understand, this passive volume is only used for groundwater storage. This makes me wonder whether any passive storage is also being considered for the unsaturated storage. Sorry in case I missed this, but I am feeling a bit confused here. It is also not clear to me how mixing between active and passive storage has been calculated.

Reply:

We do not consider an explicit passive storage volume for the unsaturated zone. In reality, there may be such hydrologically passive volumes (i.e. dS/dt = 0) in the unsaturated zone, though.

The first one is the water stored in pores at water content below the permanent wilting point and thus essentially bound indefinitely, as it cannot be drained nor extracted by vegetation. The absolute magnitude of this volume is, depending on the wilting point, very small and thus considered to be negligible here and in similar studies (e.g. Birkel et al., 2010; Harman, 2015; Benettin et al., 2017 and many others).

*The second storage compartment that could be seen as a hydrologically passive storage volume is the unsaturated zone **below** and/or **outside** the root zone. In that zone, vegetation cannot extract significant volumes of water below field capacity. The pores therefore remain filled to field capacity much of the year, except for moments when a wetting front passes through. However, exchange (i.e. "mixing") with water in the "active" stores can and does occur. Indeed, we have previously added such a hydrologically passive mixing volume, representing the transition zone between the root zone and the groundwater, in a similar study (Hrachowitz et al., 2015). However, we found that the additional parameters cannot be reliably constrained with the available data, thereby increasing model uncertainty.*

In the present study, we also tested initial model formulations including such a store. However, it was found that it does not improve the results nor that it is meaningfully constrained by the available data. Here in the Wüstebach, the passive mixing volume in the unsaturated zone has an upper plausible limit of <1000 mm due to the position of the groundwater table (see also replies to Reviewer #1). In the way the model is implemented now, this additional mixing volume is implicit in $S_{S,p}$. In other words, were we to introduce an individual passive unsaturated mixing volume of ~1000 mm, $S_{S,p}$ would be reduced by approximately the same value. Such a trade-off, however, does not influence any of the results, as water going through such an unsaturated passive volume, subsequently only passes through S_S. Thus, the two can be aggregated without introducing relevant uncertainties. The same implicit reasoning was applied in many successful previous tracer studies (e.g. Birkel et al., 2010; Harman, 2015; Benettin et al., 2017 and many others).

*The mixing between active and passive stores was done using a standard SAS-function: a technique that has been well described and successfully tested in a large body of literature cited in the original manuscript (e.g. Botter et al., 2011; van der Velde, 2010; Benettin et al., 2013, 2017; Harman, 2015; Rinaldo et al., 2015 and many others), but also reproduced in this manuscript in some detail (section 4.2.2 and in particular l.336-339). Briefly, the estimated outflow $Q_S(t)$ from the active groundwater store $S_{S,a}(t)$ at each time step t is a composition of ages that is sampled (i.e. "mixed") according to the SAS-function from the **total** groundwater storage, i.e. $S_{S,T}(t)=S_{S,a}(t)+S_{S,p}$. We will further clarify this in the revised version of the manuscript.*

Comment:

Another crucial issue is the assumption that roots only take from the unsaturated zone. While this might be the case for the direct uptake, indirectly the uptake of water from the unsaturated zone will have the effect that an upward gradient is established

which will cause groundwater to rise into the unsaturated zone. So, indirectly roots can access water from the saturated zone. This process seems to be ignored here.

Reply:

We agree that roots can create suction pressures that, together with pure capillary rise and upwelling groundwater, can result in upward fluxes. While the latter is explicitly accounted for in the model as flux $R_{S,R}$ (Figure 3; Equations 11, 13 and 24; l.261-262), the first is implicit in how $S_{U,max}$ is estimated: it is the volume of water that was in the past accessible and accessed by vegetation. It therefore includes any upward capillary water fluxes.

Comment:

Based on the points above, I would argue that the calibration parameter S_Umax is difficult to interpret. It sounds like it is the size of the unsaturated storage, but I would argue it is more a parameter describing catchment functioning.

Reply:

*As clarified above (as well as explained in the original manuscript and the references therein), $S_{U,max}$ has indeed a clear and hydrologically meaningful definition. It is the maximum water volume that can be stored in the pores of the unsaturated root zone between field capacity and permanent wilting point at the catchment scale and, most importantly, which is **accessible and accessed by roots** (sometimes also referred to as "available water" or "plant available water"). This vegetation accessible water volume at the catchment scale is therefore a meaningful measure for the catchment-scale effective influence zone of roots, implicitly accounting for spatial heterogeneity of soils as well as for the spatial heterogeneity in the depths and densities of root systems. It is also a subsurface property that regulates much of the hydrological response and which could be, provided we have suitable observation technology available at some time in the future, practically obtained by measuring **all** roots and **all** soil porosities in a catchment multiple times over a certain period. As it could be **directly measured**, albeit only theoretically at this point, it **represents also a real catchment-scale quantity** and not only some abstract number. Note, that $S_{U,max}$ does not describe the unsaturated zone outside/below the root-zone. Also note that $S_{U,max}$ is a conceptual volume (and as such it is a theoretically directly measurable quantity, as explained above) that does not necessarily match to a specific position in the soil. It is rather a catchment-integrated pore volume that aggregates all locations and depths where roots are present.*

Comment:

Overall, I am afraid that the results obtained in the study are both catchment- and model-dependent. The authors need to make a more convincing case why their results are generally valid.

Reply:

We agree, the results depend on the decision taken and choices made throughout the modelling process. This is the case for any modelling study. For this reason and to limit uncertainties we only report results from processes that could at least to some degree be confronted with data. For example, we estimated $S_{U,max}$ (1) from water balance data alone and (2) as model

calibration parameter and then compared these values. In spite of uncertainties, they are broadly consistent with each other. Similarly, we only analysed stream water travel time distributions and not, for example, evaporation travel time distributions, as in the model only the stream water isotopic composition could be directly confronted with and compared to observed data. Furthermore, in an attempt to make the model as robust and reliable as possible, we constrained, evaluated and tested the model with an extended multi-objective and multi-variable calibration strategy, that goes far beyond of what many other modelling studies do. Lastly, we have also devoted the entire Section 5.4 to a detailed and honest discussion of the limitations of the modelling experiment, stressing that the results and interpretations are of course model-dependent (l.599). Given the above points, we nevertheless think that the results provide a rather reliable test of our research hypotheses. However, as with any other hypothesis, the test could be even stricter if the necessary data were available (Hrachowitz and Clark, 2017).

As discussed in one of the replies above, as much as we would like, the available data does not allow us to generalize the result. As also mentioned above, we will therefore emphasize the local character of the results more in the revised manuscript.

References:

Benettin, P., Soulsby, C., Birkel, C., Tetzlaff, D., Botter, G., & Rinaldo, A. (2017). Using SAS functions and high- resolution isotope data to unravel travel time distributions in headwater catchments. Water Resources Research, 53(3), 1864-1878.

Birkel, C., Tetzlaff, D., Dunn, S. M., & Soulsby, C. (2010). Towards a simple dynamic process conceptualization in rainfall– runoff models using multi- criteria calibration and tracers in temperate, upland catchments. Hydrological Processes: An International Journal, 24(3), 260-275.

Botter, G., Bertuzzo, E., & Rinaldo, A. (2011). Catchment residence and travel time distributions: The master equation. Geophysical Research Letters, 38(11).

Coenders-Gerrits, A. M. J., Van der Ent, R. J., Bogaard, T. A., Wang-Erlandsson, L., Hrachowitz, M., & Savenije, H. H. G. (2014). Uncertainties in transpiration estimates. Nature, 506(7487), E1-E2.

Fenicia, F., Savenije, H. H., Matgen, P., & Pfister, L. (2008). Understanding catchment behavior through stepwise model concept improvement. Water Resources Research, 44(1).

Harman, C. J. (2015). Time- variable transit time distributions and transport: Theory and application to storage- dependent transport of chloride in a watershed. Water Resources Research, 51(1), 1-30.

Hrachowitz, M., & Clark, M. P. (2017). HESS Opinions: The complementary merits of competing modelling philosophies in hydrology. Hydrol. Earth Syst. Sci, 21(8), 3953-3973.

Hrachowitz, M., Fovet, O., Ruiz, L., & Savenije, H. H. (2015). Transit time distributions, legacy contamination and variability in biogeochemical $1/f\alpha$ scaling: how are hydrological response dynamics linked to water quality at the catchment scale?. Hydrological Processes, 29(25), 5241-5256.

Hrachowitz, M., Benettin, P., et al. (2016). Transit times—The link between hydrology and water quality at the catchment scale. Wiley Interdisciplinary Reviews: Water, 3(5), 629-657.

Jasechko, S. (2018). Plants turn on the tap. Nature Climate Change, 8(7), 562-563.

Jasechko, S., Sharp, Z. D., Gibson, J. J., Birks, S. J., Yi, Y., & Fawcett, P. J. (2013). Terrestrial water fluxes dominated by transpiration. Nature, 496(7445), 347-350.

Mianabadi, A., Coenders-Gerrits, M., Shirazi, P., Ghahraman, B., & Alizadeh, A. (2019). A global Budyko model to partition evaporation into interception and transpiration. Hydrology and Earth System Sciences, 23(12), 4983-5000.

Nijzink, R., Hutton, C., Pechlivanidis, I., Capell, R., Arheimer, B., Freer, J., ... & Hrachowitz, M. (2016). The evolution of root-zone moisture capacities after deforestation: a step towards hydrological predictions under change?. Hydrology and Earth System Sciences, 20(12), 4775-4799.

Rinaldo, A., Benettin, P., Harman, C. J., Hrachowitz, M., McGuire, K. J., Van Der Velde, Y., ... & Botter, G. (2015). Storage selection functions: A coherent framework for quantifying how catchments store and release water and solutes. Water Resources Research, 51(6), 4840-4847.

Samaniego, L., Kumar, R., & Attinger, S. (2010). Multiscale parameter regionalization of a grid- based hydrologic model at the mesoscale. Water Resources Research, 46(5).

Schlesinger, W. H., & Jasechko, S. (2014). Transpiration in the global water cycle. Agricultural and Forest Meteorology, 189, 115-117.

Stockinger, M. P., Lücke, A., McDonnell, J. J., Diekkrüger, B., Vereecken, H., & Bogena, H. R. (2015). Interception effects on stable isotope driven streamwater transit time estimates. Geophysical research letters, 42(13), 5299-5308.

Van Der Velde, Y., Torfs, P., Van Der Zee, S., & Uijlenhoet, R. (2012). Quantifying catchment- scale mixing and its effect on time- varying travel time distributions. Water Resources Research, 48(6).

Wei, Z., Yoshimura, K., Wang, L., Miralles, D., Jasechko, S., & Lee, X. (2017). Revisiting the contribution of transpiration to global evapotranspiration. Geophysical Research Letters, 44(6), 2792-2801.

Replies to comments of Reviewer #4

Comment:

This manuscript presents the effects of partial deforestation on water storage and water ages in the German Wüstebach catchment. For this study, the authors performed water balance analyses and modelling exercises based on 7 years of hydrometric and water stable isotope data. One major finding of the study is that the vegetation-accessible storage volume in the unsaturated zone, SUmax*, was significantly reduced after the partial deforestation; the authors hypothesize that this reduction in *SUmax* can largely be explained with young water being routed quickly to the stream during wet conditions, so that less water reached the unsaturated zone *SU*.

The paper is well written and the figures are informative. I only have some minor comments and questions that the authors should address.

Reply:

We highly appreciate the reviewer's positive assessment of our manuscript and thank her/him for the thoughtful detailed comments.

Comment:

The physical meaning of *SUmax* not fully clear to me: its definition in the introduction is "water-filled pore volume between field capacity and permanent wilting point that is within the reach of active roots". This suggests that *SUmax* depends on water content in the soil and the active rooting depth. Does this mean that *SUmax* will decrease when water influx is reduced and/or roots become shorter? Then, the major result of the study (i.e., *SUmax* is reduced after deforestation; L421-424) is not surprising but rather expected because fewer roots will lead to a smaller catchment-average active rooting depth.

Reply:

We believe that our addition "water-filled" made the definition unclear. $S_{U,max}$ is the "pore volume between field capacity and permanent wilting point that is within the reach of active roots". As such it describes the __maximum__ (i.e. the upper bound, "capacity") possible water volume that can be __held__ against gravity (i.e. above field capacity) __and__ that can be __accessed__ by vegetation.

Indeed, $S_{U,max}$ is completely independent of the actual water content in the soil at any time. For practical purposes, it is can be considered constant over short time-scales < 2-3 years (although of course in reality it is continuously changing and adapting, albeit at mostly very low rates). In more humid climates, $S_{U,max}$ is typically smaller than elsewhere (e.g. Gao et al., 2014) – when there is constant water supply, e.g. when it is frequently raining, these frequent rains sustain rather near-surface soil water contents for much of the year. Vegetation therefore does not need to develop an extensive root-system to be able to access sufficient water. The opposite is true e.g. for more arid environments. In other words, when the water influx is reduced, $S_{U,max}$ will need to increase if vegetation wants to survive. Vegetation does so by developing more extensive root systems (either by individual plants growing deeper/denser roots or by specific, not sufficiently adapted plants dying and being replaced by

more adapted ones). Indeed, the major result of this study is not surprising – fewer roots lead to a smaller catchment-scale root-accessible pore space $S_{U,max}$.

As actual root observations are very scarce in space and time, the critical questions for hydrology are: **(1) how large is this root-accessible pore space at the catchment scale** *and* **(2) how much does it change after deforestation?**

We showed that $S_{U,max}$ can not only be quantified at the catchments-scale (as a few previous studies also suggested, e.g. Gentine et al., 2012; Gao et al., 2014) but that also its post-deforestation change can be quantified and that this change is a plausible explanation for younger water ages during wet conditions.

We will clarify the definition of $S_{U,max}$ in the revised manuscript.

Comment:

L135: How many measurements of rooting depth are available to justify the general assumption that the maximum rooting depth across the catchment is 50cm? What is the depth of the groundwater table and is it possible that capillary rise from the groundwater supplies these shallow-rooted plants?

Reply:

There is only anecdotal and indicative information about root-systems in the study catchment. However, there is no indication of systematic and wide-spread presence of deeper roots.

In the riparian zone, the groundwater table can reach the surface for a few days during the wet winter months, when transpiration is very low and which is therefore largely irrelevant for the estimation of $S_{U,max}$. During the growing season, which is critical for $S_{U,max}$, the groundwater table remains well below 1 m most of the time in the riparian zone, as shown by Bogena et al. (2015) and it can be expected to be considerably deeper on the hillslopes.

It is indeed possible and likely that groundwater sustains soil moisture levels and thus indirectly supplies vegetation. This is explicitly accounted for in our model as flux $R_{S,R}$ (Figure 3; Equations 11, 13 and 24; l.261-262).

We will clarify this in the revised manuscript.

Comment:

Are there any additional data that support your claim of a large groundwater storage in the Wüstebach catchment? It is surprising to me that no groundwater table and soil moisture observations have been considered for explaining many of the processes you propose.

Reply:

We agree that such a large mixing volume is indeed surprising and apart from the tracer observations we do not have direct evidence for the underlying reasons. However, we discuss potential explanations for that in the original manuscript. Although a "large groundwater storage" **can** *be the cause, it* **does not necessarily have to be**. *One alternative hypothesis is that old groundwater may enter the system from outside the defined catchment and replace (i.e. push out) younger water as unobserved groundwater export (l.606-621).*

In case there is no such groundwater exchange, something needs to buffer the high precipitation variability to the much dampened pattern observed in the stream tracer compositions, which do exhibit almost no fluctuations that go beyond measurement uncertainty. Following our current, rather well-developed understanding of tracer hydrology, such an effect can almost exclusively be caused by a large water storage volume that allows for sufficient "mixing" (e.g. Maloszewksi and Zuber, 1982; McGuire and McDonnell, 2006).

Based on our reply to the previous comment and thus assuming a conservative upper bound of catchment-average depth of the groundwater table at ~ 5 m (assuming that the lowest groundwater table at each point in the catchment is at the elevation of the nearest stream), porosity of the silty clay loam (Bogena et al., 2018) soil of 0.4 and field capacity at a relative pore water content of 0.5 suggests an upper storage limit ~ 1000 mm in the unsaturated zone. As no further significant storage volumes besides the unsaturated zone are known and in case there is no significant exchange of groundwater (see above) in the study catchment, only the groundwater remains as the required storage volume.

To answer the second part of the above comment, it is true that in the study catchment a lot of data is available. However, these data are largely inferred from point-scale measurements. Incorporating this information in catchment-scale models is challenging if not impossible to do in a meaningful way. For example, while our root-zone reservoir S_U represents the catchment-average water content in the root-zone, which soil moisture observations should this be compared to? The ones in 5 cm depth? In 10 cm? 50 cm? Or an average of that? What if there are in reality no roots at that depth at a given location? To avoid introducing a further level of assumptions, we therefore did not make use of point-scale measurements in our study. We will clarify that in the revised manuscript.

Comment:

How dry, drying, wet and wetting-up periods were defined (L545, L561, Fig. 8)?

Reply:

We imposed four thresholds to classify time steps along a spectrum to these periods. Briefly, periods with flows above Q_{25} were classified as wet, periods with flows below Q_{75} were defined as dry, increasing flows between Q_{25} and Q_{75} as wet-up period and receding between Q_{25} and Q_{75} as drying.

Comment:

Fig. 8 and Sect. 5.3: How was the daily young water fraction calculated and what is the associated uncertainty? Are your interpretations robust with respect to the uncertainties in *Fyw*?

Reply:

The daily young water fractions were extracted from the daily travel time distributions as the fraction of water volumes that is younger than 3 months (i.e. 32 days). Due to the lack of computational capacity we were unfortunately only able to provide uncertainty estimates for the long-term average $F_{yw,avg}$ as shown in Figure 8a and 8b in the original manuscript. We will clarify this.

Comment:

L434: From Fig 2d it is hard to see how well the model simulated theδ18O time series because the data points cover each other too much.

Reply:

We agree that Figure 2 will benefit from some adaptations. Specifically for Figure 2d we will therefore (1) aggregate the precipitation tracer composition to monthly values and (2) add an additional subplot with a zoomed-in version for one individual year pre- and one year post-deforestation.

Comment:

Fig 8d, c: It is not clear to me, which data points were used to obtain these regression lines? Especially the dark-blue regression lines (wet conditions) do not seem to fit the blue data points at all, and thus, the associated regression slopes should be considered with caution (e.g. in L588).

Reply:

We agree that the individual groups of data points are difficult to distinguish. To nevertheless allow the reader to better assess the strength of these relationships we will add the associated R^2 and p-values.

References:

Bogena, H. R., Bol, R., Borchard, N., Brüggemann, N., Diekkrüger, B., Drüe, C., ... & Missong, A. (2015). A terrestrial observatory approach to the integrated investigation of the effects of deforestation on water, energy, and matter fluxes. Science China Earth Sciences, 58(1), 61-75.

Gao, H., Hrachowitz, M., Schymanski, S.J., Fenicia, F., Sriwongsitanon, N., & Savenije, H.H.G. (2014). Climate controls how ecosystems size the root zone storage capacity at catchment scale. Geophysical Research Letters, 41(22), 7916-7923.

Małoszewski, P., & Zuber, A. (1982). Determining the turnover time of groundwater systems with the aid of environmental tracers: 1. Models and their applicability. Journal of hydrology, 57(3-4), 207-231.

McGuire, K. J., & McDonnell, J. J. (2006). A review and evaluation of catchment transit time modeling. Journal of Hydrology, 330(3-4), 543-563.

~~Deforestation reduces the~~<ins>Reduction of</ins> vegetation-accessible water storage <ins>capacity after deforestation</ins>~~in the unsaturated soil and~~ affects catchment travel time distributions and <ins>increases</ins> young water fractions <ins>in a headwater catchment</ins>

Markus Hrachowitz[1], Michael Stockinger[2,3], Miriam Coenders-Gerrits[1], Ruud van der Ent[1], Heye Bogena[2], Andreas Lücke[2], Christine Stumpp[3]

[1]Department of Watermanagement, Faculty of Civil Engineering and Geosciences, Delft University of Technology, Stevinweg 1, 2628CN Delft, Netherlands
[2]Institute of Bio- and Geosciences, Agrosphere Institute (IBG-3), Forschungszentrum Jülich, Wilhelm-Johnen-Straβe, 52425 Jülich, Germany
[3]Institute for Soil Physics and Rural Water Management, University of Natural Resources and Life Sciences Vienna, Muthgasse 18, 1190 Vienna, Austria

Correspondence to: Markus Hrachowitz (m.hrachowitz@tudelft.nl)

Abstract. Deforestation can considerably affect transpiration dynamics and magnitudes at the catchment-scale and thereby alter the partitioning between drainage and evaporative water fluxes released from terrestrial hydrological systems. However, it has so far remained problematic to directly link reductions in transpiration to changes in the physical properties of the system and to quantify these changes of system properties at the catchment-scale. As a consequence, it is difficult to quantify the effect of deforestation on parameters of catchment-scale hydrological models. This in turn leads to substantial uncertainties in predictions of the hydrological response after deforestation but also to a poor understanding of how deforestation affects principal descriptors of catchment-scale transport, such as travel time distributions and young water fractions. The objectives of this study <ins>in the Wüstebach experimental catchment</ins> are therefore to <ins>provide a mechanistic explanation of *why* changes in the partitioning of water fluxes can be observed</ins> ~~quantify the effects of~~ after deforestation ~~in the Wüstebach experimental catchment~~ and how this further affects the storage and release dynamics of water. <ins>More specifically, we test the hypotheses that (1) the observed changes can</ins>~~on the partitioning of water fluxes and to~~ directly <ins>be attributed to</ins>~~associate these~~ changes <ins>in the water storage volume in the unsaturated soil that is within the reach of active roots ($S_{U,max}$), that (2) changes in $S_{U,max}$ can be estimated at the catchment-scale to meaningfully adjust the associated parameter of a hydrological model and that (3) changes in $S_{U,max}$ eventually affect travel time distributions and increase young water fractions in the Wüstebach</ins>~~to changes in parameters of a hydrological model with integrated tracer routine based on the concept of storage age selection functions.~~ Simultaneously modelling stream flow and stable water isotope dynamics using meaningfully adjusted model parameters both for the pre- and post-deforestation periods, respectively, ~~a~~<ins>the</ins> hydrological model with integrated tracer routine based on the

1

concept of storage age selection functions model is used to track fluxes through the system and to estimate the effects of deforestation on catchment travel time distributions and young water fractions F_{yw}.

It was found that deforestation led to a significant increase of stream flow, accompanied by corresponding reductions of evaporative fluxes. This is reflected by an increase of the runoff ratio from $C_R = 0.55$ to 0.68 in the post-deforestation period despite similar climatic conditions. This reduction of evaporative fluxes could be linked to a reduction of the catchment-scale water storage volume in the unsaturated soil ($S_{U,max}$) that is within the reach of active roots and thus accessible for vegetation transpiration from ~225 mm in the pre-deforestation period to ~ 90 mm in the post-deforestations period. The hydrological model, reflecting the changes in the parameter $S_{U,max}$ indicated that in the post-deforestation period stream water was characterized by slightly, yet statistically not significantly higher mean fractions of young water (F_{yw} ~ 0.13) than in the pre-deforestation period (F_{yw} ~ 0.11). In spite of these limited effects on the overall F_{yw}, considerable changes were found for wet periods, during which post-deforestation fractions of young water increased to values F_{yw} ~ 0.40 for individual storms. Deforestation also caused a significantly increased sensitivity of young water fractions to discharge under wet conditions from dF_{yw}/dQ = 0.25 to 0.43.

Overall, this study provides quantitative evidence that deforestation resulted in changes of vegetation-accessible storage volumes $S_{U,max}$ and that these changes are not only responsible for changes in demonstrates that deforestation has not only the potential to affect the partitioning between drainage and evaporation as well as the vegetation-accessible storage volumes $S_{U,max}$, and thus the fundamental hydrological response characteristics of the Wüstebach catchments, but also for changes in catchment-scale tracer circulation dynamics. In particular for wet conditions, deforestation caused higher proportions of younger water to reach the stream, implying faster routing of stable isotopes and plausibly also solutes through the subsurface.

1 Introduction

Plant transpiration is, globally, the largest continental water flux (Jasechko, 2018). Notwithstanding considerable uncertainties (Coenders-Gerrits, 2014), its magnitude depends on the interplay between canopy water demand and subsurface water supply (Eagleson, 1982; Milly and Dunne, 1994; Donohue et al., 2007; Yang et al., 2016; Jaramillo et al., 2018; Mianabadi et al., 2019). The latter is regulated by water volumes that are within the reach of roots and can be taken up by plants. Many plant species across humid climate zones develop only rather shallow root systems (Schenk, 2005) that do not directly tap the groundwater (Fan et al., 2017). In such terrestrial hydrological systems that are dominated by shallow-rooting vegetation, the water filled pore volume between field capacity and permanent wilting point that is *within the reach of active roots* becomes a core property of many terrestrial hydrological systems (Rodriguez-Iturbe et al., 2007). This maximum vegetation-accessible water storage volume in the unsaturated root-zone of soils, hereafter referred to as vegetation-accessible water storage capacity $S_{U,max}$ [mm], constitutes a major partitioning point of water fluxes. Ias it regulates the temporally varying ratio between drainage, such as groundwater recharge or shallow lateral flow, on the one hand and transpiration fluxes on the other hand (Savenije and Hrachowitz, 2017), which can in turn generate considerable feedback effects on downwind precipitation and

2

drought generation (e.g. Seneviratne et al., 2013; Ellison et al., 2017; Teuling, 2018; Wang-Erlandsson et al., 2018; Wehrli et al., 2019).

Traditionally, $S_{U,max}$ is determined as the product of root-depths or root-distributions and pore water content between field capacity and permanent wilting point. Although correct in principle, this method has several weaknesses for applications at the catchment-scale as much of the required data are typically not available at sufficient levels of detail. While soil maps and the associated soil water retention curves have become globally available at resolutions < 1km (Arrouays et al., 2017; Hengl et al., 2017), they are characterized by considerable uncertainties. Similarly, direct and detailed observations of root-systems are very scarce. They are, globally, limited to a few thousand individual plants only (e.g. Schenk and Jackson, 2002; Fan et al., 2017) and many of the observations are based on biomass extrapolations after excavating only the first meter of soil or less (Schenk and Jackson, 2003). Consequently, soil and root data largely remain inaccurate snapshots in space. As such, they are likely to be inadequate reflections of the spatial heterogeneity of soils and roots. In addition, these available data are also mostly snapshots in time and therefore disregard the adaptive behaviour of plant communities, whose compositions, and thus characteristics, at ecosystem level continuously evolve over multiple scales in space and time in response to changes in ambient conditions (e.g. Laio et al., 2006; Brunner et al., 2015; Tron et al., 2015).

There is increasing evidence that vegetation does not only actively adapt to its (changing) environment, but that it does so in an way that allows the most efficient use of available energy and resources (e.g. Guswa, 2008; Schymanski et al., 2008). The vegetation, i.e. a collective of individual different plants within an area of interest that is present at any given moment at any given location has survived past conditions. This in itself is a manifestation of the successful adaption of individual plants to their environment in the past. They have optimally allocated resources to balance sub- and above-surface growth to simultaneously meet water, nutrient and light requirements. This implies that these plants developed root-systems that, amongst other factors, ensure continuous access to *sufficient* water – but not more – to bridge dry periods. An individual plant that is not adapted to meet its water and nutrient requirements through its root-system as well as its light requirements through its foliage system in competition with other plants will disappear and be replaced by a better adapted plant. The root-system of vegetation at ecosystem level, and the associated vegetation-accessible water storage capacity $S_{U,max}$, is therefore at a dynamic equilibrium with and responding to the ever changing conditions of its environment. Similarly, any type of direct human interference with vegetation, such as deforestation, has an impact on transpiration water demand, the extent and structure of active root-systems and consequently on $S_{U,max}$ (Nijzink et al., 2016a).

For a meaningful quantification of $S_{U,max}$ at larger scales, such as the catchment-scale, it is therefore necessary to adopt a Darwinian perspective (Harman and Troch, 2014) and to estimate effective values of $S_{U,max}$, reflecting the collective and adaptive behaviour of all individual plants within a catchment. Results from many previous studies suggest, broadly speaking, three methods to do so. The first is the use of inverse approaches that treat $S_{U,max}$ as model calibration parameter (Fenicia et al., 2008; Speich et al., 2018; Bouaziz et al., 2020; Knighton et al., 2020). Alternatively, the second type of methods is based on optimality principles that maximize variables such as net primary production or carbon gain (Kleidon, 2004; Guswa, 2008; Hwang et al., 2009; Yang, et al., 2016; Speich et al., 2018, 2020), nitrogen uptake (McMurtrie et al., 2012) or transpiration

3

rates (Collins and Bras, 2007; Sivandran and Bras, 2012). Lastly, $S_{U,max}$ and its evolution over time can be directly estimated through magnitudes of annual water deficits as determined from observed water balance data (Gentine et al., 2012; Donohue et al., 2012; Gao et al., 2014; DeBoer-Euser et al., 2016).

For transpiration, shallow-rooting plants extract pore water of unsaturated soils that is held against gravity, i.e. between field capacity and permanent wilting point, and within the reach of roots. Significant vertical or lateral drainage only occurs at water contents above field capacity. ~~Transpiration~~ By extracting soil water below that, transpiration therefore ~~effectively~~ generates a root-zone water storage reservoir between field capacity and permanent wilting point that is characterized by a storage capacity $S_{U,max}$, i.e. a *maximum* vegetation-accessible storage volume, and that is at any given moment filled with a specific water volume $S_U(t)$, depending on the past sequence of water inflow and release.

Storage reservoirs~~volumes~~ as $S_{U,max}$, or others such as groundwater bodies, are key for hydrological functioning (Sprenger et al., 2019b) as they provide a buffer against hydrological extremes, such as floods and droughts. With larger storage reservoirs, the hydrological memory of a system can increase~~s~~ as more water can be stored and held over longer periods of time (e.g. Hrachowitz et al., 2015; Sprenger et al., 2019b). This also implies that while increased actual volumes of water stored in and thus the degree of filling of storage reservoirs, e.g. $S_U(t)$, can reduce water ages (Harman, 2015), increased sizes of storage reservoirs, e.g. $S_{U,max}$, can increase water ages, thereby both controlling catchment ~~residence time distributions (RTD) and~~ travel time distributions (TTD; Soulsby et al., 2010). As fundamental descriptors of hydrological functioning ~~RTDs and~~ TTDs describe the age structure of water held in and released from catchments (Birkel et al., 2015; Rinaldo et al., 2015), which is critical for regulating solute transport and thus nutrient and contaminant dynamics (Hrachowitz et al., 2016).

However, neither the effects of land cover change (Blöschl et al., 2019) nor the individual roles of different storage compartments in terrestrial hydrological systems are well understood (McDonnell et al., 2010; Penna et al., 2018, 2020). This is mostly a consequence of the lack of suitable observational technology to directly observe their respective volumes at larger scales. It remains therefore also unclear how deforestation affects $S_{U,max}$ (e.g. due to a less developed and complex rooting system for subsequent younger vegetation) and how changes in $S_{U,max}$ may propagate to affect both, the partitioning of water fluxes as well as the age structure of water stored in and released from catchments as described by residence and travel time distributions.

For the study site of this paper, the Wüstebach experimental catchment (Germany), a previous study quantified the effects of deforestation on the partitioning of water fluxes (Wiekenkamp et al., 2016). It was found that forest removal significantly reduced evaporative fluxes. This led to more persistent higher soil moisture levels and eventually to increases in stream flow. Similarly, in the same catchment, Wiekenkamp et al. (2020) found evidence for increased post-deforestation occurrence of preferential flows while Stockinger et al. (2019) reported minor post-deforestation reductions in travel times.

To establish a quantitative mechanistic link between these studies we here aim to trace back and attribute the above reported post-deforestation changes in the hydrological response of the Wüstebach to deforestation-induced changes in (subsurface) system properties. The overall objective of this study is thus to analyse whether changes in these (subsurface) properties can explain *why* deforestation affects water flux partitioning and reduces travel times in the Wüstebach in an attempt to improve

4

our quantitative understanding of critical zone processes (Brooks et al., 2015). ~~The objective of this study in the Wüstebach experimental catchment (Germany) is thus to analyse to which extent post-deforestation changes in the water balance can be attributed to changes in catchment-scale effective $S_{U,max}$ and to quantify the associated consequences on RTDs, TTDs and~~
135 ~~young water fractions F_{yw}.~~ Specifically we test the hypotheses that (1) ~~deforestation affects water storage dynamics and the partitioning of water fluxes into transpiration and drainage, (2) the~~ post-deforestation changes in water storage dynamics and partitioning of water fluxes are largely a direct consequence of a reduction of the catchment-scale effective vegetation-accessible water storage capacity in the unsaturated root-zone ($S_{U,max}$) after deforestation and that (2~~3~~) the deforestation-induced reduction of $S_{U,max}$ affects the shape of travel time distributions and results in shifts towards higher fractions of young
140 water in the stream.

2 Study site

The experimental Wüstebach headwater catchment (0.39 km^2; Fig. 1a) is part of the Lower Rhine/Eifel Observatory of the Terrestrial Environmental Observatories network (TERENO; Bogena et al., 2018) located in the Eifel National Park in
145 Germany (50°30'16"N, 06°20'00"E). The catchment is characterized by a humid, temperate climate with warm summers, mild winters and a mean annual temperature of around 7° C (Zacharias et al., 2011). Mean annual precipitation is about 1200 mm yr^{-1} and mean annual runoff about 700 mm yr^{-1} (Fig. 2). Although most of the precipitation occurs in the winter months, the fraction that falls as snow is typically less than 10 % of the annual precipitation and snow cover is present for no more than 3-4 weeks per year.
150 The catchment is drained by a perennial 2nd-order stream and extends from 595 to 630 m asl. The landscape is characterized by the gentle slopes of the surrounding hills and a flatter riparian area close to the stream, covering approximately 10 % of the catchment (Fig. 1a). The underlying bedrock is largely Devonian shales with sandstone inclusions (Richter, 2008) covered by periglacial layers (Borchardt, 2012). While cambisols dominate the hillslopes, gleysols and histosols characterize much of the riparian area (Bogena et al., 2015). The average soil depth in the catchment reaches about 1.6 m with a maximum of 2 m (Graf
155 et al., 2014). In 1946, after the Second World War, the catchment was homogeneously and completely afforested (Fig. 1) with Sitka spruce (*Picea sitchensis*) and Norway spruce (*Picea abies*; Etmann, 2009). The maximum observed rooting depth of these spruce trees in the catchment is 50 cm and no roots were observed below this depth. In the course of the development of the area into a national park approximately 21 % of the catchment, including the entire riparian zone, were deforested in September 2013 and kept largely vegetation free since (Wiekenkamp et al., 2016; Fig. 1).

160

3 Data

3.1 Hydro-meteorological data

Daily hydro-meteorological data were available for the period 01/10/2009 – 30/09/2016 (Fig. 2). Precipitation P [mm d^{-1}] and mean daily temperature T [^{o}C] were available from the Monschau-Kalterherberg meteorological station operated by the German Weather Service (Deutscher Wetterdienst DWD station 3339), located 9 km northwest of the Wüstebach catchment. Stream discharge Q [mm d^{-1}] at the outlet of the Wüstebach was observed with a V-notch weir for low flow measurements and a Parshall flume for medium to high flows (Bogena et al., 2015). Daily potential evaporation E_P [mm d^{-1}] was estimated using the Penman-Monteith equation.

3.2 Stable isotope data

Regular weekly δ^{18}O data from bulk precipitation samples collected in a cooled wet deposition gauge at the meteorological station Schleiden-Schöneseiffen (Meteomedia station) 3 km northeast of the catchment, were available for the period 01/10/2010 – 24/09/2012. After that, precipitation was sampled at half-daily intervals until 30/09/2016 using an automatic, cooled sampler (Eigenbrodt GmbH, Germany). The half-daily samples were precipitation volume-weighed to daily sampling intervals (Stockinger et al., 2016, 2017). Weekly stream water grab samples for stable water isotope analysis were taken at the outlet of the Wüstebach catchment in the 01/10/2010 – 30/09/2016 period (Fig. 3a).

Isotope analysis was carried out using laser-based cavity ringdown spectrometers (L2120-i/L2130-i, Picarro Inc.). Internal standards calibrated against VSMOW, Greenland Ice Sheet Precipitation (GISP) and Standard Light Antarctic Precipitation (SLAP2) were used for calibration and to ensure long-term stability of analyses (Brand et al., 2014). The long-term precision of the analytical system was ≤ 0.1 ‰ for δ^{18}O.

4 Methods

To quantify effects of deforestation on $S_{U,max}$ and, due to the role of $S_{U,max}$ as a mixing volume~~as a consequence of that,~~ also on the age structure of water as described by TTDs~~, RTDs~~ and the associated young water fractions F_{yw}, the following stepwise experiment was designed: (1) quantify changes in the partitioning of annual water fluxes between the pre- and the post-deforestation periods based on observed water balance data; (2) estimate the effect of these changes on the magnitudes of pre- and post-deforestation $S_{U,max}$, respectively, using the same data; (3) calibrate a hydrological model to simultaneously reproduce stream flow and stream δ^{18}O dynamics for the pre-deforestation period; (4) use the calibrated parameter sets to run the model in the post-deforestation period and evaluate the model's post-deforestation performance without further calibration; (5) re-calibrate the model for the post-deforestation period and evaluate if changes in calibrated $S_{U,max}$ (and other parameters) are plausible and reflect changes in $S_{U,max}$ directly estimated from water balance data in step (2); and finally (6) use the calibrated

pre- and post-deforestation parameter sets, respectively, to track modelled water fluxes through the system and quantify changes in TTDs, ~~RTDs~~ and F_{yw} between the pre- and the post-deforestation periods.

4.1 Water balance-based estimation of $S_{U,max}$

195   To survive, plants need continuous access to water to satisfy canopy water demand. The root-systems of vegetation are therefore adapted to provide access to water volumes that correspond to annual water deficits that result from the combination of (1) the phase lag between and (2) the difference in the respective magnitudes of seasonal precipitation and solar radiation signals (Donohue et al., 2012; Gentine et al., 2012; Gao et al., 2014). On a daily basis, these water deficits $S_{D,j}(t)$ can be estimated as the cumulative sum of daily effective precipitation P_E [mm d^{-1}] minus transpiration E_T [mm d^{-1}]. The maximum

200   deficit $S_{D,j}$ for a specific year j is then equivalent to the water volume that was accessible to vegetation through its root system over that period (deBoer-Euser et al., 2016; Nijzink et al., 2016a):

$$S_{D,j}(t) = \begin{cases} \int_{t_0}^{t}\big(P_E(t) - E_T(t)\big)dt\,, & if\ S_{D,j}(t) \leq 0 \\ 0, & if\ S_{D,j}(t) > 0 \end{cases}$$

(Eq. 1)

205

$$S_{D,j} = max\big(\big|S_{D,j}(t)\big|\big)$$

(Eq. 2)

where t is the time step [d], and t_0 is the last preceding time step for which the storage deficit $S_{D,j}(t) = 0$. As an approximation,

210   Equation 1 implies that if $S_{D,j}(t) = 0$, the water content in the root-accessible pore space at day t is at field capacity and cannot hold additional water. If water supply then exceeds canopy water demand on that day, i.e. $P_E(t) - E_T(t) > 0$, this water surplus is drained from the root zone, e.g. to recharge groundwater or directly to the stream, and cannot be used for transpiration. Daily effective precipitation P_E, i.e. precipitation that actually reaches the soil, was estimated on basis of the water balance of a canopy interception storage (Nijzink et al., 2016a):

215

$$\frac{dS_I(t)}{dt} = P(t) - E_I(t) - P_E(t)$$

(Eq. 3)

Where E_I [mm d^{-1}] is daily interception evaporation and S_I [mm] the canopy interception storage. For each time step, E_I can then be computed as:

220
$$E_I(t) = \begin{cases} E_p(t), & if\ E_p(t)dt < S_I(t) \\ \dfrac{S_I(t)}{dt}, & if\ E_P(t)dt \geq S_I(t) \end{cases}$$

7

$$(Eq. 4)$$

This then further allows to estimate P_E according to:

$$P_E(t) = \begin{cases} 0, & if\ S_I(t) < I_{max} \\ \dfrac{S_I(t) - I_{max}}{dt}, & if\ S_I(t) \geq I_{max} \end{cases}$$

225
$$(Eq. 5)$$

where I_{max} [mm] is the canopy interception capacity. In the absence of more detailed information P_E was estimated with a range of different interception capacities, i.e. I_{max} = 0, 1, 2, 3, and 4 mm, in a sensitivity analysis approach.

Note that the catchment average P_E after deforestation was estimated as the areal weighted mean of P_E in the deforested area (21% of catchment area) computed with an assumed I_{max} = 0 mm and P_E from the remaining area computed based on the above

230 range of I_{max} between 0 and 4 mm. In a next step, assuming negligible groundwater imports or exports (cf. Bouaziz et al., 2018), data errors and storage changes, long-term mean transpiration $\overline{E_T}$ was estimated according to the water balance:

$$\overline{E_T} = \overline{P_E} - \overline{Q}$$

$$(Eq. 6)$$

235 Where $\overline{P_E}$ [mm d^{-1}] is the long-term mean effective precipitation and $\overline{Q}$ [mm d^{-1}] is the long-term mean observed stream discharge. Daily transpiration E_T [mm d^{-1}] for use in Eq. (1) is then estimated by scaling the long-term mean transpiration to the signal of daily potential evaporation to approximate the seasonal fluctuation of energy input (Bouaziz et al., 2020):

$$E_T(t) = \left(E_P(t) - E_I(t)\right)\frac{\overline{E_T}}{\overline{E_P} - \overline{E_I}}$$

240
$$(Eq. 7)$$

A range of previous studies provided evidence that mature forests develop root-systems that allow access to sufficiently large pore water storage volumes $S_{U,max}$ to bridge droughts with return periods $T_R \sim 20$ years (Gao et al., 2014; deBoer-Euser et al., 2016; Nijzink et al., 2016a; Wang-Erlandsson et al., 2016). The maximum annual water deficits $S_{D,j}$ (Eq. 2) for all j years in

245 the pre-deforestation study period were therefore used to fit a Gumbel extreme value distribution (Gumbel, 1941). This subsequently allowed the estimation of a water deficit with a 20-year return period, which is for this study defined as vegetation-accessible water storage $S_{U,max}$ so that $S_{U,max} = S_{D,20yr}$.

Note that due to the limited length of the data series the $S_{U,max}$ estimates are rather uncertain and need to be understood as merely indicative approximations. This is in particular true for the post-deforestation period, where attempts to explicitly link

250 $S_{U,max}$ to a specific return period are subject to additional uncertainty: as the catchment was not reforested and natural recovery of vegetation is negligible (see aerial images in Figure 1), it is not implausible to assume that the development of the root-

8

system after the disturbance is far from equilibrium and likely to be actively evolving over time. Also note that although E_T is, for brevity, referred to as transpiration throughout this manuscript, it also contains soil evaporation. However, no explicit and quantitative distinction could be made between these two fluxes with the available data. A further critical assumption of the above method required that roots do not tap the groundwater and that water for transpiration is exclusively extracted from the unsaturated soil. In contrast to other landscapes (Fan et al., 2017; Roebroek et al., 2020), it is likely that this assumption largely holds in the Wüstebach as throughout the catchment the groundwater levels, also in the riparian zone, remains largely below a depth of 50 cm during the relatively dry growing season (Bogena et al., 2015) when storage deficits S_D typically accumulate (~ May to October) and no roots have so far been observed for the dominant *picea* species below that depth in the Wüstebach catchment. This is also broadly consistent with the results of Evaristo and McDonnell (2017), who show rather limited groundwater use by *picea* species.

4.2 Model architecture

A semi-distributed, process-based catchment model, iteratively customized and tested within the previously developed DYNAMITE modular modelling framework (Hrachowitz et al., 2014; Fovet et al., 2015), was adapted with additional, hydrologically passive storage volumes to allow for simultaneous representation of water fluxes and tracer transport (Hrachowitz et al., 2013) based on the general concept of storage-age selection functions (SAS; Rinaldo et al., 2015). This model type was chosen over simpler, more data-based methods (e.g. McGuire and McDonnell, 2006; Kirchner, 2016) as it did not only allow a simultaneous representation of water and tracer fluxes but also allowed to attribute observed pattern to specific process hypotheses and the associated model parameters that represent (subsurface) system properties, thereby providing potential quantitative mechanistic explanations of why deforestation affects the hydrology in the Wüstebach. As an intermediate model type between purely data-driven (e.g. Kirchner, 2016) and spatially explicit physically-based models (e.g. Maxwell et al., 2016), it requires assumptions on underlying processes and effective parameters and does not allow a detailed spatial analysis. Yet this model type provides the possibility to test these process hypotheses at the scale of the semi-distributed model units thereby integrating and accounting for the natural heterogeneity of system properties across the model domain (Hrachowitz and Clark, 2017).

4.2.1 Hydrological model

The model domain of the Wüstebach catchment was spatially discretized into two functionally distinct response units, i.e. hillslopes and riparian areas. These are represented in the model as two parallel suites of storage components, linked by a common groundwater body as shown in Figure 4 (e.g. Euser et al., 2015; Nijzink et al., 2016b). According to elevation data and distribution of soil types (Fig.1), 90% of the catchment area was classified as hillslope and the remaining 10% as riparian area. Below a threshold temperature T_T [ºC] precipitation P [mm d^{-1}] accumulates as snow P_S [mm d^{-1}] in S_{Snow} [mm]. Above that temperature precipitation is falling as rain P_R [mm d^{-1}] and snow melt P_M [mm d^{-1}] is released from S_{Snow} according to a melt factor F_M [mm d^{-1} ºC^{-1}] using a simple degree-day method (e.g. Arsenault et al., 2015; Ala-aho et al., 2017; Gao et al.,

9

2017). The total liquid water input $P_R + P_M$ [mm d^{-1}] entering the hillslope is routed through the canopy interception storage $S_{I,H}$ [mm]. Water that is not evaporated as $E_{I,H}$ [mm d^{-1}] enters the unsaturated root-zone $S_{U,H}$ [mm], whose storage capacity is defined by the calibration parameter $S_{U,max,H}$ [mm]. Water can be released from $S_{U,H}$ as combined root-zone transpiration and soil evaporation flux $E_{T,H}$ [mm d^{-1}] or eventually recharge the groundwater $S_{S,a}$ [mm] over a fast, preferential recharge pathway as $R_{F,H}$ [mm d^{-1}] and a slower percolation flux $R_{S,H}$ [mm d^{-1}]. Similarly, water entering the riparian zone, i.e. $P_R + P_M$ [mm d^{-1}], is routed through $S_{I,R}$ [mm]. Excess water $P_{E,R}$ [mm d^{-1}] that is not evaporated infiltrates into the unsaturated root-zone $S_{U,R}$ [mm], defined by calibration parameter $S_{U,max,R}$ [mm]. In addition, a fraction of the upwelling groundwater $R_{S,R}$ [mm d^{-1}] replenishes $S_{U,R}$ and thus, in addition to precipitation, sustains soil moisture levels in the riparian zone, while the remainder Q_S [mm d^{-1}] drains directly into the stream. While water stored in $S_{U,R}$ is available for transpiration (and soil evaporation) $E_{T,R}$ [mm d^{-1}], water that cannot be held is released as $R_{F,R}$ [mm d^{-1}] to a fast responding reservoir $S_{F,R}$ [mm] from where it ~~is~~ reaches the stream as Q_R [mm d^{-1}]. The relevant model equations can be found in Table 1.

4.2.2 Tracer transport model

The $\delta^{18}O$ composition of water fluxes and storages was tracked through the model using the storage age selection approach (SAS; Rinaldo et al., 2015), which allows a catchment-scale description of conservative transport based on time-variant travel time distributions. The method builds on the fact that a water volume S [mm] stored in any storage component can, at any moment t [d], consist of parcels of water of different age T [d]. The composition of ages in the stored volume at t depends on the history of water inflows and outflows. Consequently, it evolves over time as new inputs enter into and outflows are released from the storage component, whereby each inflow I [mm d^{-1}] and outflow volume O [mm d^{-1}] can have a different age composition. A convenient way to implement the SAS approach is the use of age-ranked storage $S_T(T,t)$ [mm], which represents, "at any time t the cumulative volumes of water in a storage component as ranked by their age T" (Benettin et al., 2017). Similarly, decomposing each inflow and outflow of a storage component into their respective cumulative, age-ranked volumes $I_T(T,t)$ and $O_T(T,t)$ [mm d^{-1}], respectively, then allows to update the age-ranked storage $S_T(T,t)$ at each time step according to the general water age balance (Botter et al., 2011; van der Velde et al., 2012; Benettin et al., 2015a, 2017; Harman, 2015):

$$\frac{\partial S_{T,j}(T,t)}{\partial t} + \frac{\partial S_{T,j}(T,t)}{\partial T} = \sum_{n=1}^{N} I_{T,n,j}(T,t) - \sum_{m=1}^{M} O_{T,m,j}(T,t)$$

(Eq.36)

where the term $\partial S_T/\partial T$ represents the aging of water in storage. Reflecting the slightly more abstract approach by Rodriguez and Klaus (2019) and similar to previous studies based on the functionally equivalent mixing coefficient approach (e.g. Fenicia et al., 2010; McMillan et al., 2012; Birkel and Soulsby, 2016; Hrachowitz et al., 2015), the water age balance is here individually formulated for each storage reservoir j (e.g. $S_{I,H}$, $S_{U,H}$, etc.), which each can have varying numbers N and M of

10

315   inflows I (e.g. P_R, P_M, $R_{S,H}$, etc.) and outflows O (e.g. P_M, $R_{S,H}$, Q_S, etc.), respectively (see Figure 4). It is assumed that the entire volume of a precipitation signal P(t) entering the system at t has an age T of zero so that the associated $I_{T,P,j}(T,t) = P_T(T,t) = P(t)$ for all T. As all other inflows to any following storage component in the system are outflows of storage components prior in the sequence (see Figure 4), the corresponding $I_{T,n,j}(T,t)$ entering a storage component are identical to the $O_{T,m,j}(T,t)$ released from the storage component above.

320   Each age-ranked outflow $O_{T,m,j}(T,t)$ of a specific storage component j depends on the outflow volume $O_{m,j}(t)$ along this outflow pathway and the cumulative age distribution $P_{o,m,j}(T,t)$ of that outflow:

$$O_{T,m,j}(T,t) = O_{m,j}(t)P_{O,m,j}(T,t)$$

325   (Eq.37)

The outflow volume $O_{m,j}(t)$ is estimated via the hydrological model (see Section 4.2.1; Figure 4) and thus assumed to be known. In contrast, the cumulative age-distribution $P_{o,m,j}(T,t)$ can in general not be directly parametrized, as it depends on the temporally varying age distribution of water in the storage component j represented by $S_{T,j}(T,t)$ and thus on the history of past inflows and outflows (Botter et al., 2011; Harman, 2015). Instead, it is possible to define a SAS function $\omega_{o,m,j}$ (or $\Omega_{o,m,j}$ in its

330   cumulative form) for each outflow m from each storage component j that describes how outflow is sampled (or selected) from the temporally varying water volumes of different age present in the age-ranked storage $S_{T,j}(T,t)$ at any time t:

$$P_{O,m,j}(T,t) = \Omega_{O,m,j}\big(S_{T,j}(T,t),t\big)$$

(Eq.38)

335   From the cumulative age-distribution $P_{o,m,j}(T,t)$ the associated probability density function, which represents the outflow age distribution $p_{o,m,j}(T,t)$, frequently also referred to as backward travel time distribution of that outflow (TTD; e.g. Benettin et al., 2015a; Wilusz et al., 2017), can be obtained according to:

$$p_{o,m,j}(T,t) = \varpi_{O,m,j}\big(S_{T,j}(T,t),t\big)\frac{\partial S_{T,j}}{\partial T}$$

(Eq.39)

340   Note that conservation of mass requires that any SAS function $\omega_{O,m,j}$ integrates to the total storage volume $S_j(t)$ present in j at any time t. To avoid the resulting need for rescaling $\omega_{O,m,j}$ at each time step, it is helpful to normalize the age-ranked storage to $S_{T,norm,j}(T,t) = S_{T,j}(T,t)/S_j(t)$ so that it remains bounded to the interval [0,1] and defines a residence time distribution (RTD). For this study beta distributions, which are conveniently bound between the limits [0,1] and defined by two shape parameters α and β, were used as SAS functions $\omega_{o,m,j}$ to sample water of different age for outflows from storage components. The

345   parameters β were fixed at a value of 1 for all SAS functions $\omega_{o,m,j}$ used here. However, there is substantial evidence for preferential flow through macropores in the shallow subsurface (e.g. Weiler and Naef, 2003; Zehe et al., 2006, 2007; Weiler and McDonnell, 2007; Beven, 2010; Beven and Germann, 2013; Klaus et al., 2013; Angermann et al., 2017; Loritz et al.,

11

2017). Such preferential flow can, with increasing wetness, increasingly bypass water volumes stored in small pores with little exchange (Sprenger et al., 2016, 2018, 2019a; Cain et al., 2019; Evaristo et al., 2019; Knighton et al., 2019). This then leads to an increasing preferential release of younger water as the system becomes wetter (Brooks et al., 2010). To mimic this, the shape parameters α of the preferential fluxes $R_{F,H}$ and $R_{F,R}$ released from the two unsaturated root-zone storage components S_j = $S_{U,H}$ and $S_{U,R}$ (Figure 4), were allowed to vary as a function of the water volumes stored in $S_{U,H}$ and $S_{U,R}$, respectively (Hrachowitz et al., 2013; van der Velde et al., 2015):

$$\alpha_{m,j}(t) = 1 - \left(\frac{S_j(t)}{S_{U,max,j}} (1 - \alpha_0) \right)$$

(Eq.40)

Where α_0 is a calibration parameter representing a lower bound so that $\alpha_{m,j}(t)$ can vary between α_0 and 1. A value of $\alpha_{m,j} = 1$ indicates complete mixing in dry conditions. Any value below that entails incomplete mixing and thus increases the preference towards releasing younger water in wet conditions (Benettin et al., 2017). Although there is evidence for the presence of preferential flow in other components of the system, such as in the groundwater (e.g. Berkowitz and Zehe, 2020), initial model testing suggested that the inclusion of the additional calibration parameters is not warranted by the available data. For simplicity and following the principle of model parsimony we assumed complete mixing for all other outflows from all other storage components (Figure 4; cf. Fenicia et al., 2010; Kuppel et al., 2018a; Rodriguez et al., 2018). Parameter α was therefore fixed to value of 1 for these SAS functions.

The $\delta^{18}O$ precipitation input signals are damped to the level of fluctuation observed in the stream by subsurface storage volumes that remain to some extent hydrologically passive (e.g. Birkel et al., 2011b). While the hydrologically active storage volumes are represented by the individual storage components of the model (Figure 4; Equations 8-14), an additional hydrologically passive storage volume $S_{S,p}$ [mm] was added as a calibration parameter to the active groundwater storage $S_{S,a}$. (Zuber, 1986; Hrachowitz et al., 2015, 2016), so that $S_{S,tot} = S_{S,a} + S_{S,p}$ (Figure 4). While $dS_{S,p}/dt = 0$, the age-ranked groundwater storage was computed as $S_{T,Ss,tot}$ and the outflows from the groundwater component consequently thus sampled from the entire storage volume $S_{S,tot}$, thereby representing the combined contributions from $S_{S,a}$ and $S_{S,p}$ to the age structure of the outflow Q_S according to Eq. 39.

Each individual volume with different age in $I_{T,n,j}(T,t)$ and, as a consequence, also in $S_{T,j}(T,t)$ is also characterized by a different tracer concentration $C_{I,n,j}(I_{T,n,j}(T,t),t)$ and $C_{S,j}(S_{T,j}(T,t),t)$, respectively. For a conservative tracer such as $\delta^{18}O$ that is not significantly affected by decay, evapoconcentration, retention or any other biogeochemical transformation (e.g. Bertuzzo et al., 2013; Benettin et al., 2015b; Hrachowitz et al., 2015) the concentration $C_{O,m,j}(t)$ in any outflow at any time t can then be obtained from:

12

$$C_{O,m,j}(t) = \int_0^{S_j} C_{S,j}\big(S_{T,j}(T,t),t\big)\varpi_{O,m,j}\big(S_{T,j}(T,t),t\big)dS_T$$

(Eq.41)

In contrast to other regions (e.g. Soulsby et al., 2017; Kuppel et al., 2018a), isotopic fractionation in the Wüstebach was previously observed to mostly affect canopy interception evaporation (Stockinger et al., 2015). Fractionation was therefore here accounted for in the two interception storage components ($S_{I,H}$, $S_{I,R}$). Following the approach described by Birkel et al. (2014), the respective δ^{18}O compositions $C_{S,S_{I,H}}$ and $C_{S,S_{I,R}}$ were accordingly updated for every time step.

385 Due to data availability, age tracking was here limited to 4 years in the pre- and 3 years in the post-deforestation period. For age beyond that it can only be said that water is older than these 4 and 3 years, respectively. The ~~RTDs and~~ TTDs reported hereafter are thus truncated at these ages. The model generates TTDs for all fluxes and storage components (Figure 4) for each time step. As a summary metric, we will here use the fraction of young water F_{yw} as robust descriptor of the left tail of TTDs. Following the definition of Kirchner (2016), F_{yw} is here the fraction of water that is younger than 3 months, which can be extracted directly from any TTD generated by the model. Note, we here only analyse water ages in stream flow as these are the only ones that are directly constrained by available data, while for all other model components, such as transpiration E_T, such direct data support was not available, and the resulting age estimates may thus be characterized by considerable additional uncertainty.

4.3 Model calibration and post-calibration evaluation

395 The model was run with a daily time step and has a total of 14 free calibration parameters, which were calibrated for the model to simultaneously reproduce flow and δ^{18}O dynamics in the stream. The uniform prior parameter distributions (Table 2) were sampled using a Monte Carlo approach with 10^6 realizations. To limit equifinality (Beven, 2006) and to ensure robust posterior parameter distributions for a meaningful process representation (e.g. Kuppel et al., 2018b), an extensive multi-objective calibration strategy was applied. Briefly, this was done using a total of 14 performance metrics that describe the model's skill to reproduce different signatures associated to streamflow (E_Q) and δ^{18}O dynamics ($E_{\delta^{18}O}$) as shown in Table 3.

Combining these metrics into two equally weighted classes describing stream and δ^{18}O dynamics, respectively, solutions with balanced overall model performances were then obtained using the mean Euclidean Distance D_E [-] from the "perfect" model (i.e. $D_E = 1$; Hrachowitz et al., 2014; Hulsman et al., 2020):

405
$$D_E = 1 - \sqrt{\frac{1}{2}\left(\frac{\sum_{n=1}^{N}\big(1 - E_{Q,n}\big)^2}{N} + \frac{\sum_{m=1}^{M}\big(1 - E_{\delta^{18}O,m}\big)^2}{M}\right)}$$

(Eq.42)

Where N is the number of different performance metrics describing streamflow and M the number of different performance metrics for δ^{18}O. To construct the posterior parameter distributions and the corresponding model uncertainty intervals, the

13

retained parameter sets where then weighted according to a likelihood measure $L = D_E^p$ (cf. Freer et al., 1996), where the
410 exponent p was set to a value of 2 to emphasize models with good overall calibration performance.

In a first step, the model was calibrated for the pre-deforestation period 01/10/2009 – 31/08/2013. Note that due to a lack of regular and weekly $\delta^{18}O$ precipitation data before 01/10/2010, the performance metric $E_{\delta^{18}O}$ describing the $\delta^{18}O$ dynamics was computed from that date onwards only. The feasible parameter sets were then used to test the model without further calibration in the post-deforestation period. In a second step, the model was re-calibrated for the 01/09/2013 – 30/09/2016
415 post-deforestation period and the changes in the resulting model performance and posterior distributions compared to those from the pre-deforestation calibration. The estimation of the effects of deforestation on ~~RTDs and~~ TTDs is based on model parameter sets obtained from calibration in the pre-deforestation and post-deforestation periods, respectively.

5 Results and Discussion

420 ### 5.1 Deforestation effects on the hydrological system

Initial analysis of water balance data suggests that the hydro-meteorological conditions as expressed by the aridity index $I_A = \overline{E_P}/\overline{P}$, do not show significant differences between the pre-deforestation ($I_A = 0.50 \pm 0.02$) and the post-deforestation periods ($I_A = 0.51 \pm 0.03$), respectively (Figure 5a). However, and in spite of these comparable climatic conditions, the results~~data~~ show a shift in the partitioning of water fluxes between runoff Q and actual evaporation E_A (note that $E_A = E_I + E_T$). While the
425 fraction of precipitation that was released into the atmosphere as vapour was reduced ($\overline{E_A}/\overline{P}$; Figure 5a), the mean runoff ratio ($C_R = 1 - \overline{E_A}/\overline{P}$) increased correspondingly from $C_R = 0.55 \pm 0.04$ to $C_R = 0.68 \pm 0.03$ after deforestation of 21 % of the catchment with p = 0.049 based on a Wilcoxon rank sum test. These results correspond well with the findings of an earlier study in the Wüstebach, based on a shorter study period (2011 – 2015; Wiekenkamp et al., 2016), which estimated an increase of C_R from ~ 0.58 to ~ 0.66 during that period using eddy-covariance measurements. In absolute terms this entails that,
430 notwithstanding rather stable mean annual precipitation $P = 1269 \pm 24$ mm yr^{-1} and potential evaporation $E_P = 632 \pm 9$ mm yr^{-1} over the entire study period, the annual actual evaporation E_A decreased from 576 ± 11 mm yr^{-1} to 401 ± 6 mm yr^{-1} whereas annual runoff Q increased by ~ 25 % from 694 ± 47 mm yr^{-1} to 870 ± 63 mm yr^{-1}.

The overall pattern found here also broadly reflect the effects of land cover/use change in many different environments (Creed et al., 2014; Jaramillo and Destouni, 2014; Renner et al., 2014, van der Velde et al., 2014; Moran-Tejada et al., 2015; Nijzink
435 et al., 2016; Zhang et al., 2017; Jaramillo et al., 2018). The vast majority of these studies suggest that forest removal leads to an increase in the runoff ratio C_R at the cost of reduced evaporation E_A, although the magnitudes of these changes do substantially vary between individual catchments and studies, which is consistent with our physical understanding of the importance of forest for transpiration in hydrological systems. Under the assumption that reduction of E_A is largely a direct consequence of forest removal in the Wüstebach, a plausible hypothesis to directly attribute this shift in water partitioning

14

440   from E_A to Q to a physical process can be formulated as follows: the roots of harvested trees stopped extracting water for transpiration from the subsurface. In addition, the decrease of turbulent exchange of vapour with depth effectively limits soil evaporation to the first few centimetres of the soil (e.g. Brutsaert, 2014). Thus, the felling of trees led to a situation where under comparable atmospheric water demand E_P, water volumes held at depths below that and previously within the reach of active roots became largely unavailable for transpiration and evaporation after deforestation. This implies that the water

445   volumes accessible to satisfy atmospheric water demand, i.e. $S_{U,max}$ and I_{max}, are drastically reduced.

In our study, this becomes evident when comparing the catchment-scale maximum annual storage deficits $S_{D,j}$ (Eq. 2) of the pre- and post-deforestation periods, respectively, which are indicative of differences in soil depths affected by E_A in the two periods. In spite of similar climatic conditions, the mean annual maximum storage deficit in the pre-deforestation period is significantly higher (p = 0.047) than in the post-deforestation period. In the pre-deforestation period values between 105 ± 23

450   mm for $I_{max} = 0$ mm and 95 ± 21 mm for $I_{max} = 4$ mm, respectively, were found (Figure 5b). Whereas in the post-deforestation period the mean storage deficit only reached between 49 ± 10 mm and 33 ± 7 mm for the same values of I_{max} (Figure 5b). Note that in both periods, $S_{D,j}$ is relatively insensitive to the magnitude of I_{max} (cf. Gerrits et al., 2009). From the above maximum annual storage deficits $S_{D,j}$, the corresponding catchment-scale vegetation-accessible water storage capacity, assuming vegetation adaptation to dry conditions with 20-year return periods (see Section 4.1), was estimated at values of $S_{U,max} = 225$

455   ± 62 mm for the pre-deforestation ($R^2 = 0.91$, p = 0.04; Figure 5c) and $S_{U,max} = 90 \pm 149$ mm for the post-deforestation period ($R^2 = 0.83$, p = 0.27; not shown). Directly reflecting reductions of E_A, these estimated reductions in storage deficits are consistent with observed post-deforestation increases in soil moisture (Wiekenkamp et al., 2016). Note, however, that in particular the estimates for the post-deforestation period are characterized by considerable uncertainty and therefore need to be understood as merely indicative as they are inferred from only 3 years of data, and a system that is likely to be far from

460   equilibrium, because the deforested part cannot have adapted yet (e.g. Nijzink et al., 2016; Teuling and Hoek van Dijke, 2020). These considerable uncertainties are also reflected in the surprisingly low post-deforestation $S_{U,max}$. Notwithstanding these limitations, the above results illustrate that here the reduction of transpiration due to deforestation is likely to go hand in hand with a considerably reduction of $S_{U,max}$ and thus the catchment-scale sub-surface pore volume between field capacity and permanent wilting point that is actively accessed by vegetation to satisfy the evaporative demand.

465   **5.2 Deforestation effects on the hydrological system**

5.2.1 Model calibration for pre-deforestation period

The model parameter sets retained as feasible after calibration in the 2009-2013 pre-deforestation period reproduce the general features of the hydrograph in that period rather well (Figures 2c,d), similar to a previous modelling study (Cornelissen et al., 2014). This is true for both, the timing and magnitudes of high flows, with an associated Nash-Sutcliffe Efficiency $E_{NS,Q} =$

470   0.79 for the best performing model in terms of D_E (Figure 6a) but also for low flows ($E_{NS,log(Q)} = 0.79$), with the exception of some overestimation in summer 2011. In addition, the model could also simultaneously mimic most other observed flow

signatures reasonably well (Figure 6a), in particular the flow duration curve ($E_{NS,FDC}$ = 0.89; Figure 6b), the peak distribution ($E_{NS,PD}$ = 0.91; Figure 6d), the auto correlation function ($E_{NS,AC}$ = 0.90; Figure 6f) and the runoff ratio ($E_{R,CR}$ = 0.97). Similarly, the model captures the substantial attenuation of the precipitation $\delta^{18}O$ variability, while at the same time largely preserving the limited but visible low-frequency temporal fluctuations in the stream $\delta^{18}O$ composition (Figures 3a,b). In comparison to the flow performance metrics the Nash-Sutcliffe Efficiency of the $\delta^{18}O$ composition for the best model is somewhat lower ($E_{NS,\delta18O}$ = 0.38; Figure 6a), which mostly results from the low variability of such a damped signal, where even very small absolute errors and a few scattered outliers can lead to very low Nash-Sutcliffe Efficiencies (cf. Hrachowitz et al., 2009).

The posterior distributions (Table 2, Figure 7) show that most model parameters are reasonably well identified. Individually calibrated for their respective landscape class, i.e. hillslope and riparian zone, $S_{U,max,H}$ = 246 mm (5/95th IQR: 233 – 309 mm) and $S_{U,max,R}$ = 234 mm (194 – 287 mm) showed similar optimal values and distributions (Figures 7a,b), reflecting the catchment-wide relatively homogenous forest cover in the pre-deforestation period (Figure 1). Remarkably, these values also come close to the water balance-derived catchment-scale estimates of $S_{U,max}$ = 225 ± 62 mm, as described in 5.1 (Figure 5c).

5.2.2 Application of pre-deforestation model to post-deforestation period

In a next step, the parameter sets obtained from the above calibration in the pre-deforestation period were used to run the model without further re-calibration in the post-deforestation period. This entails the implicit and clearly wrong assumption that the physical characteristics of the system remained unaffected by deforestation. The consequence of that can be seen in Figures 2c and 2d (red line). While the low flows remain well reproduced, the post-deforestation application of the model substantially and systematically underestimates high flows, partly by 50% or more, such as in November 2013 or August 2014. The inability of the model to reproduce post-deforestation high-flow dynamics of the system is also evident in the ~~partly much~~ lower model performance metrics associated with high flows (Figure 6a). Besides the time series of flow ($E_{NS,Q}$ = 0.63), notably the model's skill to capture the peak distribution ($E_{NS,PD}$ = 0.81; Figure 6e), the autocorrelation function ($E_{NS,AC}$ = 0.71; Figure 6g) and the runoff ratio ($E_{R,CR}$ = 0.73) were negatively affected. In contrast to the pre-deforestation period, the modelled runoff ratio C_R = 0.52 (0.48 – 0.67) in the post-deforestation period considerably underestimates the observed C_R = 0.68 ± 0.03 (Figure 5a). The above implies that the model also overestimates post-deforestation evaporative fluxes E_A. Therefore, it can, without re-calibration, not deal with the observed changes in the partitioning between drainage and evaporative fluxes (Figure 5a). A likely explanation for the pattern produced by the model is that, in contrast to the real world, no reduction in E_A due to the reduced forest cover is achieved because the model still relies on the catchment-scale vegetation-accessible storage volume $S_{U,max}$ that characterizes the extent of the catchment-scale active root-system before deforestation. This $S_{U,max}$ falsely provides sufficient water supply to sustain E_A at high levels comparatively close to E_P throughout the year (see red line in Figure 2b), although, in the parts of the catchment where trees were removed, water stored at depths below a few centimetres is not available for significant evaporation anymore. Such an overestimation of $S_{U,max}$ implies also that in the model a more pronounced water storage deficit can and does develop throughout dry periods. The model therefore assumes that soils dry out to deeper depths. Consequently, to establish connectivity and to eventually generate flow during and after rainstorms, more

16

505 water needs to be stored in the model than in the real world system to overcome this deficit. This water is then in the model held against gravity and thus only available for evaporation but not for drainage. Although it is reasonable to assume that groundwater recharge is affected in a similar way, the model can better reproduce low flows. The reason for this is that the draining groundwater body, which sustains summer low flows, is, due to limited recharge during these drier periods, largely disconnected from and thus largely unaffected by subsurface – vegetation interaction in shallower parts of the subsurface. In

510 the parts of the catchment where trees were removed a similar reasoning also holds for the interception capacity I_{max} and the associated likely overestimation of interception evaporation E_I, yet, due to the smaller magnitude of I_{max}, to a lesser extent than for $S_{U,max}$. The above described problems for the high flow periods are accompanied by the model's inability to describe the post-deforestation $\delta^{18}O$ dynamics in stream water ($E_{NS,\delta18O} < 0$). While this is partly an effect of the above explained low signal-to-noise ratio of such a damped signal and thus of the chosen performance metric, the model also struggles to adequately

515 reproduce the low-frequency fluctuations, such as between February and July 2014, when the model indicated rather stable $\delta^{18}O$ values while the observed values show a slight yet clear decrease over the same period (not shown). This is also underlined by the more than doubling of the mean absolute errors of $\delta^{18}O$ from MAE = 0.09 ‰ in the pre-deforestation period to MAE = 0.21 ‰ in the post-deforestation period. Together with the significant lower overall model performance metric D_E (Figure 6a), these results illustrate that the pre-deforestation model parameter sets provide an unsuitable characterization of the system

520 characteristics in the post-deforestation period.

5.2.3 Recalibrate model for post-deforestation period

To estimate the effect of forest removal on the characteristics of the hydrological system and thus on the model parameters, the model was in a next step recalibrated for the post-deforestation period. This led to a significant improvement of the overall model performance from D_E = 0.22 to 0.58 (Figure 6a). It can be observed that the recalibrated model can much better reproduce the increased high flows in that period (Figures 2c,d), as reflected by improvements in the performance metrics

525 associated with high flows (Figure 6a), but most notably $E_{NS,Q}$ = 0.69, $E_{NS,PD}$ = 0.93 (Figure 6e) or $E_{NS,AC}$ = 0.87 (Figure 6g). In addition and perhaps most importantly, the runoff ratio also increased and was with a modelled value of C_R = 0.58 (0.56 – 0.61) closer to the observed C_R ($E_{R,CR}$ = 0.84). This further implies that, in contrast to the initial model, the recalibrated model also features expected reductions of evaporative fluxes E_A by about 10%, which can be seen in Figure 2b. In addition, analysis

530 of the modelled fluxes indicates that a higher proportion of flows, mostly during wet-up periods, is rapidly released from the root-zones as fluxes $R_{F,H}$ and $R_{F,R}$ (Figure 4; Table 1), representing preferential flows. Such a post-deforestation increase in preferential flow occurrence is supported by observations recently reported by Wiekenkamp et al. (2020). Mirroring the improvements in the reproduction of flows, recalibration also allowed the model to better capture the stream water $\delta^{18}O$ dynamics ($E_{NS,\delta18O}$ = 0.24; MAE = 0.10 ‰; Figure 6a). While there is little change in the model's ability to mimic the general

535 level of damping of the $\delta^{18}O$ signal and its low-frequency fluctuations, the more pronounced, albeit in absolute terms still small, high-frequency fluctuations, as short-term response to individual storms are better described (Figures 3a,b).

17

It is of course unsurprising that recalibration leads to an improved model performance in the post-deforestation period. Without further analysis, such a mere model fitting exercise allows in the presence of model equifinality only little insight into the underlying processes (Beven, 2006; Kirchner, 2006). To gain more confidence that the improvements in the recalibrated model are at least partly due to the right reasons (Kirchner, 2006), the changes in the posterior parameter distributions resulting from the two calibration runs were thus analysed. It was hypothesized above that reductions in evaporative fluxes are directly linked to reduced water volumes accessible and available for evaporation and transpiration at the catchment-scale. In the theoretical ideal case, the representations of the associated storage capacities in the model, i.e. the parameters $S_{U,max}$ and I_{max}, should thus be the only ones to significantly change after deforestation. However, note that this is unlikely for two reasons. First, while it is plausible to assume that these storage capacities are significantly affected by forest removal, it is not unlikely that other system characteristics and their mutual interactions, thus far unknown and not considered, are similarly influenced, potentially causing considerable ontological uncertainty. Second, model parameter interactions that arise as artefacts to compensate overly simplistic process representations and/or data uncertainty are also likely to affect parameters seemingly unrelated to deforestation.

Inspection of the posterior parameter distributions reveals that the catchment-scale $S_{U,max}$ experienced considerable reductions after recalibration. While in the hillslope parts of the catchment, which were less affected by deforestation (~ 10% of the hillslope area; Figure 1) an average decrease by ~ 75 mm to $S_{U,max,H}$ = 137 mm (118 – 249 mm) can be seen (Figure 7a), the completely deforested riparian area exhibits an average decrease by ~ 130 mm to $S_{U,max,R}$ = 67 mm (53 – 126 mm; Figure 7b). As an indicative value, the area-weighted catchment-average $S_{U,max}$ = 120 mm of the best performing parameter set falls remarkably well into the plausible range of $S_{U,max}$ = 90 ± 149 mm as described in Section 5.1. Similarly, significant reductions in I_{max} can be observed, which are with average reduction of ~ 2 mm not as pronounced on the less deforested hillslopes (Figure 7d) than in the riparian areas where $I_{max,R}$ decreased on average by ~ 3 mm (Figure 7e). Comparing to the posterior distributions of other parameters, the results illustrate that the storage parameters $S_{U,max}$ and I_{max} of the riparian zone, and to a lesser extent of the hillslope, were subject to the most pronounced changes. In contrast, for most other parameters, the 5/95th interquantile range of the pre- and post-deforestation posterior distributions largely remained overlapping (Figure 7). Yet, it can also be observed that the individual parameter values associated with the best model solutions in the pre- and post-deforestation periods, respectively, do vary to a stronger degree for most parameters. Notwithstanding the distinct overall effects of forest removal on the individual posterior distributions, this clearly highlights the influence of parameter compensation effects and related uncertainties. This is also illustrated by a few parameters, such as $R_{S,max}$ (Figure 7c, Equation 22), that remain poorly constrained. Note that in spite of uncertainties introduced by the associated compensation effects, in particular $S_{U,max}$ remains rather well constrained. However, after preliminary unsuccessful testing, no further attempts were made to re-calibrate only the above discussed four storage parameters, i.e. $S_{U,max,H}$, $S_{U,max,R}$, $I_{max,H}$ and $I_{max,R}$, acknowledging the limitations introduced by parameter compensation effects.

Overall the results suggest that the model formulation together with the multi-objective calibration strategy ensured the identification of solutions that provide a robust description of the system and allow a simultaneous representation of flow and

18

isotope dynamics in the stream. There are indications that at least some processes and parameters can be directly linked to real world quantities. In particular, the results provide supporting evidence that the parameters $S_{U,max,H}$ and $S_{U,max,R}$ are not merely abstract quantities, but that it is not implausible to assume that they, taken together, provide a catchment-scale representation of vegetation-accessible and -accessed water volumes as defined by Equation 2.

5.3 Deforestation effects on travel time distributions, SAS-functions and young water fractions

While the volume weighted mean $\delta^{18}O$ compositions of observed precipitation with -7.9 ‰ and stream water with -8.2 ‰ are comparable, a substantial difference in their ~~respective~~ fluctuations, with standard deviations of 3.6 ‰ and 0.2 ‰, respectively, is evident (Figures 3a,b). This difference suggests a remarkably elevated degree of damping rarely found elsewhere (e.g. Speed et al., 2010), indicative of the importance of old water contributions to the stream in the study catchment. No significant difference in damping ratios was observed between the pre- and post-deforestation period, which further corroborates the prevalence of old water.

Tracking the $\delta^{18}O$ signals through the model then allowed to estimate ~~residence (RTD) and~~ travel time distributions (TTD). Note that any results reported hereafter are necessarily conditional on the assumptions made in and the uncertainties arising from the modelling process.

In general and consistent with the observed high degree of damping, it was found that pre-deforestation the system was characterized by rather old water. ~~On average only ~ 16% of the water stored in the system is younger than three years, as illustrated by the range of the truncated marginal RTDs that combine water stored in all model storage components (Figure 7b). The young water fractions (F_{yw}), here defined as the fractions of water younger than three months (Kirchner, 2016), are similarly low but exhibit somewhat more pronounced variations from < 0.01 to 0.04 between dry and wet periods. In contrast,~~ Tthe range of truncated TTDs of stream water not only shows more variability in response to changing wetness conditions but also somewhat younger water, with on average about 24 % of the discharge younger than 3 years (Figure 8b). Stream water can contain up to 30 % young water (i.e. F_{yw} ~ 0.30) for individual storm events in the wet period, while frequently dropping to < 1 % during elongated summer dry periods (Figures 8c, 9a), similar to what has been reported elsewhere (e.g. Gallart et al., 2020b). It can also be observed that the age composition of stream water (Figure 8c) and the associated F_{yw} (Figure 9a) do considerably vary throughout wet periods. Dry periods are characterized by considerably less variability and more stable stream water TTDs. This is a consequence of increased bypass flow that has little interaction with resident water as the system gets wetter and which may reach the stream over preferential flow paths and increased contributions from the riparian zone with its shorter flow paths. In other words, in a wet system where little additional water can be stored, the precipitation volumes of individual storm events control the shape of TTDs (Heidbüchel et al, 2020). In the summer dry season, however, precipitation is to a higher degree buffered in the root-zone and used for transpiration (Stockinger et al., 2014). Conversely, stream flow is then mostly sustained by groundwater which is characterized by large volumes of older water. This effectively attenuates fluctuations by the proportionally much lower volumes of younger precipitation water that cannot be stored and is thus quickly released to the stream. This is further corroborated by the significantly higher sensitivity of F_{yw} to changes in

19

stream flow in wet periods as compared to dry periods (Figure 9c). In spite of the low mean F_{yw} ~ 0.11 (Figure 9a), the above also entails that very fast switches towards higher young water fractions can be observed when the system is wetting up after dry periods as well as for storm events throughout the wet season. In general, the above observations are also encapsulated in the catchment-overall storage age selection functions ω, that represent the ratio of stream water TTD over the combined RTD of all model storage elements (Benettin et al., 2015a). While for dry periods under-sampling of young water ages with relatively little variability is evident, it can also be seen that in particular during wet-up and wet periods a considerable, yet highly variable preference for very young water can be seen (Figure 10a), similar to what has been reported previously in other environments (e.g. Benettin et al, 2015a; Remondi et al., 2018).

The overall picture did not change in the post-deforestation period. ~~Water stored in the subsurface remains to be characterized by RTDs with very low young water fractions F_{yw} between < 0.01 and 0.04 with limited sensitivity to changes in wetness conditions (Figure 7i)~~. Similar to the pre-deforestation period, the TTDs can exhibit ~~much more~~considerable variability ~~compared to RTDs~~, depending on the wetness conditions. However, in contrast to the pre-deforestation period and irrespective of the wetness conditions, ~~partly~~ considerable shifts towards younger water can be observed for the TTDs (Figure 8d-g). While individual summer storms led to increases of almost exclusively very young water <10 – 20 days in the stream (Figure 8d), considerable shifts towards younger water can be observed throughout the entire spectrum of tracked ages during wet-up and wet conditions (Figure 8e-f). During the wet period ~ 28 % of the stream water are on average younger than the tracked three years (Figure 8i). The mean F_{yw} only slightly increased to 0.13 (Figure 9b), compared to 0.11 in the pre-deforestation period (Figure 9a), which corroborates earlier results by Stockinger et al. (2019) that suggested only minor fluctuations in mean F_{yw} over multiple moving time windows. For individual winter storm events, however, F_{yw} increased to up to ~ 0.40 (Figures 8j, 9b) compared to F_{yw} of up to ~ 0.30 in the pre-deforestation period (Figures 8c, 9a). Besides the generally higher F_{yw} during wet periods, the F_{yw} became more sensitive to flow during wet-up and wet conditions, with dF_{yw}/dQ ~ 0.27 and 0.43, respectively (Figure 9d), similar to what has been previously reported by von Freyberg et al. (2018) and Gallart et al. (2020a). At the end of dry periods and the beginning of the wet period, elsewhere also referred to as "autumn flush" (e.g. Dawson et al., 2011), the switches towards younger water at given flow levels occur considerably faster in the post-deforestation period than in the pre-deforestation period. Therefore, where, at the same discharge, previously relatively little young water reached the stream, a much higher fraction of young water can now be observed in the stream. Underlining the role of transpiration (e.g. Douinot et al., 2019; Kuppel et al., 2020), this is a direct effect of the reduced evaporative removal of relatively young near-surface water (Maxwell et al., 2019), which in turn is intimately linked to the reduced water supply for evaporative fluxes, i.e. smaller storage volumes $S_{U,max}$ and I_{max}. This modelled relatively young, surface-near water, not taken up by vegetation anymore is thus to a higher degree flushed from the system mostly via preferential flow paths to the stream (i.e. $R_{F,H}$, $R_{F,R}$) and thus bypassing older resident water with little exchange, which is consistent with recent observations of more frequent activation of preferential flow paths (Wiekenkamp et al., 2020). Once connectivity and the associated higher degree of bypass flow are established in the wet period, the peak sensitivity of dF_{yw}/dQ to flow increased to ~ 0.43, as under these conditions when little additional water can be stored in the shallow subsurface, F_{yw} is largely controlled by magnitude of the individual

20

precipitation signals and to a lesser extent by the footprint of the pre-storm history of evaporative fluxes in the shallow subsurface storage. In contrast, no significant changes could be observed for the sensitivity of F_{yw} to discharge during dry

640   periods, as during that period, the composition of water ages is controlled by large volumes of old water. The above described post-deforestation changes are also manifest in the corresponding storage age selection function ω (Figure 10b) for that period. While the degree of under-sampling of young water during dry periods significantly decreased, a substantially higher preference for young water during wet-up and wet periods can be observed than during the pre-deforestation period, with a clear overall shift towards younger water for all wetness conditions.

645

5.4 Uncertainties, unresolved questions and limitations

As emphasized above, all results are conditional on the assumptions taken throughout the modelling process. These assumptions, present in model structure, parameterization and parameters, can lead to uncertainties. Yet, notwithstanding these potential uncertainties, extensive preliminary model testing together with the use of multiple model calibration and evaluation

650   criteria suggest that there is relatively strong evidence to support the main results in this study: the post-deforestation reduction of evaporative fluxes can, at least partially, be linked to a relatively clear reduction in the catchment-scale storage capacities $S_{U,max}$ and I_{max}, which in turn triggered a shift towards younger water ages in the stream, particularly during wet-up and wet conditions.

This is further corroborated when comparing the estimates of $S_{U,max}$ to estimates of physically plausible upper limits of $S_{U,max}$.

655   By definition, $S_{U,max}$ is physically bound by the depth of the groundwater table. Although fluctuating, the groundwater table in the Wüstebach remains at depths below 1 m for much of the year even in the riparian zone (Bogena et al., 2015) and can be expected to be considerably deeper on the hillslopes. Thus assuming a conservative upper bound of catchment-average depth of the groundwater table at ~ 5 m, assuming that the lowest groundwater table at each point in the catchment is at the elevation of the nearest stream, a porosity of the silty clay loam soil of 0.4 (Bogena et al., 2018) and field capacity at a relative pore

660   water content of 0.5 suggests an upper limit of $S_{U,max,GW}$ ~ 1000 mm. However, actual roots are very often shallower than these 5 m of the groundwater table. Although sufficient detailed data on root depths are not available in the study catchment, there is no evidence for systematic and wide-spread roots extending to below 2 m. This is broadly consistent with direct experimental evidence that roots of temperate forests in general (Schenk and Jackson, 2002) and *Picea* species in particular mostly remain rather shallow (< 1 m; e.g. Schmid and Kazda, 2001) and with indirect evidence that *Picea* species rarely tap groundwater and

665   are thus comparatively shallow (e.g. Evaristo and McDonnell, 2017). As a conservative back-of-the-envelope calculation, assuming thus a maximum plausible catchment-average root depth of 2 m, which comes close to the average observed soil depth reported in Graf et al. (2014), rather suggests a physically plausible upper limit of $S_{U,max,RD}$ ~ 400 mm, which is not exceeded by the water balance inferred catchment-scale estimates of $S_{U,max} = 225 \pm 62$ mm.

Note that the above also suggests the presence of an unsaturated transition zone between the root-zone and the groundwater

670   table, i.e. $S_{U,max,TZ} = S_{U,max,GW} - S_{U,max,RD}$ ~ 600 mm. In the absence of root water uptake and likely negligible soil evaporation

in that zone the water content will remain close to field capacity for much of the year, except for days when a wetting front infiltrates towards the groundwater. This transition zone can therefore be considered as hydrologically largely passive so that at time scales of more than a few days $dS/dt \sim 0$. However, this zone also provides a mixing volume that affects tracer circulation and thus water ages (Hrachowitz et al., 2015). Given its hydrologically passive nature and following the idea of a parsimonious model to limit uncertainty, we here, in a simplification, implicitly added the mixing volume $S_{U,max,TZ}$ to the passive groundwater mixing volume $S_{S,p}$

For a meaningful interpretation, two specific observations resulting from our analysis warrant special scrutiny. First, both, water balance (cf. Figure 5b) and model calibration-based catchment-scale estimations of $S_{U,max}$ (Figures 7a,b) suggest post-deforestation median $S_{U,max}$ reductions of ≥ 50 % as a consequence of clear cutting only 21 % of the catchment (Figure 1). While this may be surprising at the first, it can be plausibly explained by considerable further thinning of the remaining forest in 2015, two years after deforestation and thus by reduced catchment-scale transpiration demand. Yet, no detailed and systematic data on the degree of forest thinning is available to meaningfully test this hypothesis.

Second, our results suggest that a passive mixing volume $S_{S,p}$ of at least ~ 10.000 mm is necessary for the model to attenuate the amplitudes of the precipitation $\delta^{18}O$ signals to those in the stream water. Although, $S_{S,p}$ is rather well constrained (Figure 7h), there has in the past been no hydrogeological evidence for the presence of such a surprisingly large groundwater volume nor for its hydrological relevance in the study catchment. Indeed, the authors are not aware of any catchment-scale study that reported similarly high values for $S_{S,p}$ or functionally equivalent parameters (e.g. Birkel et al., 2011a,b; Hrachowitz et al., 2013,2015; Benettin et al., 2013,2015a; Harman, 2015; van der Velde et al., 2015). Yet, to achieve the degree of damping observed in the stream water, such a volume is necessary, if the current understanding of conservative tracer dynamics holds e.g. Maloszewski and Zuber, 1982; McGuire and McDonnell, 2006). Reflecting our insufficient knowledge to which depths exchange with surface water occurs (e.g. Condon et al., 2020), a potential explanation for this observation is that the frequently layered and fractured structure of the Devonian shale bedrock may provide relatively high-permeability pathways for the circulation of and exchange with water at depth. Another, yet, given the current understanding of the Wüstebach (e.g. Graf et al., 2014), less likely hypothesis is the presence of significant lateral groundwater exchange (e.g. Bouaziz et al., 2018). In other words the possibility that the subsurface catchment does not match with the surface catchment (Figure 1) and that older groundwater is imported from "outside" the surface catchment, while an equivalent volume of younger groundwater is exported, maintaining the mass balance. These are hypotheses to be tested in future studies, as the currently available data do not allow a conclusive answer to this question.

6 Conclusions

The small Wüstebach catchment experienced significant deforestation in 2013. Analyzing the effects of this deforestation on the hydrology and stable isotope circulation dynamics in the study catchment our main findings are:

22

(1) Water balance data suggest that deforestation led to a significant increase of stream flow, accompanied by corresponding reductions of evaporative fluxes. This is reflected by an increase of the runoff ratio from $C_R = 0.55$ to 0.68 in the post-deforestation period despite similar climatic conditions, supporting previous results based on eddy covariance measurements (Wiekenkamp et al., 2016).

(2) Based on water balance data, this reduction of evaporative fluxes, as a consequence of reduced vegetation water uptake, could at least partly be linked to a reduction of the catchment-scale water storage volume in the unsaturated soil ($S_{U,max}$) that is within the reach of active roots and thus accessible for vegetation transpiration from ~225 mm in the pre-deforestation period to ~ 90 mm in the post-deforestations period.

(3) Estimating $S_{U,max}$ as calibration parameter of a process-based hydrological model led to similar conclusions. The catchment-average calibrated model parameters representing $S_{U,max}$ for both, the pre- and deforestation periods, respectively, correspond with ~ 240 mm and ~ 120 mm remarkably well with $S_{U,max}$ directly estimated from water balance data. Other model parameters, assumed to have a less direct link to vegetation, exhibited much lower levels of systematic change following deforestation.

(4) Using the model to track the age composition of stream water suggested that, in general, water reaching the stream in the pre-deforestation period was rather old with a mean young water fraction $F_{yw} \sim 0.11$. In spite of the overall low F_{yw}, clear shifts in the shape of travel time distributions towards younger water can be seen under wet conditions with young water fractions increasing up to $F_{yw} \sim 0.30$.

(5) Deforestation and the associated reduction of $S_{U,max}$ led to shifts in travel time distributions towards younger water. Under wet conditions, this resulted in increases of young water fractions to up to $F_{yw} \sim 0.40$ for individual storms. In contrast, dry period travel time distributions exhibited only minor changes. Overall the mean fraction of young water in the stream increased to $F_{yw} \sim 0.13$.

(6) Deforestation resulted in a considerable increase of the sensitivity of young water fractions to discharge under wet conditions from $dF_{yw}/dQ = 0.25$ to 0.43. This implies faster switches towards younger water and thus faster routing of solutes during and shortly after storm events and thus faster routing of solutes with increasing wetness.

The above results suggest that deforestation has not only the potential to affect the partitioning between drainage and evaporation, and thus the fundamental hydrological response characteristics of catchments, but also catchment-scale tracer circulation dynamics. In particular for wet and wet-up conditions, sometimes also referred to as "autumn flush", deforestation in the Wüstebach caused higher proportions of younger water to reach the stream, implying faster routing of water and plausibly also solutes through the subsurface.

Overall, this study demonstrates that post-deforestation changes in both, the hydrological response and travel times, can to a large extent be traced back and attributed to changes in $S_{U,max}$, a readily quantifiable catchment-scale subsurface property (and model parameter) representing the maximum water volume that can be stored within the reach of roots. As such, $S_{U,max}$ and changes therein provide a quantitative, mechanistic hypothesis that can explain *why* deforestation in the Wüstebach decreased

23

evaporative fluxes, increased stream flow – particularly generated by preferential flows – and reduced travel times. The catchment-scale quantification of $S_{U,max}$ based on water balance data therefore provides a potentially valuable way towards meaningful and data-based catchment-scale representation of vegetation-accessible water where soil and root observations are not available at sufficient spatial and temporal detail to meaningfully represent their respective natural heterogeneities. In addition and perhaps more importantly, the method may also hold considerable potential for the formulation of temporally adaptive root-zone parameterizations in catchment-scale hydrological models for more reliable predictions in a changing environment.

References

Ala-Aho, P., Tetzlaff, D., McNamara, J. P., Laudon, H., & Soulsby, C. (2017). Using isotopes to constrain water flux and age estimates in snow-influenced catchments using the STARR (Spatially distributed Tracer-Aided Rainfall-Runoff) model. Hydrology and Earth System Sciences 21, 5089-5110.

Angermann, L., Jackisch, C., Allroggen, N., Sprenger, M., Zehe, E., Tronicke, J., ... & Blume, T. (2017). Form and function in hillslope hydrology: Characterization of subsurface ow based on response observations. Hydrology and Earth System Sciences 21, 3727-3748.

Arrouays, D., Lagacherie, P., & Hartemink, A.E. (2017). Digital soil mapping across the globe. Geoderma Regional 9

Arsenault, R., Poissant, D., & Brissette, F. (2015). Parameter dimensionality reduction of a conceptual model for streamflow prediction in Canadian, snowmelt dominated ungauged basins. Advances in water resources, 85, 27-44.

Benettin, P., Kirchner, J. W., Rinaldo, A., & Botter, G. (2015a). Modeling chloride transport using travel time distributions at Plynlimon, Wales. Water Resources Research, 51(5), 3259-3276.

Benettin, P., Rinaldo, A., & Botter, G. (2015b). Tracking residence times in hydrological systems: Forward and backward formulations. Hydrological Processes, 29(25), 5203-5213.

24

Benettin, P., Soulsby, C., Birkel, C., Tetzlaff, D., Botter, G., & Rinaldo, A. (2017). Using SAS functions and high-resolution isotope data to unravel travel time distributions in headwater catchments. Water Resources Research, 53(3), 1864-1878.

Berkowitz, B., & Zehe, E. (2020). Surface water and groundwater: Unifying conceptualization and quantification of the two water worlds. Hydrology and Earth System Sciences, 24.

Bertuzzo, E., Thomet, M., Botter, G., & Rinaldo, A. (2013). Catchment-scale herbicides transport: Theory and application. Advances in water resources, 52, 232-242.

Beven, K. (2006). A manifesto for the equifinality thesis. Journal of hydrology, 320(1-2), 18-36.

Beven, K. J. (2010). Preferential flows and travel time distributions: defining adequate hypothesis tests for hydrological process models. Hydrological Processes, 24(12), 1537-1547.

Beven, K., & Germann, P. (2013). Macropores and water flow in soils revisited. Water resources research, 49(6), 3071-3092.

Birkel, C., Tetzlaff, D., Dunn, S. M., & Soulsby, C. (2011a). Using lumped conceptual rainfall–runoff models to simulate daily isotope variability with fractionation in a nested mesoscale catchment. Advances in Water Resources, 34(3), 383-394.

Birkel, C., Soulsby, C., & Tetzlaff, D. (2011b). Modelling catchment-scale water storage dynamics: Reconciling dynamic storage with tracer-inferred passive storage. Hydrological Processes, 25(25), 3924-3936.

Birkel, C., Soulsby, C., & Tetzlaff, D. (2014). Developing a consistent process-based conceptualization of catchment functioning using measurements of internal state variables. Water Resources Research, 50(4), 3481-3501.

Birkel, C., Soulsby, C., & Tetzlaff, D. (2015). Conceptual modelling to assess how the interplay of hydrological connectivity, catchment storage and tracer dynamics controls nonstationary water age estimates. Hydrological Processes, 29(13), 2956-2969.

Birkel, C., & Soulsby, C. (2016). Linking tracers, water age and conceptual models to identify dominant runoff processes in a sparsely monitored humid tropical catchment. Hydrological Processes, 30(24), 4477-4493.

Blöschl, G., Bierkens, M. F., Chambel, A., Cudennec, C., Destouni, G., Fiori, A., ... & Stumpp, C. (2019). Twenty-three unsolved problems in hydrology (UPH)–a community perspective. Hydrological Sciences Journal, 64(10), 1141-1158.

Bogena, H. R., Bol, R., Borchard, N., Brüggemann, N., Diekkrüger, B., Drüe, C., ... & Missong, A. (2015). A terrestrial observatory approach to the integrated investigation of the effects of deforestation on water, energy, and matter fluxes. Science China Earth Sciences, 58(1), 61-75.

Bogena, H.R., Montzka, C., Huisman, J.A., Graf, A., Schmidt, M., Stockinger, M., ... & Lücke, A. (2018). The TERENO-Rur Hydrological Observatory: A multiscale multi-compartment research platform for the advancement of hydrological science. Vadose Zone Journal, 17(1).

Borchardt, H. (2012). Einfluss periglazialer Deckschichten auf Abflusssteuerung am Beispiel des anthropogen überprägten Wüstebaches (Nationalpark Eifel), PhD diss., Lehrstuhl für Physische Geogr. und Geo€okologie, Fak. für Georessourcen und Materialtechnik, Rheinisch-Westfälische Tech. Hochsch. Aachen, Aaachen, Germany.

Botter, G., Bertuzzo, E., & Rinaldo, A. (2011). Catchment residence and travel time distributions: The master equation. Geophysical Research Letters, 38(11).

25

Bouaziz, L., Weerts, A., Schellekens, J., Sprokkereef, E., Stam, J., Savenije, H., & Hrachowitz, M. (2018). Redressing the balance: quantifying net intercatchment groundwater flows. Hydrology and Earth System Sciences, 22(12), 6415-6434.

Bouaziz, L., Steele-Dunne, S.C., Schellekens, J., Weerts, A., Stam, J., Sprokkereef, E., Winsemius, H.C., Savenije, H.H.G., & Hrachowitz, M. (2020). Improved understanding of the link between catchment-scale vegetation accessible storage and satellite-derived Soil Water Index. Water Resources Research, 56, e2019WR026365.

Brand, W.A., Coplen, T.B., Vogl, J., Rosner, M., & Prohaska, T. (2014). Assessment of international reference materials for isotope-ratio analysis (IUPAC Technical Report). Pure and Applied Chemistry, 86(3), 425-467.

Brooks, J. R., Barnard, H. R., Coulombe, R., & McDonnell, J. J. (2010). Ecohydrologic separation of water between trees and streams in a Mediterranean climate. Nature Geoscience, 3(2), 100-104.

Brooks, P. D., Chorover, J., Fan, Y., Godsey, S. E., Maxwell, R. M., McNamara, J. P., & Tague, C. (2015). Hydrological partitioning in the critical zone: Recent advances and opportunities for developing transferable understanding of water cycle dynamics. Water Resources Research, 51(9), 6973-6987.

Brunner, I., Herzog, C., Dawes, M.A., Arend, M., & Sperisen, C. (2015). How tree roots respond to drought. Frontiers in plant science, 6, 547.

Brutsaert, W. (2014). Daily evaporation from drying soil: Universal parameterization with similarity. Water Resources Research, 50(4), 3206-3215.

Cain, M. R., Ward, A. S., & Hrachowitz, M. (2019). Ecohydrologic separation alters interpreted hydrologic stores and fluxes in a headwater mountain catchment. Hydrological Processes, 33(20), 2658-2675.

Coenders-Gerrits, A.M.J., Van der Ent, R.J., Bogaard, T.A., Wang-Erlandsson, L., Hrachowitz, M., & Savenije, H.H.G. (2014). Uncertainties in transpiration estimates. Nature, 506(7487), E1-E2.

Collins, D.B.G., & Bras, R.L. (2007). Plant rooting strategies in water-limited ecosystems. Water Resources Research, 43(6).

Condon, L. E., Markovich, K. H., Kelleher, C. A., McDonnell, J. J., Ferguson, G., & McIntosh, J. C. (2020). Where is the bottom of a watershed?. Water Resources Research, 56(3), e2019WR026010.

Cornelissen, T., Diekkrüger, B., & Bogena, H. R. (2014). Significance of scale and lower boundary condition in the 3D simulation of hydrological processes and soil moisture variability in a forested headwater catchment. Journal of hydrology, 516, 140-153.

Creed, I. F., Spargo, A. T., Jones, J. A., Buttle, J. M., Adams, M. B., Beall, F. D., ... & Green, M. B. (2014). Changing forest water yields in response to climate warming: Results from long-term experimental watershed sites across North America. Global change biology, 20(10), 3191-3208.

Criss, R. E., and W. E. Winston (2008), Do Nash values have a value? Discussion and alternate proposals, Hydrol. Proc., 22, 2723–2725.

deBoer-Euser, T., McMillan, H.K., Hrachowitz, M., Winsemius, H.C., & Savenije, H.H.G. (2016). Influence of soil and climate on root zone storage capacity. Water Resources Research, 52(3), 2009-2024.

Donohue, R., Roderick, M., & McVicar, T.R. (2007). On the importance of including vegetation dynamics in Budyko's

835   hydrological model.

Donohue, R.J., Roderick, M.L., & McVicar, T.R. (2012). Roots, storms and soil pores: Incorporating key ecohydrological processes into Budyko's hydrological model. Journal of Hydrology, 436, 35-50.

Douinot, A., Tetzlaff, D., Maneta, M., Kuppel, S., Schulte-Bisping, H., & Soulsby, C. (2019). Ecohydrological modelling with EcH2O-iso to quantify forest and grassland effects on water partitioning and flux ages. Hydrological Processes, 33(16), 2174-

840   2191.

Eagleson, P.S. (Ed.) (1982). Land surface processes in atmospheric general circulation models. Cambridge University Press.

Ellison, D., Morris, C. E., Locatelli, B., Sheil, D., Cohen, J., Murdiyarso, D., ... & Gaveau, D. (2017). Trees, forests and water: Cool insights for a hot world. Global Environmental Change, 43, 51-61.

Etmann, M. (2009). Dendrologische Aufnahmen im Wassereinzugsgebiet Oberer Wüstebach anhand verschiedener Mess- und

845   Schätzverfahren, MSc thesis, Institut für Landschaftsökologie, Univ. of Münster, Münster, Germany.

Euser, T., H. C. Winsemius, M. Hrachowitz, F. Fenicia, S. Uhlenbrook, and H. H. G. Savenije (2013), A framework to assess the realism of model structures using hydrological signatures, Hydrol. Earth Syst. Sci., 17, 1893–1912.

Euser, T., Hrachowitz, M., Winsemius, H.C., & Savenije, H.H. (2015). The effect of forcing and landscape distribution on performance and consistency of model structures. Hydrological Processes, 29(17), 3727-3743.

850   Evaristo, J., & McDonnell, J. J. (2017). Prevalence and magnitude of groundwater use by vegetation: a global stable isotope meta-analysis. Scientific reports, 7(1), 1-12.

Evaristo, J., Kim, M., van Haren, J., Pangle, L. A., Harman, C. J., Troch, P. A., & McDonnell, J. J. (2019). Characterizing the fluxes and age distribution of soil water, plant water, and deep percolation in a model tropical ecosystem. Water Resources Research, 55(4), 3307-3327.

855   Fan, Y., Miguez-Macho, G., Jobbágy, E.G., Jackson, R.B., & Otero-Casal, C. (2017). Hydrologic regulation of plant rooting depth. Proceedings of the National Academy of Sciences, 114(40), 10572-10577.

Fenicia, F., Savenije, H.H.G., Matgen, P., & Pfister, L. (2008). Understanding catchment behavior through stepwise model concept improvement. Water Resources Research, 44(1).

Fenicia, F., Wrede, S., Kavetski, D., Pfister, L., Hoffmann, L., Savenije, H. H., & McDonnell, J. J. (2010). Assessing the

860   impact of mixing assumptions on the estimation of streamwater mean residence time. Hydrological Processes, 24(12), 1730-1741.

Fovet, O., Ruiz, L., Hrachowitz, M., Faucheux, M., & Gascuel-Odoux, C. (2015). Hydrological hysteresis and its value for assessing process consistency in catchment conceptual models. Hydrology and Earth System Sciences, 19(1), 105-123.

Freer, J., Beven, K., & Ambroise, B. (1996). Bayesian estimation of uncertainty in runoff prediction and the value of data: An

865   application of the GLUE approach. Water Resources Research, 32(7), 2161-2173.

Gallart, F., von Freyberg, J., Valiente, M., Kirchner, J. W., Llorens, P., & Latron, J. (2020a). An improved discharge sensitivity metric for young water fractions. Hydrology and Earth System Sciences, 24(3), 1101-1107.

Gallart, F., Valiente, M., Llorens, P., Cayuela, C., Sprenger, M., & Latron, J. (2020b). Investigating young water fractions in a small Mediterranean mountain catchment: both precipitation forcing and sampling frequency matter. Hydrological Processes.

Gao, H., Hrachowitz, M., Schymanski, S.J., Fenicia, F., Sriwongsitanon, N., & Savenije, H.H.G. (2014). Climate controls how ecosystems size the root zone storage capacity at catchment scale. Geophysical Research Letters, 41(22), 7916-7923.

Gao, H., Ding, Y., Zhao, Q., Hrachowitz, M., & Savenije, H. H. (2017). The importance of aspect for modelling the hydrological response in a glacier catchment in Central Asia. Hydrological Processes, 31(16), 2842-2859.

Gentine, P., D'Odorico, P., Lintner, B.R., Sivandran, G., & Salvucci, G. (2012). Interdependence of climate, soil, and vegetation as constrained by the Budyko curve. Geophysical Research Letters, 39(19).

Gerrits, A. M. J., Savenije, H. H. G., Veling, E. J. M., & Pfister, L. (2009). Analytical derivation of the Budyko curve based on rainfall characteristics and a simple evaporation model. Water Resources Research, 45(4).

Graf, A., Bogena, H.R., Drüe, C., Hardelauf, H., Pütz, T., Heinemann, G., & Vereecken, H. (2014). Spatiotemporal relations between water budget components and soil water content in a forested tributary catchment. Water resources research, 50(6), 4837-4857.

Gumbel, E. J. (1941). The return period of flood flows. The annals of mathematical statistics, 12(2), 163-190.

Guswa, A.J. (2008). The influence of climate on root depth: A carbon cost-benefit analysis. Water Resources Research, 44(2).

Harman, C., & Troch, P.A. (2014). What makes Darwinian hydrology" Darwinian"? Asking a different kind of question about landscapes. Hydrology and Earth System Sciences, 18(2), 417.

Harman, C. J. (2015). Time-variable transit time distributions and transport: Theory and application to storage-dependent transport of chloride in a watershed. Water Resources Research, 51(1), 1-30.

Heidbüchel, I., Yang, J., Musolff, A., Troch, P., Ferré, T., & Fleckenstein, J. H. (2020). On the shape of forward transit time distributions in low-order catchments. Hydrology and Earth System Sciences 24, 2895–2920.

Hengl, T., de Jesus, J. M., Heuvelink, G. B., Gonzalez, M. R., Kilibarda, M., Blagotić, A., ... & Guevara, M. A. (2017). SoilGrids250m: Global gridded soil information based on machine learning. PLoS one, 12(2).

Hrachowitz, M., & Clark, M. P. (2017). HESS Opinions: The complementary merits of competing modelling philosophies in hydrology. Hydrol. Earth Syst. Sci, 21(8), 3953-3973.

Hrachowitz, M., Soulsby, C., Tetzlaff, D., Dawson, J. J. C., Dunn, S. M., & Malcolm, I. A. (2009). Using long-term data sets to understand transit times in contrasting headwater catchments. Journal of Hydrology, 367(3-4), 237-248.

Hrachowitz, M., Savenije, H., Bogaard, T.A., Tetzlaff, D., & Soulsby, C. (2013). What can flux tracking teach us about water age distribution patterns and their temporal dynamics?. Hydrology and Earth System Sciences, 17, 533–564.

Hrachowitz, M., Fovet, O., Ruiz, L., Euser, T., Gharari, S., Nijzink, R., ... & Gascuel-Odoux, C. (2014). Process consistency in models: The importance of system signatures, expert knowledge, and process complexity. Water resources research, 50(9), 7445-7469.

28

Hrachowitz, M., Fovet, O., Ruiz, L., & Savenije, H.H.G. (2015). Transit time distributions, legacy contamination and variability in biogeochemical 1/f^n scaling: how are hydrological response dynamics linked to water quality at the catchment scale?. Hydrological Processes, 29(25), 5241-5256.

Hrachowitz, M., Benettin, P., Van Breukelen, B.M., Fovet, O., Howden, N.J., Ruiz, L., ... & Wade, A.J. (2016). Transit times—The link between hydrology and water quality at the catchment scale. Wiley Interdisciplinary Reviews: Water, 3(5), 629-657.

Hulsman, P., Winsemius, H.C., Michailovsky, C., Savenije, H.H.G. & Hrachowitz, M. (2020). Using altimetry observations combined with GRACE to select parameter sets of a hydrological model in data scarce regions. Hydrology and Earth System Sciences, 24.

Hwang, T., Band, L., & Hales, T.C. (2009). Ecosystem processes at the watershed scale: Extending optimality theory from plot to catchment. Water Resources Research, 45(11).

Jaramillo, F., & Destouni, G. (2014). Developing water change spectra and distinguishing change drivers worldwide. Geophysical Research Letters, 41(23), 8377-8386.

Jaramillo, F., Cory, N., Arheimer, B., Laudon, H., Van Der Velde, Y., Hasper, T. ., ... & Uddling, J. (2018). Dominant effect of increasing forest biomass on evapotranspiration: interpretations of movement in Budyko space. Hydrology and Earth System Sciences, 22(1), 567-580.

Jasechko, S. (2018). Plants turn on the tap. Nature Climate Change, 8(7), 562-563.

Jothityangkoon, C., M. Sivapalan, and D. L. Farmer (2001), Process controls of water balance variability in a large semi-arid catchment: Downward approach to hydrological model development, J. Hydrol., 254(1), 174–198.

Kirchner, J. W. (2006). Getting the right answers for the right reasons: Linking measurements, analyses, and models to advance the science of hydrology. Water Resources Research, 42(3).

Klaus, J., Zehe, E., Elsner, M., Külls, C., & McDonnell, J. J. (2013). Macropore flow of old water revisited: experimental insights from a tile-drained hillslope. Hydrology and Earth System Sciences, 17(1), 103.

Kleidon, A. (2004). Global datasets of rooting zone depth inferred from inverse methods. Journal of Climate, 17(13), 2714-2722.

Knighton, J., Souter-Kline, V., Volkman, T., Troch, P. A., Kim, M., Harman, C., ... & Walter, M. T. (2019). Seasonal and topographic variations in ecohydrological separation within a small, temperate, snow-influenced catchment. Water Resources Research, 55(8), 6417-6435.

Knighton, J., Singh, K., & Evaristo, J. (2020). Understanding Catchment-Scale Forest Root Water Uptake Strategies Across the Continental United States Through Inverse Ecohydrological Modeling. Geophysical Research Letters, 47(1), e2019GL085937.

Kuppel, S., Tetzlaff, D., Maneta, M., & Soulsby, C. (2018a). EcH2O-iso 1.0: water isotopes and age tracking in a process-based, distributed ecohydrological model. Geoscientific Model Development.

29

Kuppel, S., Tetzlaff, D., Maneta, M. P., & Soulsby, C. (2018b). What can we learn from multi-data calibration of a process-based ecohydrological model?. Environmental Modelling & Software, 101, 301-316.

Kuppel, S., Tetzlaff, D., Maneta, M. P., & Soulsby, C. (2020). Critical zone storage controls on the water ages of ecohydrological outputs. Geophysical Research Letters, 47(16), e2020GL088897.

Laio, F., D'Odorico, P., & Ridolfi, L. (2006). An analytical model to relate the vertical root distribution to climate and soil properties. Geophysical Research Letters, 33(18).

Loritz, R., Hassler, S. K., Jackisch, C., Allroggen, N., van Schaik, L., Wienhöfer, J., & Zehe, E. (2017). Picturing and modeling catchments by representative hillslopes. Hydrology and Earth System Sciences, 21, 1225-1249.

Małoszewski, P., & Zuber, A. (1982). Determining the turnover time of groundwater systems with the aid of environmental tracers: 1. Models and their applicability. Journal of hydrology, 57(3-4), 207-231.

Maxwell, R. M., Condon, L. E., Kollet, S. J., Maher, K., Haggerty, R., & Forrester, M. M. (2016). The imprint of climate and geology on the residence times of groundwater. Geophysical Research Letters, 43(2), 701-708.

Maxwell, R. M., Condon, L. E., Danesh-Yazdi, M., & Bearup, L. A. (2019). Exploring source water mixing and transient residence time distributions of outflow and evapotranspiration with an integrated hydrologic model and Lagrangian particle tracking approach. Ecohydrology, 12(1), e2042.

Mezentsev, V. (1955). Back to the computation of total evaporation. Meteorologia i Gidologia, 5. 24-26.

McDonnell, J.J., McGuire, K., Aggarwal, P., Beven, K.J., Biondi, D., Destouni, G., ... & Lyon, S. (2010). How old is streamwater? Open questions in catchment transit time conceptualization, modelling and analysis. Hydrological Processes, 24(12), 1745-1754.

McGuire, K. J., & McDonnell, J. J. (2006). A review and evaluation of catchment transit time modeling. Journal of Hydrology, 330(3-4), 543-563.

McMillan, H., Tetzlaff, D., Clark, M., & Soulsby, C. (2012). Do time-variable tracers aid the evaluation of hydrological model structure? A multimodel approach. Water Resources Research, 48(5).

McMurtrie, R.E., Iversen, C.M., Dewar, R.C., Medlyn, B.E., Näsholm, T., Pepper, D.A., & Norby, R.J. (2012). Plant root distributions and nitrogen uptake predicted by a hypothesis of optimal root foraging. Ecology and evolution, 2(6), 1235-1250.

Milly, P.C., & Dunne, K.A. (1994). Sensitivity of the global water cycle to the water-holding capacity of land. Journal of Climate, 7(4), 506-526.

Mianabadi, A., Coenders-Gerrits, M., Shirazi, P., Ghahraman, B., & Alizadeh, A. (2019). A global Budyko model to partition evaporation into interception and transpiration. Hydrology and Earth System Sciences, 23(12), 4983-5000.

Montanari, A., and E. Toth (2007), Calibration of hydrological models in the spectral domain: An opportunity for scarcely gauged basins?, Water Resour. Res., 43, W05434, doi:10.1029/2006WR005184.

Morán-Tejeda, E., Zabalza, J., Rahman, K., Gago-Silva, A., López-Moreno, J. I., Vicente-Serrano, S., ... & Beniston, M. (2015). Hydrological impacts of climate and land-use changes in a mountain watershed: Uncertainty estimation based on model comparison. Ecohydrology, 8(8), 1396-1416.

Nash, J. E., and J. V. Sutcliffe (1970), River flow forecasting through conceptual models: part 1—A discussion of principles, J. Hydrol., 10, 282–290.

Nijzink, R., Hutton, C., Pechlivanidis, I., Capell, R., Arheimer, B., Freer, J., ... & Hrachowitz, M. (2016a). The evolution of root-zone moisture capacities after deforestation: a step towards hydrological predictions under change?. Hydrology and Earth System Sciences, 20(12), 4775-4799.

Nijzink, R.C., Samaniego, L., Mai, J., Kumar, R., Thober, S., Zink, M., ... & Hrachowitz, M. (2016b). The importance of topography-controlled sub-grid process heterogeneity and semi-quantitative prior constraints in distributed hydrological models. Hydrology & Earth System Sciences, 20(3), 1151–1176

Penna, D., Hopp, L., Scandellari, F., Allen, S. T., Benettin, P., Beyer, M., ... & Volkmann, T. H. (2018). Ideas and perspectives: Tracing terrestrial ecosystem water fluxes using hydrogen and oxygen stable isotopes-challenges and opportunities from an interdisciplinary perspective. Biogeosciences, 15(21), 6399-6415.

Penna, D., Geris, J., Hopp, L., & Scandellari, F. (2020). Water sources for root water uptake: Using stable isotopes of hydrogen and oxygen as a research tool in agricultural and agroforestry systems. Agriculture, Ecosystems & Environment, 291, 106790.

Renner, M., Brust, K., Schwärzel, K., Volk, M., & Bernhofer, C. (2014). Separating the effects of changes in land cover and climate: a hydro-meteorological analysis of the past 60 yr in Saxony, Germany. Hydrology and Earth System Sciences, 18, 389-405.

Richter, F. (2008), Bodenkarte zur Standorterkundung. Verfahren Quellgebiet Wüstebachtal (Forst), Geologischer Dienst Nordrhein-Westfalen, Krefeld, Germany.

Rinaldo, A., Benettin, P., Harman, C. J., Hrachowitz, M., McGuire, K.J., Van Der Velde, Y., ... & Botter, G. (2015). Storage selection functions: A coherent framework for quantifying how catchments store and release water and solutes. Water Resources Research, 51(6), 4840-4847.

Rodriguez, N. B., McGuire, K. J., & Klaus, J. (2018). Time-varying storage–water age relationships in a catchment with a mediterranean climate. Water Resources Research, 54(6), 3988-4008.

Rodriguez, N. B., & Klaus, J. (2019). Catchment travel times from composite StorAge Selection functions representing the superposition of streamflow generation processes. Water Resources Research.

Rodriguez-Iturbe, I., D'Odorico, P., Laio, F., Ridolfi, L., & Tamea, S. (2007). Challenges in humid land ecohydrology: Interactions of water table and unsaturated zone with climate, soil, and vegetation. Water Resources Research, 43(9).

Roebroek, C. T., Melsen, L. A., Hoek van Dijke, A. J., Fan, Y., & Teuling, A. J. (2020). Global distribution of hydrologic controls on forest growth. Hydrology and Earth System Sciences, 24(9), 4625-4639.

31

Formatiert: Deutsch (Deutschland)

Savenije, H.H.G., & Hrachowitz, M. (2017). HESS Opinions "Catchments as meta-organisms–a new blueprint for hydrological modelling". Hydrol. Earth Syst. Sci, 21(2), 1107-1116.

Sawicz, K., T. Wagener, M. Sivapalan, P. A. Troch, and G. Carrillo (2011), Catchment classification: Empirical analysis of hydrologic similarity based on catchment function in the eastern USA, Hydrol. Earth Syst. Sci., 15, 2895–2911.

Seneviratne, S.I., Wilhelm, M., Stanelle, T., van den Hurk, B., Hagemann, S., Berg, A., ... & Claussen, M. (2013). Impact of soil moisture-climate feedbacks on CMIP5 projections: First results from the GLACE-CMIP5 experiment. Geophysical Research Letters, 40(19), 5212-5217.

Schenk, H.J. (2005). Vertical vegetation structure below ground: scaling from root to globe. In Progress in botany (pp. 341-373). Springer, Berlin, Heidelberg.

Schenk, H.J., & Jackson, R.B. (2002). Rooting depths, lateral root spreads and below-ground/above-ground allometries of plants in water-limited ecosystems. Journal of Ecology, 90(3), 480-494.

Schenk, H. J., & Jackson, R. B. (2003). Global distribution of root profiles in terrestrial ecosystems. ORNL DAAC.

Schymanski, S.J., Sivapalan, M., Roderick, M.L., Beringer, J., & Hutley, L B. (2008). An optimality-based model of the coupled soil moisture and root dynamics. Hydrology and earth system sciences, 12(3), 913-932.

Shamir, E., B. Imam, H. V. Gupta, and S. Sorooshian (2005), Application of temporal streamflow descriptors in hydrologic model parameter estimation, Water Resour. Res., 41, W06021, doi:10.1029/2004WR003409.

Sivandran, G., & Bras, R.L. (2012). Identifying the optimal spatially and temporally invariant root distribution for a semiarid environment. Water Resources Research, 48(12).

Speich, M.J., Lischke, H., & Zappa, M. (2018). Testing an optimality-based model of rooting zone water storage capacity in temperate forests. Hydrology and Earth System Sciences, 22(7), 4097-4124.

Speich, M. J., Zappa, M., Scherstjanoi, M., & Lischke, H. (2020). FORests and HYdrology under Climate Change in Switzerland v1. 0: a spatially distributed model combining hydrology and forest dynamics. Geoscientific Model Development, 13(2), 537-564.

Soulsby, C., Tetzlaff, D., & Hrachowitz, M. (2010). Are transit times useful process-based tools for flow prediction and classification in ungauged basins in montane regions?. Hydrological Processes, 24(12), 1685-1696.

Soulsby, C., Braun, H., Sprenger, M., Weiler, M., & Tetzlaff, D. (2017). Influence of forest and shrub canopies on precipitation partitioning and isotopic signatures. Hydrological Processes, 31(24), 4282-4296.

Speed, M., Tetzlaff, D., Soulsby, C., Hrachowitz, M., & Waldron, S. (2010). Isotopic and geochemical tracers reveal similarities in transit times in contrasting mesoscale catchments. Hydrological Processes: An International Journal, 24(9), 1211-1224.

Sprenger, M., Leistert, H., Gimbel, K., & Weiler, M. (2016). Illuminating hydrological processes at the soil-vegetation-atmosphere interface with water stable isotopes. Reviews of Geophysics, 54(3), 674-704.

Sprenger, M., Tetzlaff, D., Buttle, J., Laudon, H., & Soulsby, C. (2018). Water ages in the critical zone of long-term experimental sites in northern latitudes. Hydrology and Earth System Sciences.

32

Sprenger, M., Llorens, P., Cayuela, C., Gallart, F., & Latron, J. (2019a). Mechanisms of consistently disjunct soil water pools over (pore) space and time.

1035   Sprenger, M., Stumpp, C., Weiler, M., Aeschbach, W., Allen, S.T., Benettin, P., ... & McDonnell, J.J. (2019b). The demographics of water: a review of water ages in the critical zone. Reviews of Geophysics, 57(3), 800-834.

Stockinger, M. P., Bogena, H. R., Lücke, A., Diekkrüger, B., Weiler, M., & Vereecken, H. (2014). Seasonal soil moisture patterns: Controlling transit time distributions in a forested headwater catchment. Water resources research, 50(6), 5270-5289.

1040   Stockinger, M. P., Lücke, A., McDonnell, J. J., Diekkrüger, B., Vereecken, H., & Bogena, H. R. (2015). Interception effects on stable isotope driven streamwater transit time estimates. Geophysical research letters, 42(13), 5299-5308.

Stockinger, M. P., Bogena, H. R., Lücke, A., Diekkrüger, B., Cornelissen, T., & Vereecken, H. (2016). Tracer sampling frequency influences estimates of young water fraction and streamwater transit time distribution. Journal of hydrology, 541, 952-964.

1045   Stockinger, M. P., Lücke, A., Vereecken, H., & Bogena, H. R. (2017). Accounting for seasonal isotopic patterns of forest canopy intercepted precipitation in streamflow modeling. Journal of Hydrology, 555, 31-40.

Teuling, A. J. (2018). A hot future for European droughts. Nature Climate Change, 8(5), 364-365.

Teuling, A. J., & van Dijke, A. J. H. (2020). Forest age and water yield. Nature, 578(7794), E16-E18.

Tron, S., Perona, P., Gorla, L., Schwarz, M., Laio, F., & Ridolfi, L. (2015). The signature of randomness in riparian plant root

1050   distributions. Geophysical Research Letters, 42(17), 7098-7106.

Turc, L. (1954). Le bilan d'eau des sols. Relations entre les precipitations, l'evaporation et l'ecoulement. Ann. Agron., 5, 491-596

Van Der Velde, Y., Torfs, P. J. J. F., Van Der Zee, S. E. A. T. M., & Uijlenhoet, R. (2012). Quantifying catchment-scale mixing and its effect on time-varying travel time distributions. Water Resources Research, 48(6).

1055   Van der Velde, Y., Vercauteren, N., Jaramillo, F., Dekker, S. C., Destouni, G., & Lyon, S. W. (2014). Exploring hydroclimatic change disparity via the Budyko framework. Hydrological Processes, 28(13), 4110-4118.

van der Velde, Y., Heidbüchel, I., Lyon, S. W., Nyberg, L., Rodhe, A., Bishop, K., & Troch, P. A. (2015). Consequences of mixing assumptions for time-variable travel time distributions. Hydrological Processes, 29(16), 3460-3474.

von Freyberg, J., Allen, S. T., Seeger, S., Weiler, M., & Kirchner, J. W. (2018). Sensitivity of young water fractions to hydro-

1060   climatic forcing and landscape properties across 22 Swiss catchments. Hydrology and Earth System Sciences, 22(7), 3841-3861.

Wang-Erlandsson, L., Bastiaanssen, W.G., Gao, H., Jägerrmeyr, J., Senay, G.B., Van Dijk, A., ... & Savenije, H.H. (2016). Global root zone storage capacity from satellite-based evaporation.

Wang-Erlandsson, L., Fetzer, I., Keys, P. W., Van Der Ent, R. J., Savenije, H. H., & Gordon, L. J. (2018). Remote land use

1065   impacts on river flows through atmospheric teleconnections. Hydrology and Earth System Sciences, 22(8), 4311-4328.

Wehrli, K., Guillod, B.P., Hauser, M., Leclair, M., & Seneviratne, S.I. (2019). Identifying Key Driving Processes of Major Recent Heat Waves. Journal of Geophysical Research: Atmospheres, 124(22), 11746-11765.

Weiler, M., & Naef, F. (2003). An experimental tracer study of the role of macropores in infiltration in grassland soils. Hydrological Processes, 17(2), 477-493.

Weiler, M., & McDonnell, J. J. (2007). Conceptualizing lateral preferential flow and flow networks and simulating the effects on gauged and ungauged hillslopes. Water resources research, 43(3).

Wiekenkamp, I., Huisman, J.A., Bogena, H.R., Graf, A., Lin, H.S., Drüe, C., & Vereecken, H. (2016). Changes in measured spatiotemporal patterns of hydrological response after partial deforestation in a headwater catchment. Journal of hydrology, 542, 648-661.

Wilusz, D. C., Harman, C. J., & Ball, W. P. (2017). Sensitivity of catchment transit times to rainfall variability under present and future climates. Water Resources Research, 53(12), 10231-10256.

Yadav, M., T. Wagener, and H. V. Gupta (2007), Regionalization of constraints on expected watershed response behavior for improved predictions in ungauged basins, Adv. Water Resour., 30, 1756–1774.

Yang, Y., Donohue, R.J., & McVicar, T.R. (2016). Global estimation of effective plant rooting depth: Implications for hydrological modeling. Water Resources Research, 52(10), 8260-8276.

Yilmaz, K. K., H. V. Gupta, and T. Wagener (2008), A process-based diagnostic approach to model evaluation: Application to the NWS distributed hydrologic model, Water Resour. Res., 44, W09417, doi:10.1029/2007WR006716.

Zacharias, S., Bogena, H., Samaniego, L., Mauder, M., Fuß, R., Pütz, T., ... & Bens, O. (2011). A network of terrestrial environmental observatories in Germany. Vadose Zone Journal, 10(3), 955-973.

Zehe, E., Lee, H., & Sivapalan, M. (2006). Dynamical process upscaling for deriving catchment scale state variables and constitutive relations for meso-scale process models.

Zehe, E., Elsenbeer, H., Lindenmaier, F., Schulz, K., & Blöschl, G. (2007). Patterns of predictability in hydrological threshold systems. Water Resources Research, 43(7).

Zhang, M., Liu, N., Harper, R., Li, Q., Liu, K., Wei, X., ... & Liu, S. (2017). A global review on hydrological responses to forest change across multiple spatial scales: Importance of scale, climate, forest type and hydrological regime. Journal of Hydrology, 546, 44-59.

Zuber, A. (1986). On the interpretation of tracer data in variable flow systems. Journal of Hydrology, 86(1-2), 45-57.

Copernicus Publications
The Innovative Open Access Publisher

Table 1: Water balance, state and flux equations used in the hydrological model. Symbols shown in bold are model parameters. Subscripts H and R indicate hillslope and riparian zone, respectively. Model variables: P **is total precipitation [mm d⁻¹],** P_S **is solid precipitation (snow)]mm d⁻¹],** P_M **is snow melt [mm d⁻¹],** P_R **is rain [mm d⁻¹],** P_E **is effective precipitation [mm d⁻¹],** E_P **is potential evaporation [mm d⁻¹],** E_I **is interception evaporation [mm d⁻¹],** R_F **is preferential recharge [mm d⁻¹],** R_S **is slow recharge [mm d⁻¹],** E_T **is transpiration [mm d⁻¹],** Q_S **is flow from slow responding reservoir [mm d⁻¹],** Q_R **is flow from the fast responding riparian reservoir [mm d⁻¹],** Q **is the total flow [mm d⁻¹] and** E_A **is the total actual evaporation [mm d⁻¹]. Model parameters:** T_T **is the threshold temperature [ºC],** F_M **is a melt factor [mm d⁻¹ ºC⁻¹],** I_{max} **is the interception capacity [mm],** $S_{U,max}$ **is the root-zone storage capacity [mm],** γ **is a shape factor [-],** $R_{S,max}$ **is the maximum percolation rate [mm d⁻¹],** L_P **is a transpiration water stress factor [-],** f_{QS} **is a factor determining the fraction of groundwater flow that is upwelling into the riparian zone [-],** k_S **is the storage coefficient of the slow responding reservoir [d⁻¹],** k_R **is the storage coefficient for the fast responding riparian reservoir [d⁻¹] and** f **is the areal fraction of the riparian zone [-].**

Landscape unit	Storage component	Water balance	Eq.	Constitutive equations	Eq.
Hillslope	Snow storage	$dS_{snow}/dt = P_S - P_M$	(8)	$P_S = \begin{cases} P, & T < T_T \\ 0, & T \geq T_T \end{cases}$	(15)
				$P_M = \begin{cases} 0, & T < T_T \\ min\left(F_M(T - T_T), \frac{S_{snow}}{dt}\right), & T \geq T_T \end{cases}$	(16)
	Interception storage	$dS_{I,H}/dt = P_R + P_M - P_{E,H} - E_{I,H}$	(9)	$P_R = \begin{cases} 0, & T < T_T \\ P, & T \geq T_T \end{cases}$	(17)
				$P_{E,H} = max\left(0, \frac{S_{I,H} - I_{max,H}}{dt}\right)$	(18)
				$E_{I,H} = min\left(E_P, \frac{S_{I,H} - P_{E,H}}{dt}\right)$	(19)
	Unsaturated root-zone storage	$dS_{U,H}/dt = P_{E,H} - R_{F,H} - R_{S,H} - E_{T,H}$	(10)	$S'_{U,H} = (1 + \gamma)S_{U,max,H}\left(1 - \left(1 - \frac{S_{U,H}}{S_{U,max,H}}\right)^{\left(\frac{1}{1+\gamma}\right)}\right)$	(20)
				$R_{F,H} = P_{E,H} - \left(S_{U,max,H} + S_{U,H} + S_{U,max,H}\left(1 - \frac{P_{E,H}dt + S_{U,H}'}{(1+\gamma)S_{U,max,H}}\right)^{(1+\gamma)}\right)dt^{-1}$	(21)
				$R_{S,H} = min\left(R_{S,max}\frac{S_{U,H}}{S_{U,max,H}}, \frac{S_{U,H}}{dt}\right)$	(22)
				$E_{T,H} = min\left((E_P - E_{I,H})min\left(\frac{S_{U,H}}{S_{U,max,H}}\frac{1}{L_P}, 1\right), \frac{S_{U,H}}{dt}\right)$	(23)
	Slow responding storage	$dS_{S,a}/dt = (1 - f)(R_{F,H} + R_{S,H}) - R_{S,R} - Q_S$	(11)	$R_{S,R} = f_{QS}S_{S,a}(1 - e^{-k_S t})dt^{-1}$	(24)
				$Q_S = (1 - f_{QS})S_{S,a}(1 - e^{-k_S t})dt^{-1}$	(25)
Riparian zone	Interception storage	$dS_{I,R}/dt = P_R + P_M - P_{E,R} - E_{I,R}$	(12)	$P_{E,R} = max\left(0, \frac{S_{I,R} - I_{max,R}}{dt}\right)$	(26)
				$E_{I,R} = min\left(E_P, \frac{S_{I,R} - P_{E,R}}{dt}\right)$	(27)
	Unsaturated root-zone storage	$dS_{U,R}/dt = P_{E,R} + R_{S,R}/f - R_{F,R} - E_{T,R}$	(13)	$S'_{U,R} = (1 + \gamma)S_{U,max,R}\left(1 - \left(1 - \frac{S_{U,R}}{S_{U,max,R}}\right)^{\left(\frac{1}{1+\gamma}\right)}\right)$	(28)
				$R_{F,R} = P_{E,R} + \frac{R_{S,R}}{f} - \left(S_{U,max,R} + S_{U,R} + S_{U,max,R}\left(1 - \frac{P_{E,R}dt + S_{U,R}'}{(1+\gamma)S_{U,max,R}}\right)^{(1+\gamma)}\right)dt^{-1}$	(29)
				$E_{T,R} = min\left((E_P - E_{I,R})min\left(\frac{S_{U,R}}{S_{U,max,R}}\frac{1}{L_P}, 1\right), \frac{S_{U,R}}{dt}\right)$	(30)
	Fast responding storage	$dS_{F,R}/dt = R_{F,R} - Q_R$	(14)	$Q_R = S_{F,R}(1 - e^{-k_R t})dt^{-1}$	(31)
				$Q = Q_S + f Q_R$	(32)
				$E_I = (1 - f)E_{I,H} + f E_{I,R}$	(33)
				$E_T = (1 - f)E_{T,H} + f E_{T,R}$	(34)
				$E_A = E_I + E_T$	(35)

Table 2: Parameter prior distributions and 5/95th percentiles of the posterior distributions. Note that *) parameter *f*, characterizing the areal proportion of the riparian zone was fixed according to soil and elevation data and **) the interception capacity I_{max} was assumed to be identical on the hillslopes and the riparian zone in the pre-deforestation period.

Model	Parameter	Prior distribution	Posterior distribution	
			Pre-deforestation	Post-deforestation
Hydrological model	f [-]*	0.1	0.1	0.1
	F_M [mm d^{-1} ^{o}C^{-1}]	1.0 – 5.0	2.1 – 4.2	1.8 – 4.6
	f_{QS} [-]	0.00 – 0.20	0.02 – 0.11	0.01 – 0.10
	$I_{max,H}$ [mm]	0.0 – 6.0	0.8 – 4.5	0.1 – 1.7
	$I_{max,R}$ [mm]**	0.0 – 6.0	0.8 – 4.5	0.0 – 0.9
	k_R [d^{-1}]	0.01 – 2.00	0.20 – 1.60	0.40 – 1.40
	k_S [d^{-1}]	0.01 – 0.15	0.04 – 0.07	0.03 – 0.09
	L_p [-]	0.0 – 1.0	0.2 – 0.7	0.1 – 0.2
	$R_{S,max}$ [mm d^{-1}]	0.0 – 2.0	0.2 – 1.9	0.4 – 1.6
	$S_{U,max,H}$ [mm]	0 – 400	233 – 309	118 – 249
	$S_{U,max,R}$ [mm]	0 – 400	194 – 287	53 – 126
	T_T [^{o}C]	-1.5 – 1.5	-0.6 – 1.2	-0.7 – 1.0
	γ [-]	0.0 – 5.0	0.3 – 4.2	0.7 – 4.3
Tracer model	α_0 [-]	0.00 – 1.00	0.77 – 0.99	0.58 – 0.96
	$S_{S,p}$ [mm]	1000 – 30 000	8132 – 16 457	8387 - 16314

1125

Table 3: Signatures of flow and δ^{18}O and the associated performance metrics used for model calibration and evaluation. The performance metrics used include the Nash-Sutcliffe efficiency (E_{NS}), the volume error (E_V) and the relative error (E_R).

Variable/Signature	Symbol	Performance Metric	Reference
Time series of flow	Q	$E_{NS,Q}$	Nash and Sutcliffe (1970)
	log(Q)	$E_{NS,log(Q)}$	
	Q	$E_{V,Q}$	Criss and Winston (2008)
Flow duration curve	FDC	$E_{NS,FDC}$	Jothityangkoon et al. (2001)
Flow duration curve high flow period	FDC,h	$E_{NS,FDCh}$	Yilmaz et al. (2008)
Peak distribution	PD	$E_{NS,PD}$	Euser et al. (2013)
Rising limb density	RLD	$E_{R,RLD}$	Shamir et al. (2005)
Declining limb density	DLD	$E_{R,DLD}$	Sawicz et al. (2011)
Autocorrelation function of flow	AC	$E_{NS,AC}$	Montanari and Toth (2007)
Lag-1 autocorrelation	AC1	$E_{R,AC1}$	Hrachowitz et al. (2014)
Lag-1 autocorrelation low flow period	AC1,l	$E_{R,AC1,l}$	Fovet et al. (2015)
Runoff ratio	CR	$E_{R,CR}$	Yadav et al. (2007)
Time series of δ^{18}O in stream water	δ^{18}O	$E_{NS,\delta18O}$	Birkel et al. (2011a)

1130

1135

1140

37

Figure 1: Map of the Wüstebach study catchment showing the spatial distribution of soil types. The riparian zone is defined by the parts of the catchment covered by Gleysols, Planosols and Halfbogs. The red line indicates the outline of the deforested part of the catchment, as can also be seen on the aerial images (Google Earth, Maxar Technologies 2020) from 2013 and 2016.

1145

1150

1155

1160

38
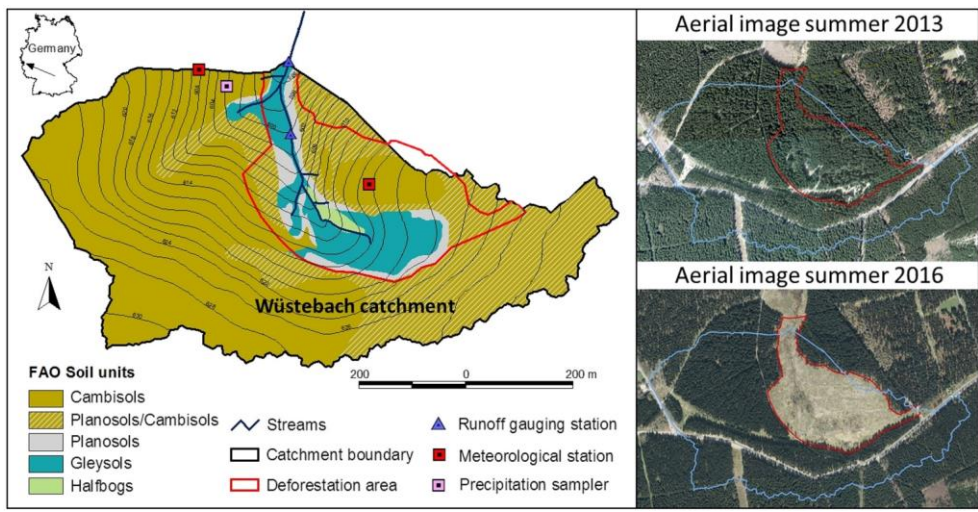
Figure 2: (a) Time series of observed weekly~~daily~~ precipitation P; **(b)** daily cumulative evaporative fluxes for the pre- and post-deforestation period, where the dark brown line indicates potential evaporation E_P and the orange lines and the yellow shaded areas show the actual evaporation E_A modelled using the best fit parameter sets and the associated 5/95th percentiles of all feasible solutions of the pre- and post-deforestation periods, respectively. The dashed red line indicates the modelled E_A in the post-deforestation period using the best fit pre-deforestation parameter set; **(c)** observed (dark blue line) and modelled daily stream flow Q; light blue line indicates best fit model and the shaded area the 5/95th percentile of all feasible solutions for the pre- and post-deforestation periods, respectively. The dashed red line indicates the modelled stream in the post-deforestation period using the best fit pre-deforestation parameter set; **(d)** zoom-in to the observed and modelled stream flow for the 10/2012 – 10/2014 period. The grey shaded area indicates the deforestation period.
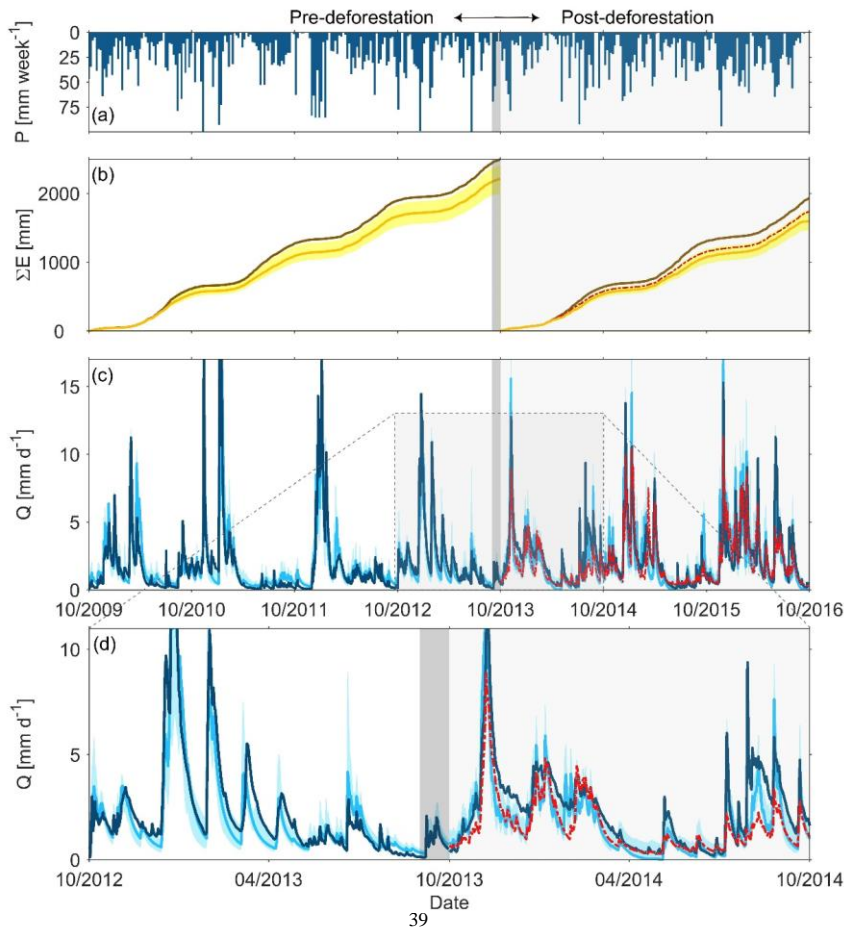
Figure 3: (a) Observed volume weighted monthly δ¹⁸O signals in precipitation (grey dots; size of dots indicates the precipitation volume) and stream flow (green dots) as well as the best fit modelled δ¹⁸O signal in the stream (green line) and the 5/95th percentile of all feasible solutions from pre- and post-deforestation calibration (green shaded area); (b) zoom-in of observed and modelled δ¹⁸O signal in the stream for the 10/2012 – 10/2014 period.

1180

40
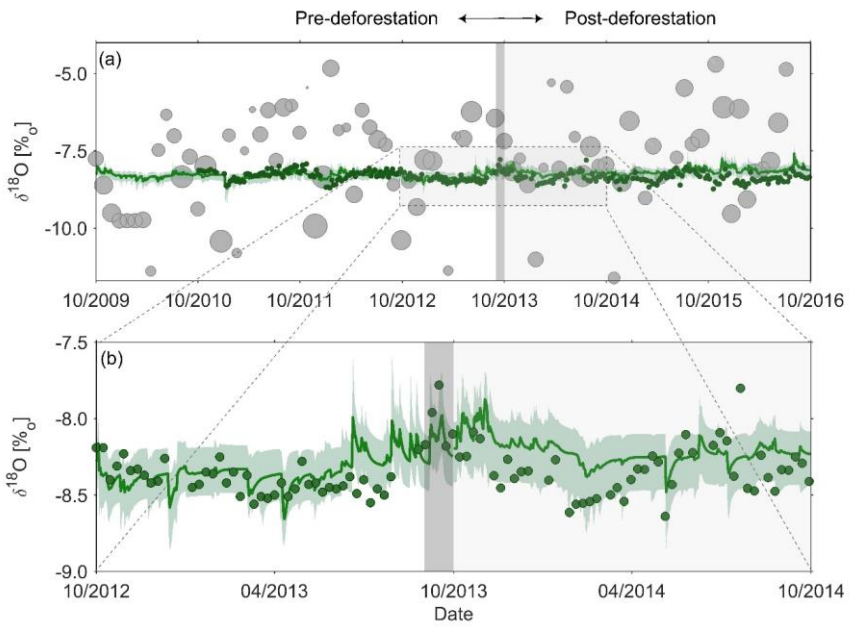
Figure 43: Model structure used in this study. The light blue boxes indicate the hydrologically active individual storage volumes in the hillslope and riparian zones, respectively. The darker blue box $S_{S,p}$ indicates a hydrologically passive, i.e. $dS_{S,p}/dt = 0$, mixing volume. The blue lines indicate liquid water fluxes, the green lines indicate vapour fluxes. Model parameters are shown in red, adjacent to the model component they are associated with. All symbols are defined in Table 1.
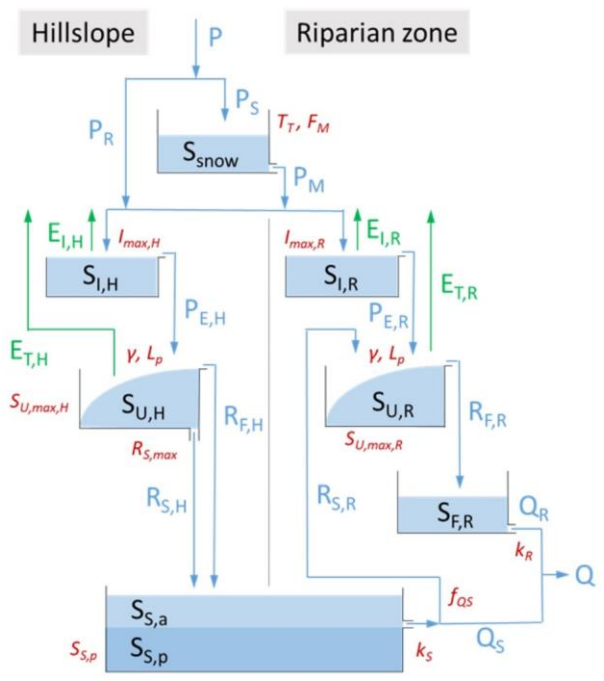
Figure 54: (a) Positions of the individual years of the study period in the Budyko framework. The x-axis shows the aridity index I_A $= E_P/P$, the y-axis indicates the evaporative ration E_A/P and the runoff ratio $C_R = 1 - E_A/P$. Pre-deforestation years are shown with blueish shades, post-deforestation years with greenish shades. The bold black lines indicate the energy and water limits, respectively. The dashed grey line is the theoretical-analytical Turc-Mezentsev relationship (Turc, 1954; Mezentsev, 1955). **(b)** The range of time series of storage deficits as computed according to equation 2, using values of I_{max} from 0 to 4 mm. The maximum annual storage deficits $S_{D,j}$ are indicated by the arrows. The grey shaded area indicates the deforestation period. **(c)** Estimation of $S_{U,max}$ as the storage deficit associated with a 20-year return period $S_{D,20yr}$ using the Gumbel extreme value distribution for the pre-deforestation period. The blueish dots indicate the range of maximum annual storage deficits $S_{D,j}$ for the four years pre-deforestation period. The dark grey shaded area indicates the envelop of least-square fits for the individual values of I_{max}. The light grey shaded area indicates the envelope of the 5/95th confidence intervals. The red line shows the plausible range for $S_{U,max}$.
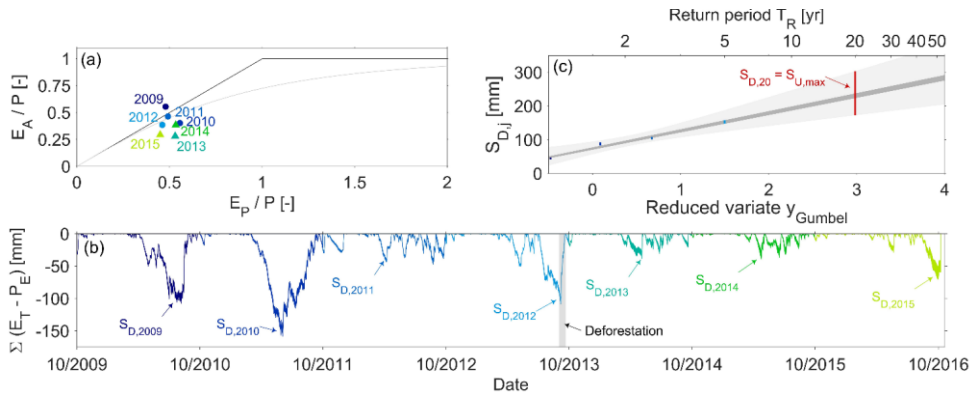
1230 **Figure 56: (a) Model performance metrics for all variables and signatures. D_E is the Euclidean distance to the perfect model. It combines all other performance metrics (Table 3) into one number (Eq.42). All performance metrics are formulated in a way that a value of 1 indicates a perfect fit. The boxplots summarize the performances of all parameter sets retained as feasible. The circle symbols indicate the performance of the best performing model in terms of D_E. The dark red shades indicate pre-deforestation model performance based on calibration in the pre-deforestation period. Orange shades indicate post-deforestation performance using the**
1235 **pre-deforestation parameter sets without further re-calibration. Yellow shades show the post-deforestation performance after model re-calibration in the post-deforestation period. (b)-(c) show flow duration curves, (d)-(e) show the peak distributions and (f)-(g) the autocorrelation functions for the pre- (red) and the post deforestation periods (orange and yellow), respectively. The black lines indicate the observed values, the dashed lines indicate the best fits and the shaded areas the 5/95th uncertainty interval of all solutions retained as feasible. The dark red shades indicate pre-deforestation model results based on calibration in the pre-deforestation**
1240 **period. Orange shades indicate post-deforestation model results using the pre-deforestation parameter sets without further re-calibration. Yellow shades show the post-deforestation model results after model re-calibration in the post-deforestation period.**
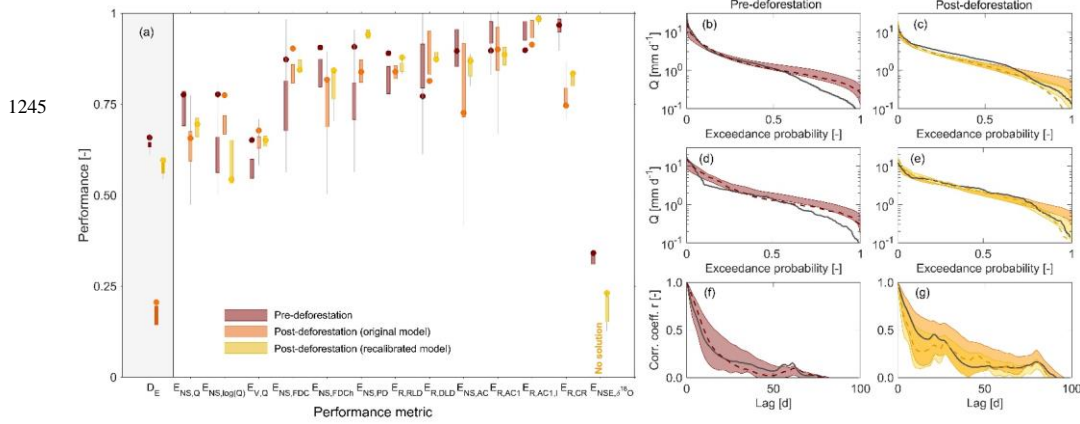
Figure 67: Posterior distributions of selected parameters shown as empirical cumulative distribution function (lines) and the associated relative frequency distributions (bars). Red shades indicate calibration in the pre-deforestation period, Yellow shades indicate post-deforestation calibration. The dots indicate the parameter values associated with respective best fit models.
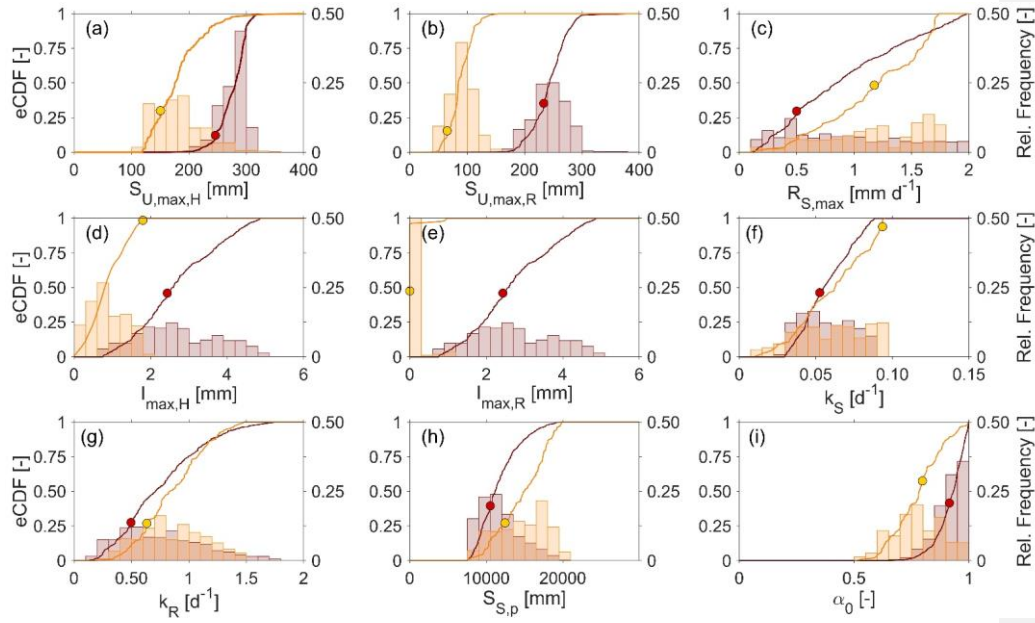
Figure 78: Panels in the left column show pre-deforestation (a) discharge, the coloured dots indicate to which period (dry, wet-up, wet, drying) the individual selected time steps belong; (b) the 5/95th percentiles of the empirical cumulative ~~RTDs (light shades) and~~ TTDs ~~(dark shades)~~ for wet (blue) and dry (red) periods, respectively; (c) the ensemble of the individual TTDs at the time steps indicated in (a). Panels in the middle column (d-g) compare the 5/95th percentiles of empirical cumulative TTDs between predeforestation (dark shades) and post-deforestation (light shades) periods for dry, wet-up, wet and drying conditions, respectively. Panels in the right column show post-deforestation (h) discharge, the coloured dots indicate to which period (dry, wet-up, wet, drying) the individual selected time steps belong; (i) the 5/95th percentiles of the empirical cumulative ~~RTDs (light shades) and~~ TTDs ~~(dark shades)~~ for wet (blue) and dry (red) periods, respectively; (j) the ensemble of the individual TTDs at the time steps indicated in (h). All distributions shown are truncated at 3 (post-deforestation) for 4 years (pre-deforestation), which coincides with the tracked period. For the remaining fractions, i.e. the difference to 1, it can only be said that they are older than 3 years but nothing more than that.

45
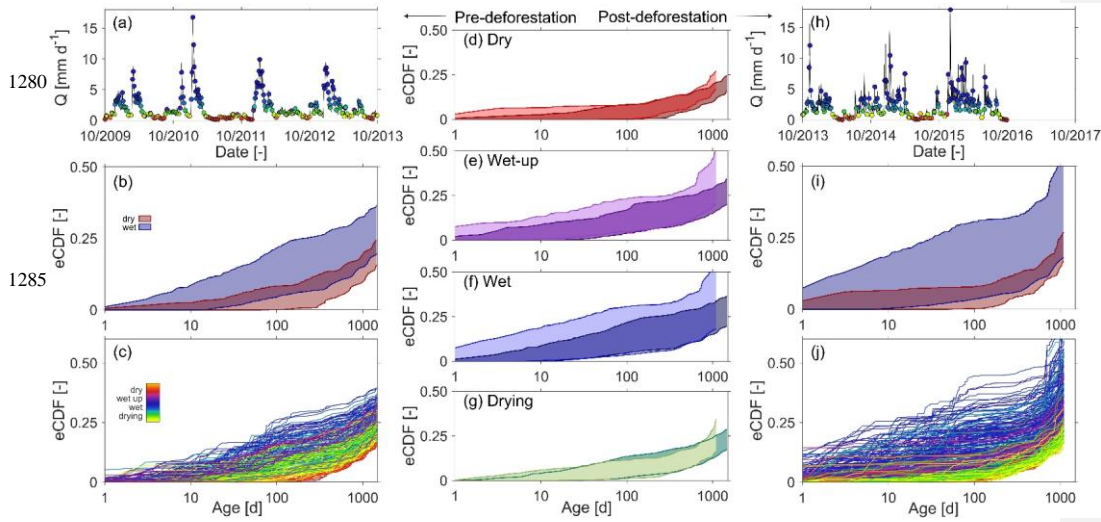
Figure 89: (a)-(b) Pre- and post-deforestation time series of young water fractions F_{yw} in discharge. The colour code indicates the transition between dry, wetting-up, wet and drying conditions. The bold black line shows the mean F_{yw} of the best model fit, the grey shaded area shows the 5/95th percentile of F_{yw} for all feasible model solutions; (c)-(d) pre- and post-deforestation sensitivity of F_{yw} to discharge, using the same colour code as above to indicate dry, wetting-up, wet and drying conditions. The arrows in (d) indicate if there are statistically significant ($\uparrow$; $p < 0.05$) changes or not ($\leftrightarrow$) in the sensitivities between the post-deforestation period and the pre-deforestation period.

46
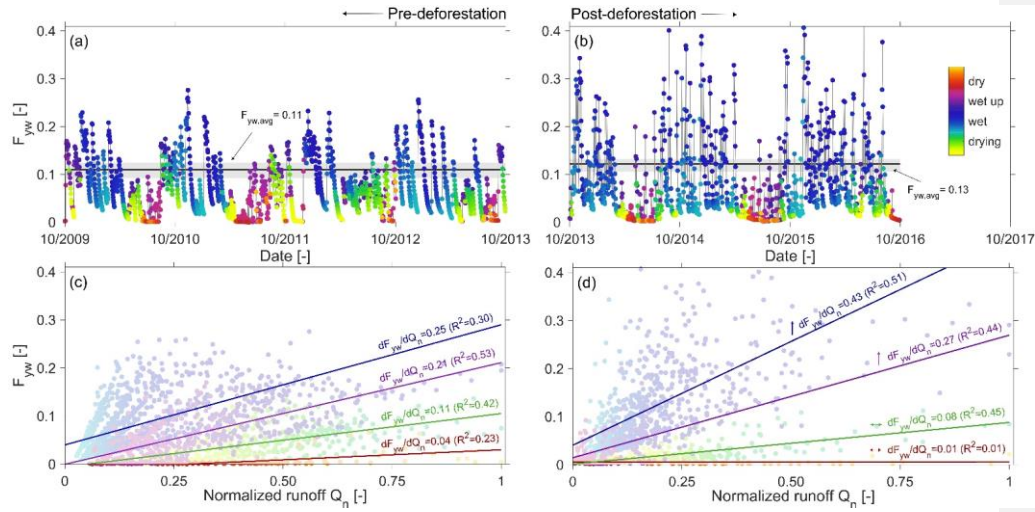
Figure 910: Individual catchment overall SAS ω-functions for individual time steps under different wetness conditions in the (a) pre-deforestation period and (b) post-deforestation period. The insets show the relative water content in $S_{U,rel,mod} = S_U/S_{U,max}$ at the individual time steps.

1310

1315

1320

47